

**SANTA CATARINA STATE UNIVERSITY – UDESC
CENTER OF TECHNOLOGICAL SCIENCES – CCT
GRADUATE PROGRAM IN APPLIED COMPUTING – PPGCA**

KRIGOR RHUANN ROSA DA SILVA

**MULTI-OBJECTIVE EVOLUTIONARY ALGORITHM APPLIED TO STEEL
DEVELOPMENT**

JOINVILLE

2024

KRIGOR RHUANN ROSA DA SILVA

**MULTI-OBJECTIVE EVOLUTIONARY ALGORITHM APPLIED TO STEEL
DEVELOPMENT**

Master thesis submitted to the Computer Science Department at the College of Technological Science of Santa Catarina State University in fulfillment of the partial requirement for the Master's degree in Applied Computing.

Supervisor: Rafael Stubs Parpinelli

JOINVILLE

2024

Para gerar a ficha catalográfica de teses e
dissertações acessar o link:
<https://www.udesc.br/bu/manuais/ficha>

Rosa da Silva, Krigor Rhuann

Multi-objective Evolutionary Algorithm Applied to
Steel Development / Krigor Rhuann Rosa da Silva. -
Joinville, 2024.

97 p. : il. ; 30 cm.

Supervisor: Rafael Stubs Parpinelli.

Dissertação (Mestrado) - Universidade do Estado
de Santa Catarina, Centro de Ciências Tecnológicas,
Programa de Pós-Graduação em Computação Aplicada,
Joinville, 2024.

1. Palavra-chave. 2. Palavra-chave. 3. Palavra-chave.
4. Palavra-chave. 5. Palavra-chave. I. Stubs Parpinelli,
Rafael. II. , . III. Universidade do Estado de Santa
Catarina, Centro de Ciências Tecnológicas, Programa de
Pós-Graduação em Computação Aplicada. IV. Título.

KRIGOR RHUANN ROSA DA SILVA

**MULTI-OBJECTIVE EVOLUTIONARY ALGORITHM APPLIED TO STEEL
DEVELOPMENT**

Master thesis submitted to the Computer Science Department at the College of Technological Science of Santa Catarina State University in fulfillment of the partial requirement for the Master's degree in Applied Computing.

Supervisor: Rafael Stubs Parpinelli

EXAMINATION BOARD:

Dr. Rafael Stubs Parpinelli
UDESC (president/supervisor)

Members:

Dr. Roberto Célio Limão de Oliveira
UFPA

Dr. Yuri Kaszubowski Lopes
UDESC

Joinville, 25th of July, 2024

I dedicate this work to my parents, who have always been with me, and whose structure made it all possible.

ACKNOWLEDGEMENTS

I would like to express my gratitude, first and foremost, to my family for all the support during my studies, for sharing in the achievements and uncertainties. To my friends who served as a foundation of distraction and comfort throughout this journey.

To my advisor Rafael Parpinelli, for giving me the opportunity and agreeing to guide me in this work, for his patience and help throughout this academic journey.

Last but certainly not least, I want to thank ArcelorMittal for making this work possible and believing in the partnership with UDESC. Special thanks to Fabricio Cerqueira, Fabiano Miranda, and José Francisco for their monitoring and unwavering support for the project.

”No fim tudo dá certo, e se não deu certo é
porque ainda não chegou no fim.”

(Fernando Sabino)

ABSTRACT

The development of new types of steel is a constant challenge in the metallurgical sector, as researchers tirelessly seek to create lighter and stronger variants tailored to various industrial demands. However, the intrinsic complexity in the formation structure of steels, resulting in different types with varied property ranges, makes this process difficult and unique for each application. In this context, we propose modifications to a data-driven system using Machine Learning (ML). This system can predict the mechanical properties of steel, optimizing both the chemical composition and processing parameters. The goal is to enhance the accuracy of the new alloys concerning specific mechanical properties and achieve greater genotypic diversity in the configurations suggested by the system. For the prediction task, we trained an ensemble of Artificial Neural Networks (ANN) on metallurgical data using Automated Machine Learning (AutoML). These networks are coupled to form a single multivariate regression model. Subsequently, this joint model is integrated with a Multi-Objective Evolutionary Algorithm (MOEA), employing a two-archive strategy to pursue both solution convergence and genotypic diversity, respectively. At the end of the process, the optimization algorithm based on a surrogate model proposes new steel designs. Comparison experiments were conducted to validate the prediction model and ensure the computational validation of the optimization scheme.

Keywords: Artificial Neural Network. Optimization. Material Design. Steel. Machine Learning.

RESUMO

O desenvolvimento de novos tipos de aço é um desafio constante no setor metalúrgico, pois os pesquisadores buscam incessantemente criar variantes mais leves e mais resistentes, adaptadas às diversas demandas industriais. No entanto, a complexidade intrínseca à estrutura de formação dos aços, que resulta em diferentes tipos com variadas faixas de propriedades, torna esse processo difícil e único para cada aplicação. Neste contexto, propomos modificações em um sistema baseado em dados utilizando Aprendizado de Máquina (ML). Esse sistema é capaz de prever as propriedades mecânicas do aço, otimizando tanto a composição química quanto os parâmetros de processamento. O objetivo é aumentar a precisão das novas ligas em relação a propriedades mecânicas específicas, além de obter uma maior diversidade genotípica nas configurações sugeridas pelo sistema. Para a tarefa de previsão, treinamos um conjunto de Redes Neurais Artificiais (ANN) em dados metalúrgicos usando Aprendizado de Máquina Automatizado (AutoML). Essas redes são acopladas para formar um único modelo de regressão multivariada. Em seguida, esse modelo conjunto é integrado a um Algoritmo Evolutivo Multi-Objetivo (MOEA), utilizando uma estratégia de dois arquivos para buscar a convergência das soluções e a diversidade genotípica, respectivamente. Ao final do processo, o algoritmo de otimização baseado em modelo substituto propõe novos designs de aços. Experimentos de comparação foram realizados para validar o modelo de previsão e garantir a validação computacional do esquema de otimização.

Palavras-chave: Rede Neural Artificial. Otimização. Design de Materiais. Aços. Machine Learning.

LIST OF FIGURES

| | |
|---|----|
| Figure 1 – Overview of different steel grades in relation to strength and elongation. Source: (HALL; FEKETE, 2017) | 23 |
| Figure 2 – Stress-Strain Curve. | 26 |
| Figure 3 – General supervised learning scheme. Source: Own authorship | 28 |
| Figure 4 – Representation of a) neuron and b) neural network. Source: Adapted from Krogh (2008) | 29 |
| Figure 5 – Abstract illustration of Neural Architecture Search methods. Source: (ELSKEN; METZEN; HUTTER, 2019) | 31 |
| Figure 6 – Representation of an ensemble of artificial neural networks. Source: (ALAM; SIDDIQUE; ADELI, 2020a) | 32 |
| Figure 7 – Pareto front with two objectives, being f_1 and f_2 . Non-dominated points are in blue, and dominated points are in orange. A and B are Pareto optimal solutions that dominate C and D. Source: Inspired by (SGROTT, 2022) . . . | 34 |
| Figure 8 – Representation of the HV for a biobjective problem. Source: (FONSECA; PAQUETE; LÓPEZ-IBÁÑEZ, 2006) | 41 |
| Figure 9 – Representation of the IGD calculation for the solution set A. Source: Inspired by Ishibuchi, Masuda e Nojima (2016) | 42 |
| Figure 10 – Proposed computational system. Source: Own authorship. | 52 |
| Figure 11 – Proposed surrogate modeling flowchart. Source: (SILVA et al., 2023). | 53 |
| Figure 12 – Online parameter control using deterministic rules for Recombination and Mutation. Source: Adapted from Sgrott (2022). | 56 |
| Figure 13 – Flowchart of solution and diversity archives. Source: Own authorship. | 57 |
| Figure 14 – Flowchart of the genetic algorithm with solution and diversity archives, and reintroduction of solution. Source: Own authorship. | 58 |
| Figure 15 – Example of the staggered optimization process, 3 additional optimizations are made due to the staggering of X_{02} and 15 additional optimizations due to the staggering of X_{07} . Source: Own authorship. | 59 |
| Figure 16 – Best five ANNs found using the NAS architecture. | 63 |
| Figure 17 – Training and validation loss of training epochs using the NAS architecture. | 64 |
| Figure 18 – Performance Comparison of Models in 10-Fold Cross-Validation. | 64 |
| Figure 19 – Sensitivity analysis of 'C' for the E-ANN and B-ANN models. | 66 |
| Figure 20 – Sensitivity analysis of 'Mn' for the E-ANN and B-ANN models. | 66 |
| Figure 21 – SHAP values for a) B-ANN Model, b) E-ANN Model. | 67 |
| Figure 22 – Data cut applied to steel subtypes for each grade. | 68 |
| Figure 23 – Box plot of MAE values per mechanical properties, using the database and its limited version for each model. | 69 |

| | |
|--|----|
| Figure 24 – Box plot of MAE values per subtypes of steel grade, using the database and its limited version for each model. | 70 |
| Figure 25 – Final HV and IGD values for all MOEA tested and IF steels. | 71 |
| Figure 26 – Final HV and IGD values for all MOEA tested and BH steels. | 72 |
| Figure 27 – Final HV and IGD values for all MOEA tested and HSLA steels. | 72 |
| Figure 28 – Final HV and IGD values for all MOEA tested and DP steels. | 73 |
| Figure 29 – Final HV and IGD values for all MOEA tested and TRIP steels. | 74 |
| Figure 30 – Dispersion of mechanical properties for each MOEA for IF steel. | 75 |
| Figure 31 – Dispersion of mechanical properties for each MOEA for BH steel. | 76 |
| Figure 32 – Dispersion of mechanical properties for each MOEA for HSLA steel. | 76 |
| Figure 33 – Dispersion of mechanical properties for each MOEA for DP steel. | 76 |
| Figure 34 – Dispersion of mechanical properties for each MOEA for TRIP steel. | 77 |
| Figure 35 – Box plots of the GF values for different values of the solution reintroduction parameter. | 78 |
| Figure 36 – GF results for each type of steel and 30 runs. | 80 |
| Figure 37 – Histogram of the configurations for six chemical input variables. | 81 |
| Figure 38 – Histogram of the configurations for six process parameters input variables. | 82 |
| Figure 39 – TRIP steel dispersion of mechanical properties for (a) C1, (b) C2. | 82 |
| Figure 40 – Dispersion of mechanical properties for the a) staggered optimization b) standart optimization. | 84 |
| Figure 41 – Carbon histogram for the a) staggered optimization b) standart optimization. | 84 |
| Figure 42 – Time Taken to Display the Plots plot. | 85 |
| Figure 43 – Time taken to complete the optimization and display the results plots. | 86 |
| Figure 44 – Memory Consumed to Display the results plots. | 87 |

LIST OF TABLES

| | |
|---|----|
| Table 1 – Table referring to the number of studies found, filtered, and selected in the search. | 46 |
| Table 2 – Selected papers/theses | 51 |
| Table 3 – Search space for the NAS parameters. | 54 |
| Table 4 – Description from the model’s variables, where CE, PP, DIM, and MP stand for Chemical Element, Process Parameter, Dimension, and Mechanical Property, respectively. | 62 |
| Table 5 – Distribution of Steel Types | 62 |
| Table 6 – Dunn’s test P-values for the model performance comparison dataset (values above the main diagonal represent the values for the MAE metric, and values below the main diagonal indicate the values for the MSE metric). | 64 |
| Table 7 – Dunn’s test P-values comparing the original and cutted dataset for MAE values per mechanical properties. | 69 |
| Table 8 – Distribution of Steel Types after the limitation of the database | 70 |
| Table 9 – Dunn’s test P-values for Final HV and IGD values for all MOEA tested and IF steels (values above the main diagonal represent the values for the HV metric, and values below the main diagonal indicate the values for the IGD metric). | 71 |
| Table 10 – Dunn’s test P-values for Final HV and IGD values for all MOEA tested and BH steels (values above the main diagonal represent the values for the HV metric, and values below the main diagonal indicate the values for the IGD metric). | 72 |
| Table 11 – Dunn’s test P-values for Final HV and IGD values for all MOEA tested and HSLA steels (values above the main diagonal represent the values for the HV metric, and values below the main diagonal indicate the values for the IGD metric). | 73 |
| Table 12 – Dunn’s test P-values for Final HV and IGD values for all MOEA tested and DP steels (values above the main diagonal represent the values for the HV metric, and values below the main diagonal indicate the values for the IGD metric). | 73 |
| Table 13 – Dunn’s test P-values for Final HV and IGD values for all MOEA tested and TRIP steels (values above the main diagonal represent the values for the HV metric, and values below the main diagonal indicate the values for the IGD metric). | 74 |
| Table 14 – Critical steel mechanical properties values used for distribution analysis. | 75 |
| Table 15 – MOEAs Mean time for each run. | 77 |
| Table 16 – Optimization parameters for the two-archive strategy evaluation. | 78 |
| Table 17 – P-values for reintroduction parameter using Dunn test. | 79 |

| | |
|---|----|
| Table 18 – Mechanical property values used for each steel. | 79 |
| Table 19 – Dunn’s test P-values for each type of steel for comparing the two archives configurations. | 80 |
| Table 20 – Description from the staggered variables. | 83 |
| Table 21 – Mechanical property values used for each steel. | 83 |
| Table 22 – Speedup values for each case. | 86 |

LIST OF ABBREVIATIONS AND ACRONYMS

| | |
|----------|---|
| AI | Artificial Intelligence |
| AGE-MOEA | Adaptive Geometry Estimation based Multi-Objective Evolutionary Algorithm |
| AHSS | Advanced High-Strength Steel |
| ANN | Artificial Neural Network |
| ASE | Academic Search Engine |
| AutoML | Automated Machine Learning |
| BH | Bake Hardening |
| CD | Crowding Distance |
| CFD | Computational Fluids Dynamics |
| CRM | Cold Rolling Mill |
| DOE | Design Of Experiments |
| DP | Dual Phase |
| EA | Evolutionary Algorithm |
| EL | Elongation |
| ES | Evolutionary Strategy |
| EP | Evolutionary Programming |
| GA | Genetic Algorithm |
| GP | Genetic Programming |
| IF | Interstitial Free |
| IGD | Inverse Generational Distance |
| HDG | Hot Dip Galvanizing line |
| HSLA | High-Strength Low-Alloy |
| HSM | Hot Strip Mill |
| HSS | High-Strength Steel |
| HV | Hypervolume |
| LAB | Laboratory |
| ML | Machine Learning |
| MLP | Multi-Layer Perceptron |
| MOEA | Multi-Objective Evolutionary Algorithm |

| | |
|-----------|--|
| NAS | Neural Architecture Search |
| NSGA | Non-dominated Sorting Genetic Algorithm |
| ReLU | Rectified Linear Unit |
| RVEA | Reference Vector Guided Evolutionary Algorithm |
| SHAP | Shapley Values |
| SLR | Systematic Literature Review |
| SM | Steel Mill |
| SPEA | Strength Pareto Evolutionary Algorithm |
| Tanh | Hyperbolic Tangent |
| TRIP | Transformation Induced Plasticity |
| TS or UTS | Tensile Strength |
| xAI | Explainable Artificial Intelligence |
| YS | Yield Strength |

LIST OF SYMBOLS

| | |
|-------------|---|
| Al | Aluminium |
| B | Boron |
| C | Carbon |
| Cr | Chrome |
| F | Pareto front |
| MAE | Mean Absolute Error |
| Mn | Manganese |
| MPa | Mega Pascal |
| MSE | Mean Squared Error |
| Mo | Molybdenum |
| N | Nitrogen |
| Nb | Niobium |
| Ni | Nickel |
| P | Phosphorus |
| r | Reference point |
| S | Sulfur |
| Si | Silicon |
| Ti | Titanium |
| V | Vanadium |
| x | Generic optimization's decision variable vector |
| w | Synaptic weights from the artificial neural network |
| X_{01-27} | Independent parameters used in modeling and as decision variables in optimization |
| Y_{01-03} | Dependent parameters used in modeling |
| λ_m | m-dimensional Lebesgue measure |

CONTENTS

| | | |
|--------------|---|-----------|
| 1 | INTRODUCTION | 19 |
| 1.1 | MOTIVATION | 21 |
| 1.2 | OBJECTIVES | 21 |
| 1.3 | DOCUMENT STRUCTURE | 22 |
| 2 | BACKGROUND | 23 |
| 2.1 | STEEL AND PROPERTIES | 23 |
| 2.1.1 | STEEL TYPES | 23 |
| 2.1.1.1 | <i>Interstitial Free Steels (IF)</i> | 24 |
| 2.1.1.2 | <i>Bake Hardening Steels (BH)</i> | 24 |
| 2.1.1.3 | <i>High Strength Low-Alloy Steels (HSLA)</i> | 24 |
| 2.1.1.4 | <i>Dual-Phase Steels (DP)</i> | 25 |
| 2.1.1.5 | <i>Transformation Induced Plasticity Steels (TRIP)</i> | 25 |
| 2.1.2 | STEEL PROPERTIES | 25 |
| 2.1.2.1 | <i>Yield Strength</i> | 26 |
| 2.1.2.2 | <i>Tensile Strength</i> | 26 |
| 2.1.2.3 | <i>Elongation</i> | 27 |
| 2.2 | MACHINE LEARNING | 27 |
| 2.2.1 | SUPERVISED LEARNING | 27 |
| 2.2.2 | ARTIFICIAL NEURAL NETWORKS | 28 |
| 2.2.2.1 | <i>NEURAL NETWORK PARAMETERS</i> | 29 |
| 2.2.2.1.1 | NUMBER OF LAYERS AND NEURONS | 29 |
| 2.2.2.1.2 | DROPOUT | 30 |
| 2.2.2.1.3 | ACTIVATION FUNCTION | 30 |
| 2.2.2.1.4 | OPTIMIZER | 30 |
| 2.2.2.2 | <i>NEURAL ARCHITECTURE SEARCH</i> | 31 |
| 2.2.3 | ENSEMBLE MODELS | 32 |
| 2.3 | MULTI-OBJECTIVE OPTIMIZATION | 32 |
| 2.3.0.1 | <i>DOMINANCE AND PARETO OPTIMALITY</i> | 33 |
| 2.3.1 | EVOLUTIONAY ALGORITHMS AND MULTI-OBJECTIVE EVOLUTIONARY ALGORITHMS | 34 |
| 2.3.1.1 | <i>GENETIC ALGORITHM</i> | 35 |
| 2.3.1.2 | <i>NONDOMINATED SORTING GENETIC ALGORITHM (NSGA)</i> | 36 |
| 2.3.1.3 | <i>REFERENCE VECTOR GUIDED EVOLUTIONARY ALGORITHM (RVEA)</i> | 37 |
| 2.3.1.4 | <i>ADAPTIVE GEOMETRY ESTIMATION BASED MULTI-OBJECTIVE EVOLUTIONARY ALGORITHM (AGE-MOEA)</i> | 38 |

| | | |
|--------------|---|-----------|
| 2.3.1.5 | <i>EA PARAMETER CONTROL</i> | 39 |
| 2.3.1.6 | <i>EA PARALLELIZATION</i> | 40 |
| 2.3.2 | OPTIMIZATION METRICS | 40 |
| 2.3.2.1 | <i>HYPERVOLUME</i> | 41 |
| 2.3.2.2 | <i>INVERTED GENERATIONAL DISTANCE</i> | 41 |
| 2.3.2.3 | <i>GENE FREQUENCY</i> | 42 |
| 3 | SYSTEMATIC LITERATURE REVIEW | 44 |
| 3.1 | RESEARCH METHOD | 44 |
| 3.2 | PLANNING THE REVIEW | 44 |
| 3.3 | CONDUCTING THE REVIEW | 45 |
| 3.4 | DISCUSSIONS | 47 |
| 3.4.1 | INPUT VARIABLES FOR OPTIMIZATION | 47 |
| 3.4.2 | META-HEURISTIC ALGORITHMS | 47 |
| 3.4.3 | QUANTITATIVE ANALYSIS | 48 |
| 3.4.4 | QUALITATIVE ANALYSIS | 48 |
| 3.4.5 | CONSIDERATIONS | 49 |
| 4 | PROPOSED APPROACH | 52 |
| 4.1 | REGRESSOR MODELING | 53 |
| 4.1.1 | NEURAL ARCHITECTURE SEARCH | 53 |
| 4.2 | MOEA FOR STEEL DESIGN OPTIMIZATION | 54 |
| 4.2.1 | MOEA | 55 |
| 4.2.2 | TWO-ARCHIVE STRATEGY | 56 |
| 4.2.2.1 | <i>MOEA REINTRODUCTION OF SOLUTIONS</i> | 58 |
| 4.2.3 | STAGGERED OPTIMIZATION | 59 |
| 5 | RESULTS AND ANALYSIS | 61 |
| 5.1 | REGRESSOR ANALYSIS | 61 |
| 5.1.1 | DATABASE | 61 |
| 5.1.2 | ENSEMBLE MODELING | 63 |
| 5.1.2.1 | <i>INTERPRETABILITY TECHNIQUES</i> | 65 |
| 5.1.3 | DATABASE CUTOFF | 68 |
| 5.2 | OPTIMIZATION ANALYSIS | 71 |
| 5.2.1 | MOEA ALGORITHM | 71 |
| 5.2.2 | TWO-ARCHIVES STRATEGY | 77 |
| 5.2.2.1 | <i>REINTRODUCTION PARAMETER</i> | 78 |
| 5.2.2.2 | <i>ARCHIVES PERFORMANCES</i> | 79 |
| 5.2.3 | CASE STUDY: ROTA 2030 | 83 |
| 5.2.3.1 | <i>STAGGERED OPTIMIZATION PARALLELIZATION</i> | 85 |

| | | |
|----------|---|-----------|
| 6 | FINAL CONSIDERATIONS AND FUTURE WORK | 88 |
| 6.1 | ACKNOWLEDGMENTS | 89 |
| | BIBLIOGRAPHY | 90 |

1 INTRODUCTION

The utilization of steel holds a historical significance, dating back centuries and even prehistory, when it replaced bronze in tool manufacturing (SCHWEITZER et al., 2003). This transition triggered substantial societal transformations by driving rapid agricultural development and facilitating territorial expansion through advanced weaponry, reshaping the global landscape. Over time, advancements in steel production techniques, such as the introduction of alloying elements and phase changes, enhanced its hardness and resistance. Presently, steel occupies a prominent position in the global economy, serving as a vital component across various industrial sectors.

In the realm of industrial applications, the demand for steel is characterized by essential safety and quality requirements coupled with evolving manufacturing processes and customer preferences. This dynamic has resulted in a diverse array of steel types available in the market, each exhibiting distinct microstructural characteristics determined by alloying elements and production temperatures. These factors significantly influence crystalline phase formation, grain size, and other features crucial to the mechanical properties of the resulting steel (KRAUSS, 2017).

Mechanical properties, encompassing strength, surface quality, fatigue and density, play a pivotal role in industrial applications (XIAO et al., 2023). The unique demands of each application necessitate specific steel types with particular mechanical properties. This underscores the importance of ongoing efforts to develop new steel alloys, driven by the goals of innovative design, cost reduction, weight reduction, and achieving higher mechanical property values (HUANG et al., 2022).

Recently, the use of bio-inspired optimization algorithms to find solutions in steel design has been the focus of some researchers. In problems of this nature, the typical goal is to optimize concurrent properties, and therefore, multi-objective algorithms are commonly applied, with Multi-objective Evolutionary Algorithm (MOEA) standing out. The diversity of solutions plays a fundamental role both in the context of evolutionary algorithms and steel development. In the optimization, comprehensive search space coverage allows for representing a wide range of non-dominated solutions (DEB, 2001). However, MOEA need help maintaining genotypic diversity over generations, and controlling it is crucial to avoid premature convergence, i.e., getting stuck in local optima and ensuring adequate search space exploration. Furthermore, for the steel development context, a lack of genotypic diversity can lead to similar solutions, limiting decision-makers choices for new configurations with different combinations of chemical composition and process parameters. This low number of options can take away the possibility of cheaper solutions or those better suited to the production line and its limits.

The work of Resendiz-Flores et al. (2021) employs an Artificial Neural Network (ANN) to model DP steel, in conjunction with the NSGA-II(DEB et al., 2002) algorithm, aiming to optimize process parameters for steels with fixed chemical composition. Although the choice of

the Multi-Objective Evolutionary Algorithm (MOEA) is mentioned as being made to preserve diversity, the study does not utilize complementary methods for this purpose. Additionally, it is observed that the performance of NSGA-II is inferior to more recent MOEAs, and one of the reasons for this is that NSGA-II does not take into account diversity in the objective space, as highlighted by Segura, Castillo e Schütze (2023).

Thus, techniques aimed at increasing diversity, especially genotypic diversity of solutions, aligned with low variance in the target values of desired mechanical properties, represent a significant opportunity for advancement in this field. These approaches have the potential to add industrial value through the results they generate.

This study proposes enhancements to a computational system designed for steel development as outlined in Sgrott (2022). The initial system comprises two key components. In the first part, an Artificial Neural Network (ANN) is constructed to function as a surrogate model for Interstitial Free (IF), Bake Hardening (BH), High-Strength Low-Alloy (HSLA), Dual Phase (DP), and Transformation Induced Plasticity (TRIP) steels. The ANN's architecture and hyperparameters undergo optimization through Neural Architecture Search (NAS), automating and refining the modeling stage (SGROTT et al., 2021). Inputs to the ANN include chemical composition, processing parameters, and dimensional information, while its outputs encompass mechanical properties, specifically Tensile Strength (TS or UTS), Yield Strength (YS), and Elongation (EL).

Moving to the second part, the ANN is integrated into a MOEA, where its predictions contribute to the fitness function, assessing the various optimized individuals evolved over generations. Each individual corresponds to the chemical composition, processing parameters, and dimensional information of a specific steel. The modifications introduced in this work are categorized into these two distinct parts.

For the modifications related to the first part of the Sgrott (2022), there was a comprehensive increase in the database, aiming for a more consistent balance in the number of samples for each steel type. Furthermore, the regression model derived from this database was enhanced to become an ensemble of Artificial Neural Networks (E-ANN) comprised of the five most effective configurations identified by NAS. These adjustments aim to mitigate bias in regression, preventing the system from consistently favoring steel configurations similar to a specific type. Instead, the goal is to enable a broader search, allowing for the combination of distinctive characteristics present in each steel type. Additionally, ensemble techniques are intended to more effectively distribute the generalization errors associated with each individual ANN, contributing to more precise predictions with reduced margins of error (ALAM; SIDDIQUE; ADELI, 2020b).

For the modifications related to the second part of the Sgrott (2022), the possibility of replacing the MOEA algorithm was examined due to the high variance observed in the NSAG-II results concerning the desired mechanical properties. Additionally, a new strategy involving two external repositories for promising solutions, known as archives, was implemented, focusing on convergence as assessed by the fitness and diversity of solutions as evaluated by Shannon

entropy. This approach aims to enhance the genotypic diversity of the final steel configurations provided by the system, thereby generating more viable options for decision-makers.

1.1 MOTIVATION

In the metallurgical industry, the challenges presented by clients and governments underscore the indispensable role of constant innovation in the industry's mindset. Achieving the desired characteristics for steel many times involves altering the chemical composition and process temperatures, which can be a highly complex and challenging task (ZHU; LIANG; ZOU, 2020). Computational systems and techniques such as ANN and MOEA have already proven to be influential in proposing solutions, as seen in (SGROTT, 2022). However, the increasing need for more diverse and accurate solutions is crucial, as it can bring several benefits. This includes the exploration of new configurations with varying combinations of chemical composition and process parameters, paving the way for innovative approaches to steel design. Such approaches can yield cost-effective solutions, introduce novel values and combinations for mechanical properties, or offer configurations of steels better suited to the production line and its constraints. Consequently, this not only leads to the creation of new products but also adds significant value to the company.

1.2 OBJECTIVES

The main purpose of this work is to enhance the results generated by the system that proposes new chemical compositions and processing parameters for the production of steels with desired mechanical properties. To achieve this, two main objectives have been established regarding the search mechanism used in the optimization procedure:

1. Improve the accuracy of the solutions generated in relation to the desired mechanical properties, aiming to make the majority of results more representative as a viable solution for decision-makers.
2. Achieve greater genotypic diversity in the solutions found by the optimizer, allowing the observation of various configurations of steels that possess the desired mechanical properties, thereby expanding the possibilities for decision-makers.

Additionally, some secondary objectives are listed, which will build the steps to accomplish the main objectives:

- Evaluate different multi-objective optimization algorithms to handle solution searching.
- Model the behavior of steels using Artificial Neural Networks (ANNs), employing ensemble techniques to enhance the system's generalization.

- Adjust the proportions of different types of steels in the dataset, aiming to reduce potential biases and make the search for solutions more comprehensive.
- Gain a deeper understanding of the surrogate model by applying artificial explainability techniques.

1.3 DOCUMENT STRUCTURE

The remaining chapters of this master's thesis are organized as follows: Chapter 2 delves into the essential theoretical foundations necessary for a comprehensive understanding of this work, offering insights into both metallurgical and computational aspects; Chapter 3 conducts a Systematic Literature Review (SLR), focusing on the utilization of computational methods in predicting and designing steels; Chapter 4 furnishes a comprehensive and detailed account of the proposed modifications, adopting a top-down approach to elucidate the intricacies involved; Chapter 5 elaborates on the experimental procedures, providing details on their execution, results, and subsequent analysis; Finally, Chapter 6 encapsulates the findings and concludes, also outlining potential avenues for future research directions.

2 BACKGROUND

This chapter presents the metallurgical and computational concepts needed to support this study.

2.1 STEEL AND PROPERTIES

2.1.1 STEEL TYPES

Steels are widely acclaimed for their exceptional strength, durability, and versatility, establishing them as an extensively utilized group of alloys across various industries. The distribution of steel grades concerning their strength and ductility is illustrated in Figure 1.

When examining conventional steels, we observe lower values for both strength and formability. This can be attributed to the initial development of these steels, dating back to the post-Industrial Revolution era, which was marked by significant advancements in production methods. However, over time, the limitations of these materials in terms of strength, weight, and efficiency prompted the development of Advanced High-Strength Steels (AHSS) to meet the growing demands of the modern industry.

In general, AHSS emerged in response to the increasing demand for lighter, more efficient, and safer materials across various industrial applications, notably in the automotive industry (FONSTEIN, 2015). The evolution of these steels was motivated by diverse challenges and specific engineering needs, including weight reduction, high formability performance, and adaptation to new technologies, among others. Furthermore, as depicted in Figure 1, each generation of AHSS represents a revolutionary increase in strength and, consequently, the complexity of the material.

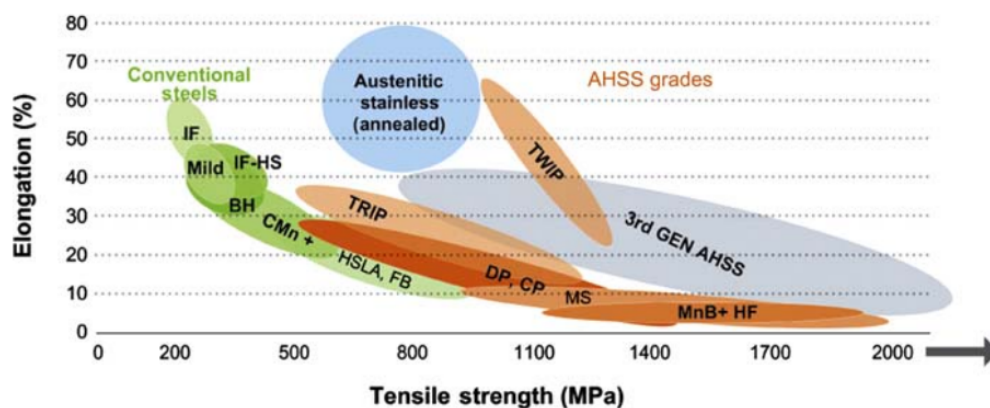


Figure 1 – Overview of different steel grades in relation to strength and elongation. Source: (HALL; FEKETE, 2017)

2.1.1.1 *Interstitial Free Steels (IF)*

Interstitial Free Steels (IF) are renowned for their exceptional formability, a characteristic attributed to their distinctive chemical composition devoid of interstitial elements like carbon and nitrogen. This unique composition results in a remarkably ductile material capable of being shaped into intricate forms without succumbing to cracking or rupturing, as extensively discussed by Sarkar (SARKAR et al., 2010a). Consequently, the absence of these interstitial elements imparts remarkable malleability to IF steels, rendering them extensively utilized in the automotive industry, particularly for crafting external body components.

In the manufacturing process of IF steels, the common practice involves the addition of niobium or titanium. This addition serves the purpose of minimizing the presence of carbon and nitrogen as interstitial solutes. Notably, niobium and titanium possess the ability to stabilize carbon and nitrogen atoms, preventing their incorporation into the crystal structure of the steel, as elucidated by Ray (RAY; JONAS; HOOK, 1994). Furthermore, meticulous temperature control is imperative during the reheating and hot rolling phases of the manufacturing process. These steps play a pivotal role in determining the crystallographic structure and grain size of the material, as emphasized by Sarkar (SARKAR et al., 2010a). These factors directly impact the final properties of the steel, highlighting the critical importance of precise control throughout the production process.

2.1.1.2 *Bake Hardening Steels (BH)*

Bake Hardening Steels (BH) represent a category of low-carbon steel distinguished by its heightened strength and hardness achieved through a specialized heat treatment process. This process involves the diffusion of carbon atoms, creating an atmosphere around dislocations. The consequence is the immobilization of these dislocations, culminating in a notable increase in strength (MOMENI et al., 2007).

The introduction of alloying elements, including niobium, titanium, molybdenum, and vanadium, plays a crucial role in influencing carbide dissolution during annealing. This, in turn, has a substantial impact on the concentration of carbon within the solution. The intricacies of this phenomenon are intricately discussed by Pereloma (PERELOMA; TIMOKHINA, 2017). The interplay between alloying elements, carbide dissolution temperature, and the strength of carbon bonding energy creates a delicate balance, giving rise to diverse microstructures and, consequently, varied final material properties. The nuanced understanding of these factors is pivotal in tailoring the properties of Bake Hardening Steels to meet specific application requirements.

2.1.1.3 *High Strength Low-Alloy Steels (HSLA)*

High Strength Low-Alloy Steels (HSLA) constitute a category of steel designed to deliver superior mechanical properties and enhanced resistance to atmospheric corrosion when compared

to conventional carbon steels. The augmentation of these properties is accomplished through a spectrum of hardening techniques, including grain refinement and precipitation strengthening, as expounded by Skobir (KONSTRUKCIJSKA, 2011). Notably, the incorporation of minute quantities of alloying elements further amplifies these effects. Elements such as aluminum, vanadium, niobium, or titanium are strategically added to the composition, contributing to the overall improvement in performance and durability of HSLA steels.

2.1.1.4 Dual-Phase Steels (DP)

Dual-phase steels (DP) are recognized for their exceptional combination of tensile strength, elongation, and heightened fatigue resistance. The manufacturing intricacies of dual-phase steels demand meticulous control over phase transformations, each representing unique states defined by specific chemical compositions, atomic bonds, and element arrangements. These transformations are intricately tied to the steel's heat treatment history. Within the steel structure, each phase manifests distinct properties, collectively contributing to the superior performance of the material, as elucidated by Krauss in the referenced literature (KRAUSS, 2017).

2.1.1.5 Transformation Induced Plasticity Steels (TRIP)

Transformation Induced Plasticity Steels (TRIP) represent an advanced class of metallic materials renowned for their exceptional mechanical properties, stemming from their unique ability to undergo phase transformations during plastic deformation (FONSTEIN, 2015). This distinctive characteristic results in a remarkable synergy of high strength and ductility.

The phase transformation is initiated by the redistribution of alloying elements within the material, leading to the formation of a stable crystalline structure that significantly enhances its strength. Notably, the presence of a stable austenitic phase imparts TRIP steels with an augmented capacity for energy absorption during deformation. This attribute makes them particularly well-suited for applications that demand a combination of high strength and toughness (FISCHER et al., 2000).

2.1.2 STEEL PROPERTIES

The diverse range of available steel types and various composition approaches stem from the constant endeavor to enhance their unique properties. However, there are various types of properties, such as thermal and electrical, among others. In this work, we focused our efforts on fundamental mechanical properties, specifically yield strength (YS), tensile strength (TS or UTS), and elongation (EL).

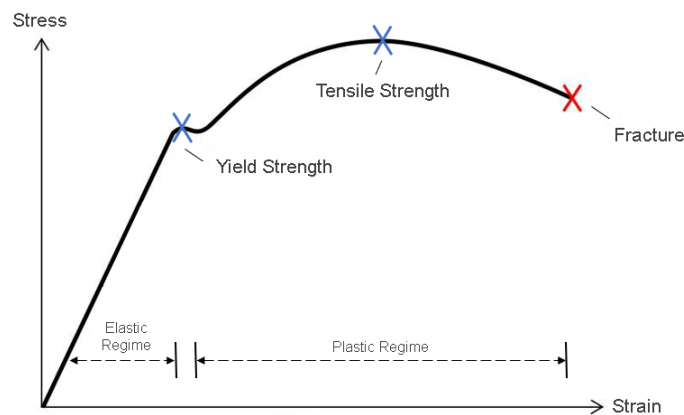


Figure 2 – Stress-Strain Curve.

The stress-strain curve, as depicted in Fig. 2, is a fundamental tool in understanding the mechanical behavior of materials, including steel. This curve is generated through a tensile test, where a specimen of the material is subjected to an increasing axial load until it fractures (BUDYNAS; NISBETH, 2016). The resulting stress and strain data are then plotted to create the curve.

Understanding the stress-strain curve is crucial for designing and analyzing structures made of steel. Its information is used to determine the material's mechanical properties, predict its behavior under different conditions and design structures that can withstand specific loads without failure.

Each of these properties carries significance within a project. In mechanical forming, for instance, tensile strength and elongation are crucial, as they are essential for the material to undergo maximum deformation (HOSFORD; CADDELL, 2011), operating within the plastic regime. However, in most other engineering applications, Yield Strength takes precedence in design, aiming to work within the material's elastic range without inducing significant deformations (CALLISTER; RETHWISCH, 2010).

2.1.2.1 Yield Strength

This is defined as the maximum stress value within the material's elastic regime (CALLISTER; RETHWISCH, 2010). In simpler terms, any deformation experienced by the material up to this stress level is reversible upon the removal of the applied load.

2.1.2.2 Tensile Strength

This is the maximum stress point required to further deform the material, now in the plastic regime (CALLISTER; RETHWISCH, 2010), resulting in permanent deformations that do not revert to the original size upon load removal.

2.1.2.3 *Elongation*

Defined as the amount of deformation sustained by the material in the plastic regime until its complete fracture.

2.2 MACHINE LEARNING

Over the past decades, machine learning (ML) has witnessed significant progress, with advancements in sophisticated learning algorithms and efficient pre-processing techniques. A notable development has been the evolution of ANNs into deep learning (DL) architectures, demonstrating superhuman performance in specific applications. Despite these benefits, challenges persist in implementing analytical models in natural business settings, including choosing suitable implementation options, addressing data bias and drift, mitigating black-box properties, and reusing preconfigured models (JANIESCH; ZSCHECH; HEINRICH, 2021). ML's applicability, particularly in tasks related to high-dimensional data like classification, regression, and clustering, has led to success in various domains, including fraud detection, credit scoring, speech and image recognition, and natural language processing (NLP) (SHINDE; SHAH, 2018).

Considering the presented problem and the available data, we can distinguish three types of machine learning: supervised learning, unsupervised learning, and reinforcement learning (JANIESCH; ZSCHECH; HEINRICH, 2021). However, in this work, we will focus on supervised learning.

2.2.1 SUPERVISED LEARNING

Supervised learning stands out in the field of data science for its remarkable effectiveness in addressing a wide range of tasks. Its popularity is grounded in the method's ability to make accurate predictions based on properly labeled datasets, placing it in a prominent position as the most common and widely publicized form of machine learning (LECUN; BENGIO; HINTON, 2015).

In supervised learning, the utilized data is referred to as "labeled," indicating that it contains examples of both inputs (referred to as features) and correct outputs (labels). Algorithms analyze an extensive set of these training pairs to infer what the desired output value would be when making predictions on new datasets. This method excels in its ability to adapt to patterns in the training data, enabling the model to generalize and make accurate predictions on unseen data (HASTIE et al., 2009).

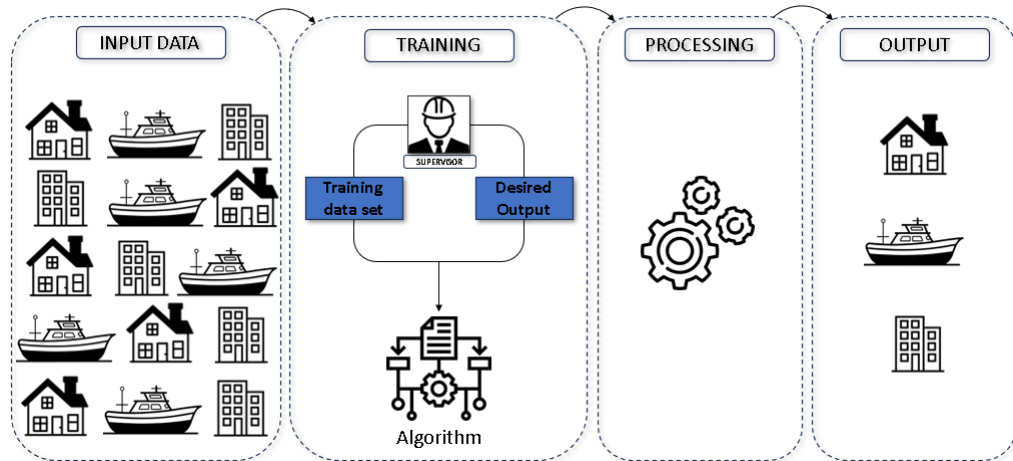


Figure 3 – General supervised learning scheme. Source: Own authorship

The learning process can be segmented into several stages, as illustrated in Figure 3. In the initial phase, depicted in the first frame, we encounter the input data. This stage encompasses the collection, cleaning, and preprocessing of the data, which are all essential steps since the quality of the data has a total impact on the final model generated and its effectiveness. Subsequently, the two phases of the learning process are training and testing.

During the training process, samples from the training data serve as input, where the learning algorithm or learner comprehends and assimilates features to construct the learning model. In the testing phase, the learning model utilizes the execution engine to make predictions for test or production data (LIU; LIU, 2011). The outcome of this process is labeled data, providing the final prediction or classified data.

2.2.2 ARTIFICIAL NEURAL NETWORKS

ANNs draw inspiration from the intricate structure of biological neural networks. The fundamental concept involves extracting linear combinations of inputs to derive characteristics, which are then modeled as a non-linear function of these derived features (HASTIE et al., 2009). This approach results in a highly potent learning method, demonstrating versatile applications across various domains, both complex and non-complex.

A neuron, referred to as a unit, functions as depicted in Figure 4a. It receives inputs from various other units or external sources, each input (x_n) being associated with a weight value (W_n) for that connection. The neuron computes the sum of the linear combination between these weights and inputs. This combined value then undergoes evaluation through an activation function, determining whether the neuron is activated and passes information or remains inactive. As the complexity of the problem increases, addressing non-linear data becomes crucial. Consequently, more artificial neuron units are required, giving rise to an artificial neuron network, as shown in Figure 4b. The organization of the neurons and their communication can vary across different types of ANN architectures (FURTADO, 2019). However, the most well-known

topology used in this work is the Multilayer Perceptron (MLP), also recognized as a feed-forward ANN.

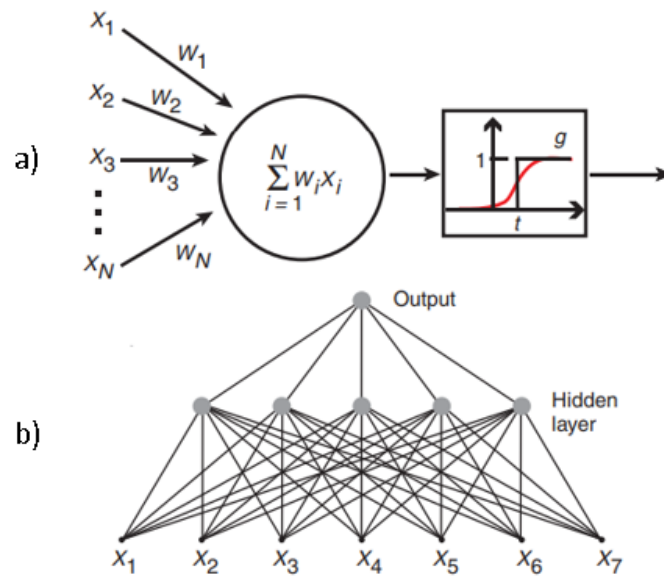


Figure 4 – Representation of a) neuron and b) neural network. Source: Adapted from Krogh (2008)

This structure comprises three types of layers: the input layer, the hidden layer(s), and the output layer. These layers are fully connected, meaning that each neuron in a layer is linked to every neuron in the subsequent layer (KROGH, 2008).

This way, these structures can be used to capture complex patterns and relationships between input and output using a large amount of data. However, they are also susceptible to problems such as overfitting and learning instability, which can result in a low generalization capacity and model accuracy (ZHANG et al., 2021).

2.2.2.1 NEURAL NETWORK PARAMETERS

ANNs are composed of multiple layers of interconnected artificial neurons, where their effectiveness highly depends on the proper selection of model parameters, such as the number of layers, the number of neurons per layer, and activation functions (ABIODUN et al., 2018). Some of the main parameters are discussed below:

2.2.2.1.1 NUMBER OF LAYERS AND NEURONS

The choice of the number of layers and the number of neurons in a neural network plays a crucial role, as increasing these values results in a greater capacity for information transfer within the network, enabling the modeling of increasingly complex problems. However, while it is possible to increase the size of the network to enhance accuracy, this increase inevitably leads to greater model complexity and, consequently, an increase in the time required for training (UZAIR; JAMIL, 2020).

Given that various factors contribute to the overall complexity of the problem, such as the intricate nature of the data and the size of the database, there is no predefined formula or method for determining these parameters. The proper definition of these aspects is subject to practical testing and the developer's experience, who must carefully consider the specific context of the problem at hand.

2.2.2.1.2 DROPOUT

The term refers to a technique where units within an RNA are deleted. When a unit is dropped out, it is temporarily removed from the network, along with all its input and output connections, and the selection of units for exclusion is done randomly. This dropout mechanism introduces noise into the training process, compelling nodes within a layer to probabilistically take on varying levels of responsibility for the inputs (SRIVASTAVA et al., 2014). This conceptualization implies that dropout might disrupt scenarios in which network layers co-adapt to rectify errors from preceding layers, thereby enhancing the model's robustness and reducing the risk of overfitting in ANNs.

2.2.2.1.3 ACTIVATION FUNCTION

The resulting value from the linear combination of all artificial neurons in the network, excluding the input ones, is necessarily subjected to the activation function. This function aims to constrain the neuron's output to a value within a reasonable range. By introducing non-linearity to the generated signal, the activation function plays a crucial role, as without it, the Artificial Neural Network (ANN) becomes a linear regression model (SHARMA; SHARMA; ATHAIYA, 2017). Therefore, the activation function is fundamental to the model learning process.

2.2.2.1.4 OPTIMIZER

The optimizer in neural networks plays a crucial role in the model training process, being essential for enhancing the accuracy and efficiency of the network. It operates by adjusting the weights and biases of the neural network to minimize the loss function, which quantifies the discrepancy between the predicted outputs of the network and the desired values (DESAI, 2020). The optimizer works iteratively to reduce this discrepancy progressively. This continuous adjustment continues until the model reaches a state where the loss function is minimized or reaches a satisfactorily low level.

Numerous optimizers are at one's disposal, each characterized by its unique features and tailored for diverse problem types and neural network architectures. The selection of an optimizer typically involves a blend of theoretical assessments regarding the algorithm, considerations related to the specific problem's characteristics, and practical experimentation.

2.2.2.2 NEURAL ARCHITECTURE SEARCH

The ability of deep learning methods to automatically extract features from unstructured data makes them very successful in solving machine translation tasks, such as image and speech recognition (WISTUBA; RAWAT; PEDAPATI, 2019). Currently, we are witnessing a transformation in the way we design network architectures for deep learning, moving away from the traditional method of manual design. Despite the significance of modifications and testing in models, this process becomes time-consuming, and effectiveness is closely tied to the experience of the responsible developer (REN et al., 2021).

Neural Architecture Search (NAS) aims to design a neural architecture that achieves the best possible performance using limited computer resources and minimal human intervention in an automated way (ELSKEN; METZEN; HUTTER, 2019). As shown in Figure 5, we can conceptualize NAS through three distinct stages: the "Search Space," which defines the architectures that can be represented in principle; the "Search Strategy," which explains how to explore the "Search Space"; and the "Performance Estimation Strategy," where we aim to estimate the process performance.

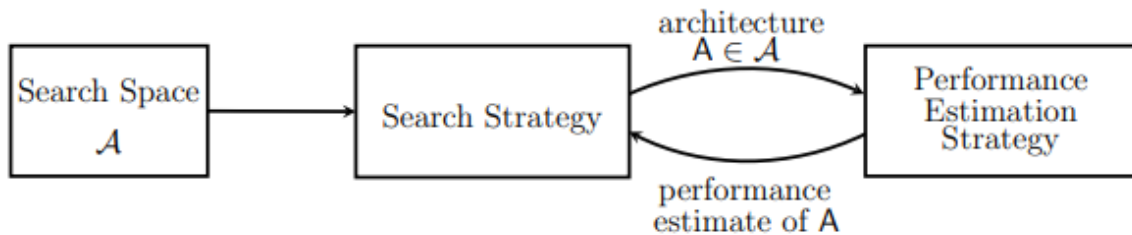


Figure 5 – Abstract illustration of Neural Architecture Search methods. Source: (ELSKEN; METZEN; HUTTER, 2019)

The exploration of new NAS types and their applications has garnered significant attention from researchers. Various search strategies are employed to empower these applications and navigate the neural architecture space. For instance, reinforcement learning, as demonstrated in (ZOPH; LE, 2017), has achieved competitive performance on benchmarks like CIFAR-10 and Penn Treebank, making it a focal point in machine learning research. Bayesian optimization, showcased in (DOMHAN; SPRINGENBERG; HUTTER, 2015), has enhanced performance on the CIFAR-10 benchmark without data augmentation. Additionally, EAs, as demonstrated in (WANG et al., 2019) who propose a hybrid PSO-GA method, in this approach, PSO guides the evolution of parameters, while GA directs the evolution of connections.

For the present study, the open-source NAS framework Auto-Keras (JIN; SONG; HU, 2019) was employed, utilizing Bayesian optimization to navigate the search space while preserving network morphism. This entails maintaining the functionality of a network while altering its neural architecture.

2.2.3 ENSEMBLE MODELS

Ensemble techniques are designed to enhance the performance of machine learning models by amalgamating multiple individual models to produce a unified result. Typically, these models undergo independent training before being amalgamated to yield the outcome. When consolidating the results of a number of ANNs into a singular value, the initial step involves identifying the nature of the problem. For classification tasks, a prevalent technique involves adhering to the majority of results, whereas, for regression, the commonly employed approach is to calculate the arithmetic mean of the results (KROGH; VEDELSBY, 1994).

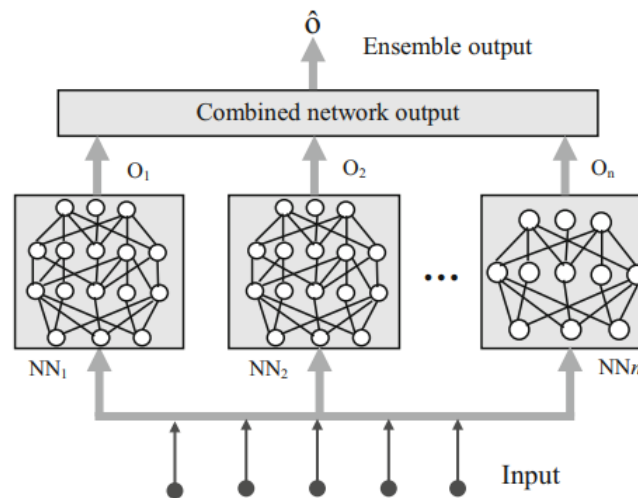


Figure 6 – Representation of an ensemble of artificial neural networks. Source: (ALAM; SIDDIQUE; ADELI, 2020a)

Combining several ANNs, as in the example shown in Figure 6, can be advantageous for the final model. Each ANN has its own parameters, structures, or data sets and, therefore, its way of generalizing patterns in relation to the database (REN; ZHANG; SUGANTHAN, 2016). The techniques used to develop these ANNs are strategically designed to give the resulting models a broad spectrum of diversity.

Consequently, individual ANNs, each with its specific traits, may manifest more pronounced errors in some areas of the input space (HANSEN; SALAMON, 1990). Through the formation of an ensemble, these errors can be harmonized, leveraging the information embedded in each ANN to generate an averaged response. This approach leads to heightened accuracy and an overall improvement in model performance.

2.3 MULTI-OBJECTIVE OPTIMIZATION

As stated by Deb e Kalyanmoy (2001), optimization consists of obtaining one or more feasible solutions that correspond to extreme values of one or more objectives. This task requires a systematic exploration of available feasible solutions, wherein a continuous comparison is conducted until reaching a point where no superior solution can be identified. This iterative

nature of the optimization process allows the identification of optimal configurations that meet the defined objectives.

A distinction arises based on the number of objective functions within a given problem. When a model representing a physical system includes only one objective function, the pursuit of discovering the optimal solution is referred to as single-objective optimization. On the other hand, when an optimization problem encompasses multiple objective functions, the challenge shifts to identifying one or more optimal solutions, classifying the endeavor as multi-objective optimization (PEREIRA et al., 2022). In this scenario, where several objective functions are optimized simultaneously, there is a need to involve many criteria to reach the final decision-making on solutions.

Mathematically, the formulation of a multi-objective optimization problem follows Equation 1, with the objective of minimizing the defined criteria. Represented by a solution vector X within the feasible search/design space, for the n decision variables as $\mathbf{X} = (x_1, x_2, \dots, x_n)$, each decision variable x_i is bound by constraints within lower (x_i^L) and upper (x_i^U) bounds. These bounds collectively form the set of variable bounds. Consequently, the feasible set solution $\mathbf{F}(x) = [f_1(x)f_2(x)\cdots f_m(x)]^T$ is derived by evaluating all objective functions f for a given solution $x \in \mathbf{X}$. The objective functions denoted as $f : \mathbf{X} \rightarrow \mathbb{R}^m$, where m defines the number of optimization objectives, collectively define the feasible set and contribute to the overall optimization process.

$$\begin{aligned} \min \mathbf{F}(x) &= [f_1(x)f_2(x)\cdots f_m(x)]^T \\ x_i^L &\leq x_i \leq x_i^U, i = 1, 2, \dots, n \end{aligned} \tag{1}$$

2.3.0.1 DOMINANCE AND PARETO OPTIMALITY

For many multi-objective optimization problems, the objectives cannot be optimized simultaneously; in other words, they are competitive. Unlike single-objective optimizations where a direct comparison among the solution set can be made to determine the best solution, in the multi-objective case, solutions can be considered Pareto optimal if none of the objective functions can be improved without deteriorating another objective value (DEB; KALYANMOY, 2001).

Since the majority of multi-objective optimization algorithms leverage this concept, it becomes imperative to formalize specific definitions of Pareto optimality, as outlined by Deb e Kalyanmoy (2001).

Definition 1 (Dominance relations). Given two decision vectors x and x' in \mathbf{X} ,

- $x \preceq x'$ (x weakly dominates x') if and only if $\mathbf{F}(x) \leq \mathbf{F}(x')$
- $x \prec x'$ (x dominates x') if and only if $x \preceq x'$ and at least one component of $\mathbf{F}(x)$ is strictly less than the corresponding one of $\mathbf{F}(x')$

- $x \prec x'$ (x strictly dominates x') if and only if $\mathbf{F}(x) < \mathbf{F}(x')$.
- $x \parallel x'$ (x and x' are incomparable) if neither x weakly dominates x' nor x' weakly dominates x .

Definition 2 (Pareto optimality and Pareto solutions). The vector $x \in \mathbf{X}$ is a Pareto optimal solution if there is no other vector in \mathbf{X} that dominates it. The set of Pareto optimal solutions is called the Pareto set, denoted \mathcal{X}_P , and the image of the Pareto set is called the Pareto front, denoted \mathcal{F}_P .

Definition 3 (Pareto set approximation). A set of vectors A in the decision space is called a Pareto set approximation if no element of this set is dominated by any other. The image of such a set in the objective space is called a Pareto front approximation.

Definition 4 (Ideal point). The ideal point $F^I = (f_1^I, f_2^I, \dots, f_M^I)$ is the vector composed with the best objective values over the search space.

As illustrated in Figure 7, consider a scenario where a candidate solution A exhibits superior performance across all optimized objectives compared to another candidate solution C. In this case, it is stated that A dominates C, similar to the relationship between B and C, where B dominates C. However, if A outperforms candidate solution B in certain objectives but performs worse in others, both solutions can be deemed optimal within a Pareto set, as long as neither of them is dominated by any other solution in the set.

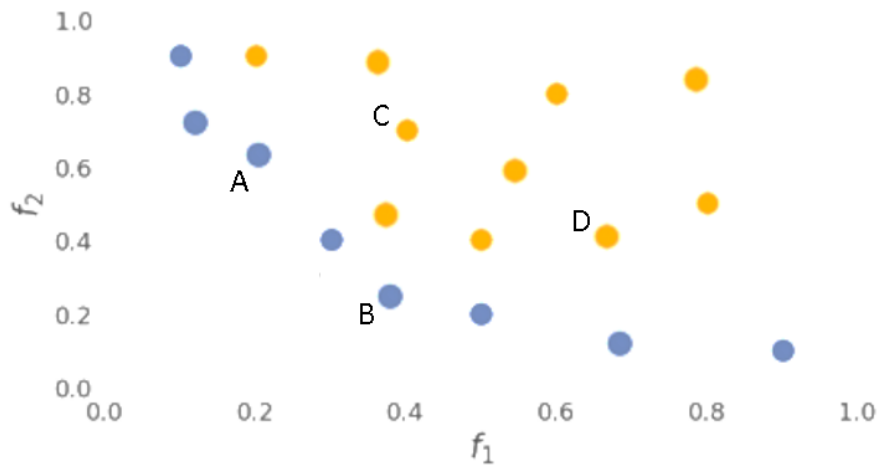


Figure 7 – Pareto front with two objectives, being f_1 and f_2 . Non-dominated points are in blue, and dominated points are in orange. A and B are Pareto optimal solutions that dominate C and D. Source: Inspired by (SGROTT, 2022)

2.3.1 EVOLUTIONARY ALGORITHMS AND MULTI-OBJECTIVE EVOLUTIONARY ALGORITHMS

Evolutionary computing is a branch of computer science research inspired by the mechanisms of natural evolution. This inspiration stems from the observable prowess of evolution in nature, where a diverse array of animal species has adapted to thrive in specific environments

(EIBEN; SMITH, 2015). Evolutionary algorithms (EAs) constitute a subset of evolutionary computing and fall within the broader category of stochastic search algorithms. In optimization, these algorithms simulate solutions within an environment, subjecting them to an evolutionary process governed by the specified constraints integrated into the simulation (KRAMER, 2017).

Evolutionary algorithms (EAs) offer a versatile and powerful approach to solving complex optimization problems. One of their main advantages lies in their ability to explore vast solution spaces, especially in cases where traditional methods may struggle, either due to the immense search space dimensions or the complexity of the objective function. In problems requiring global optimization, where finding the optimal solution is particularly challenging, evolutionary algorithms shine by efficiently navigating through diverse solution landscapes to identify optimal or near-optimal solutions (EIBEN; SMITH, 2015).

There are several types of EAs, each of which can be used for different types of challenges. According to Vikhar (2016), the main algorithms are Genetic Algorithms (GAs), Genetic Programming (GP), Evolution strategy (ES), and Evolutionary Programming (EP).

While various EAs are available, the choice in this study leans towards employing a GA due to its apt alignment with the distinctive characteristics of the problem at hand. The GAs efficiency influences the decision in addressing challenges associated with vast, ambiguously defined, and potentially non-linear search spaces, needing compelling exploration, coupled with its ability to handle problems lacking complete analytical equations for a comprehensive solution and the inherent ease of parallelization (BINITHA; SATHYA, 2012).

2.3.1.1 GENETIC ALGORITHM

Genetic Algorithms (GAs) stand out as the most well-known and widely utilized EA in the realm of optimization problems. Originating in the 1960s and 1970s, GAs were initially crafted by John Henry Holland and his students (HOLLAND, 1973). These algorithms are designed as search and optimization procedures, drawing inspiration from the principles underlying natural genetics and the process of natural selection. By artificially incorporating key concepts from genetics, GAs are adeptly engineered to construct resilient search algorithms (DEB; KALYANMOY, 2001).

At their core, GAs consist of a set of individuals called population that represent potential solutions to the problem at hand. These individuals are called chromosomes or genotypes, and each parameter within the genotype is referred to as a gene (MITCHELL, 1998). From this point on, several operations involving stochastic components are applied, making the process based on probabilistic criteria, with the aim of promoting the evolution of the population of individuals (LAMBORA; GUPTA; CHOPRA, 2019).

The success of a Genetic Algorithm (GA) hinges on choosing the correct encoding for its candidate solutions. The encoding works as the language the GA can understand; it maps the problem's parameters onto the chromosomes, ensuring the GA searches for solutions relevant to the problem at hand (CHAHAR; KATOCH; CHAUHAN, 2021). Beyond suitable

encoding, another critical element in a GA's success is the fitness function, as it guides the search towards optimal solutions within the problem's landscape. This function evaluates each candidate solution, assigning a score based on how well it aligns with the desired outcome.

The main GAs procedures are described below:

1. **Initialization:** Creates an initial population of individuals. These individuals can be generated randomly, covering the entire search space. However, a more efficient approach involves leveraging domain knowledge. By incorporating prior knowledge about the problem, the algorithm can generate feasible solutions more readily, leading to faster convergence and reduced computational time (TODOROVSKI; RAJICIC, 2006).
2. **Selection:** At each generation, GA carefully chooses individuals for reproduction, mimicking the concept of natural selection. This fitness-based process prioritizes solutions with higher performance (fitness), gradually leading to population improvement across generations (LAMBORA; GUPTA; CHOPRA, 2019). This mechanism is the core driver of GA's evolutionary power.
3. **Crossover:** After selecting promising individuals, the GA enters the recombination phase, where it mimics biological reproduction. Here, a crossover operator pairs chromosomes from different parents, exchanging genetic material to create new offspring. These offspring inherit characteristics from both parents, forming a diverse next generation. Numerous crossover operators, specialized for various applications and problem domains, have been developed over the years. Each operator has its strengths and weaknesses, affecting the effectiveness of the entire optimization process (UMBARKAR; SHETH, 2015).
4. **Mutation:** After creating fresh offspring through crossover, the GA introduces the mutation operator, which mimics random mutations in living organisms that introduce novel traits. Here, the mutation operator randomly alters individual genes within each chromosome, potentially injecting the population with entirely new genetic structures (KRAMER, 2017). This act of "throwing the dice" helps explore unseen areas of the search space, ensuring a broader spectrum of potential solutions.
5. **Evaluation and Iteration:** Each candidate solution in the new generation undergoes evaluation through a fitness function. If a pre-defined termination condition is met (e.g., maximum number of generations reached, desired solution quality achieved, or time limit exceeded), the GA halts. Otherwise, the cycle repeats, iterating through steps 2-5 again to create even better solutions.

2.3.1.2 *NONDOMINATED SORTING GENETIC ALGORITHM (NSGA)*

NSGA-II (Non-dominated Sorting Genetic Algorithm II) and NSGA-III (Non-dominated Sorting Genetic Algorithm III) are MOEAs widely used to solve optimization problems with

multiple conflicting objectives (ZHOU et al., 2011). Both algorithms rely on non-dominated solution selection and population diversity to find a set of Pareto-optimal solutions.

NSGA-II, introduced by Deb et al. (2002), is recognized for its simplicity and effectiveness. It employs a non-dominated sorting technique to rank solutions and a crowding distance operator to maintain diversity within the population. The combination of these two features allows NSGA-II to explore and exploit the solution space efficiently, preventing premature convergence to suboptimal solutions.

On the other hand, NSGA-III, which was developed later, enhances NSGA-II by introducing more sophisticated mechanisms to handle optimization problems with a more significant number of objectives. NSGA-III uses a reference point-based approach that guides the selection of solutions towards less explored regions of the objective space. This method is beneficial for problems with more than three objectives, where simple non-dominated sorting and diversity maintenance become insufficient (DEB; JAIN, 2013).

According to Deb et al. (2002), some of the main features of NSGA-II are as follows:

- NSGA-II employs non-dominated sorting to rank solutions in the population, ensuring a clear hierarchy based on Pareto dominance.
- Parent selection is conducted through a binary tournament that considers both dominance rank and crowding distance, promoting a balance between quality and diversity.
- Elitism is incorporated to preserve the best solutions from the previous generation, enhancing the algorithm's ability to retain high-quality solutions over iterations.

According to Deb e Jain (2013), some of the main features of NSGA-III are as follows:

- NSGA-III utilizes a set of reference points to guide the search for Pareto-optimal solutions, which is particularly effective in high-dimensional objective spaces.
- Parent selection involves a process that considers both non-dominated sorting and the distance to the nearest reference point, ensuring a well-distributed selection of solutions.
- Environmental selection employs a niching mechanism to maintain population diversity, preventing premature convergence and promoting a comprehensive exploration of the objective space.

2.3.1.3 REFERENCE VECTOR GUIDED EVOLUTIONARY ALGORITHM (RVEA)

The RVEA excels at tackling complex optimization problems with multiple objectives (three or more), known as many-objective optimization. Compared to traditional multi-objective evolutionary algorithms (MOEAs), it employs a distinct approach to selecting individuals for reproduction, making it particularly effective in maintaining diversity in high-dimensional spaces. Standard MOEAs often struggle with this crucial aspect when dealing with numerous objectives.

Their reliance on dominance-based selection alone can lose "pressure" in complex situations, leading to premature convergence and suboptimal solutions (DEB; JAIN, 2014).

RVEA breaks free from this limitation by adopting a selection mechanism guided by reference vectors. These vectors, strategically positioned throughout the objective space, serve as navigational markers for the search procedure, effectively segmenting the entire objective space into more tractable subspaces. Consequently, the original multi-objective optimization problem (MOP) is subdivided into several subproblems, each retaining its multi-objective nature. Individuals that closely align with their designated reference vectors while maintaining substantial diversity among themselves are given precedence in the reproduction process (QIU et al., 2021).

RVEA's main features highlighted by Cheng et al. (2016):

- **Reference Vector Guidance:** RVEA utilizes a set of reference points (vectors) distributed across the objective space. These vectors guide the search towards diverse regions of the Pareto front.
- **Angle-Penalized Distance:** Instead of directly measuring dominance, RVEA calculates the angle-penalized distance between each solution and its closest reference vector. Solutions closer to the vectors (with smaller angles) and diverse among themselves are preferred.
- **Adaptive Reference Vectors:** RVEA dynamically updates the reference vectors during the optimization process. This ensures they adapt to the evolving population and guide the search towards previously unexplored regions.
- **Elitism Mechanism:** RVEA employs an elitism strategy to preserve high-quality solutions across generations. This helps maintain progress and prevents the loss of optimal solutions due to randomness.

2.3.1.4 ADAPTIVE GEOMETRY ESTIMATION BASED MULTI-OBJECTIVE EVOLUTIONARY ALGORITHM (AGE-MOEA)

The AGE-MOEA is a multi-objective optimization algorithm inspired by NSGA-II but with critical modifications that enhance its performance. The core difference lies in its crowding distance formula, which is adapted to consider the specific geometry of the Pareto front (PANICHELLA, 2019). This allows AGE-MOEA to maintain a diverse population that is better suited to the problem at hand.

The critical feature of AGE-MOEA is its ability to estimate the geometry of the Pareto front throughout iterations. By utilizing this information, it is possible to calculate the crowding distance more accurately and distribute solutions better, avoiding clustering. This allows the algorithm to identify and preserve promising solutions in complex regions of the Pareto front, especially in problems with many objectives, where the shape of the front can be irregular and contain niches (BENALI et al., 2022).

According to Panichella (2019), some of the main points of AGE-MOEA that help in its ability to work with problems with many objectives are shown below:

1. **Probability Distribution Estimation:** AGE-MOEA leverages estimations of the underlying probability distributions to dynamically adjust mutation and crossover rates. This allows the algorithm to balance exploration and exploitation more effectively throughout the optimization process.
2. **Adaptive Environmental Selection:** The algorithm employs an adaptive environmental selection scheme that simultaneously considers both population diversity and solution quality. This ensures the population maintains a healthy balance between finding diverse solutions and converging towards optimal ones.
3. **Hierarchical Architecture:** AGE-MOEA can be implemented with a hierarchical architecture, making it suitable for tackling complex optimization problems with a large number of variables. This hierarchical structure allows the algorithm to decompose the problem into smaller sub-problems, facilitating the search for optimal solutions.

2.3.1.5 EA PARAMETER CONTROL

In EA, parameter tuning plays a crucial role, as it can significantly influence the algorithm's behavior and its ability to search for promising regions in the problem's solution space. When considering parameter adjustment, two distinct categories can be applied: offline and online tuning. In the offline category, parameters are chosen before the algorithm's execution. This requires extensive testing, making parameter tuning a complex combinatorial optimization problem in itself (EIBEN; SMIT, 2011).

On the other hand, in the online adjustment category, parameter selection is performed during the algorithm's execution according to specific rules, thereby relieving the user from the responsibility of finding the best parameter combination in advance (PARPINELLI et al., 2019).

The use of online parameter control can lead to improvements in optimization results due to its ability to adjust values dynamically, benefiting both the exploitation and exploration phases of optimization (ALETI; MOSER, 2016). According to Parpinelli et al. (2019), online control techniques can be divided into the following groups:

- **Deterministic:** In this approach, a deterministic rule changes the parameter values. The rule modifies the parameter values without using any information from the fitness function.
- **Adaptive:** This method uses information from the optimization process to adjust the parameter values. Feedback can come from the fitness or objective function itself, measurements of population diversity, or other sources.

- **Aggregated:** Here, the parameters are directly encoded in the solution vector as additional dimensions and are optimized concurrently with the primary optimization process.

2.3.1.6 EA PARALLELIZATION

The parallelization of evolutionary algorithms focuses on the intelligent distribution of tasks among multiple processors, accelerating the search for optimized solutions. This distribution can occur at different levels, from the evaluation of individuals' fitness to the application of genetic operators (ALBA; LUQUE; NESMACHNOW, 2013). The choice of the ideal parallelization model depends on various factors, such as task granularity, hardware architecture, and the characteristics of the problem to be solved.

The primary advantage is the drastic reduction in the time required to find optimized solutions. By distributing tasks among several processors, parallelization allows different parts of the algorithm to be executed simultaneously, significantly decreasing the total processing time (KONFRST, 2004). Additionally, parallelization makes evolutionary algorithms more scalable, enabling them to handle more complex problems and larger datasets efficiently (ALBA; LUQUE; NESMACHNOW, 2013). As demand increases, new processors can be added, expanding the problem-solving capacity without compromising performance.

However, implementing parallelization comes with its own set of challenges. Efficient task distribution requires careful consideration to avoid bottlenecks and ensure balanced workloads across processors. Communication overhead between processors can also impact performance, and synchronization issues may arise, necessitating robust strategies to manage them.

Several models and strategies guide the implementation of parallelization in evolutionary algorithms:

- **Fitness Evaluation Parallelism:** Distributes the evaluation of individuals' fitness across different processors.
- **Selection Parallelism:** Divides the process of selecting individuals for the next generation among multiple processors.
- **Genetic Operators Parallelism:** Distributes the application of genetic operators, such as crossover and mutation, across different processors.

2.3.2 OPTIMIZATION METRICS

Unlike single-objective optimization, where we can assess the quality of solutions based on the best fitness value, multi-objective optimization presents additional challenges. In this context, the goal is to approach the Pareto front, often unknown, evaluating the approximation quality as a multifaceted challenge. Besides the proximity to the actual Pareto front, it is crucial to consider the dispersion of solutions as a quality aspect, aiming to ensure high diversity, reflected by extensive use of the optimization objective space (AUDET et al., 2021).

To streamline the evaluation in multi-objective optimization, similar to the single-objective approach, various performance indicators or metrics have been defined. These parameters aim to measure the quality of the approximation set of the Pareto front, assigning values according to different specific objectives (LI; YAO, 2019).

2.3.2.1 HYPERVOLUME

The hypervolume indicator (HV) quantifies the volume of the objective space enclosed by the Pareto front approximation set S , bounded from above by a reference point $r \in \mathbb{R}^m$, where for all $z \in S$, $z \prec r$, as shown in Figure 8. Mathematically, the hypervolume is expressed by Equation 2.

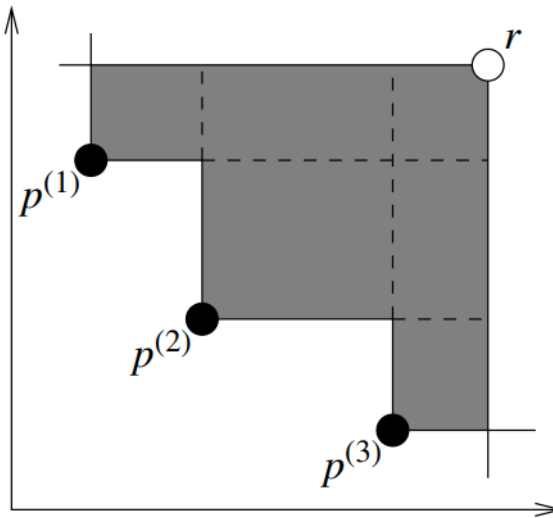


Figure 8 – Representation of the HV for a biobjective problem. Source: (FONSECA; PAQUETE; LÓPEZ-IBÁÑEZ, 2006)

$$HV(S, r) = \lambda_m\left(\bigcup_{z \in S} [z; r]\right) \quad (2)$$

The hypervolume indicator is noteworthy for addressing both the proximity to ideal points and the coverage of the solution space in the Pareto front. Its strict monotonicity implies that if a Pareto front approximation A dominates another approximation B , then $HV(A, r) > HV(B, r)$. This property makes the hypervolume widely used in the evolutionary community for seeking potentially interesting new points or for algorithm comparisons (AUDET et al., 2021).

2.3.2.2 INVERTED GENERATIONAL DISTANCE

The Inverted Generational Distance (IGD) measures the Euclidean distance of each point from a discrete representation of the Pareto front in relation to p points from the approximation set, as defined in Equation 3, where d is the distance between a point from the Pareto front and

the closest point pertaining to the Pareto approximation. Figure 9 shows an illustration of the IGD calculation.

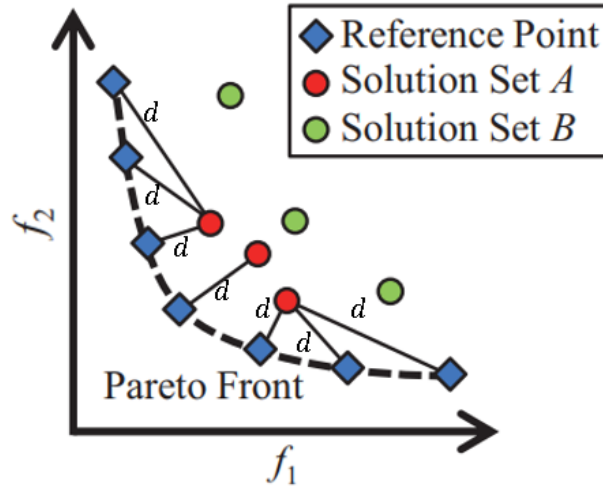


Figure 9 – Representation of the IGD calculation for the solution set A. Source: Inspired by Ishibuchi, Masuda e Nojima (2016)

$$IGD(S, F) = \frac{1}{|F|} \left(\sum_{i=1}^{|F|} d_i^p \right)^{\frac{1}{p}} \quad (3)$$

The accuracy of IGD assessment is heavily reliant on the quality of the reference set approximation to the Pareto front, as different reference sets can bias the indicator towards favoring distinct solution sets. Therefore, opting for a sizable reference set with a high resolution for the Pareto front is advisable, helping to prevent counter-intuitive assessments stemming from insufficient points in the set (AUDET et al., 2021). As a result, a low IGD value is sought, and it should indicate that the set has good combined quality of convergence.

2.3.2.3 GENE FREQUENCY

Addressing the balance between exploration and exploitation is a common challenge in evolutionary algorithms. This equilibrium is crucial as an imbalance between these phases can result in premature convergence or transform the process into a random search. One prevalent strategy to rectify this balance is adjusting optimization parameters. Genotypic diversity assessment, which centers on solution variations, is a crucial aspect of effectively monitoring exploration. Simultaneously, characterizing exploitation more appropriately involves considering phenotypic diversity, which pertains to variations in the obtained fitness values (CORRIVEAU et al., 2012).

Entropy serves as a robust tool in information theory, functioning as a metric that quantifies uncertainty or disorder within a dataset (PIRES; MACHADO; OLIVEIRA, 2014).

Shannon entropy stands out among the various entropy metrics and is widely employed by researchers to measure the extent of information loss within a population. This facilitates the evaluation of the distribution and equilibrium of solutions within the search space.

The Equation 4, presented by (CORRIVEAU et al., 2012), allows us to calculate the Shannon entropy and consequently the gene frequency (GD) within a genetic algorithm population, where n is the population size, u is the individual vector size, and p is a specific gene from the population individual. The higher the entropy, the greater the genotypic diversity, indicating more significant variation in the genes present in the solutions.

$$GF = -\frac{1}{n \cdot \log(u)} \sum_{k=1}^n \sum_{m=1}^u p_{m,k} \cdot \log(p_{m,k}) \quad (4)$$

3 SYSTEMATIC LITERATURE REVIEW

Systematic reviews constitute an approach aimed at assessing and interpreting all relevant research associated with a specific question, topic, or theme (KITCHENHAM; CHARTERS, 2007). In this way, these reviews scrutinize a more restricted set of studies with the intention of delving deeper into the existing knowledge within a specific subject, given their particular objectives.

In this context, this chapter presents a systematic literature review conducted between September and November 2022 and updated in April 2024. The goal is to identify meta-heuristic algorithms employed in the multi-objective optimization of the mechanical properties of steels, namely TS, YS, and EL, while comprehending the intricacies involved in each process.

3.1 RESEARCH METHOD

To develop the review plan, we adopted the methodology described by (KLOCK, 2018). With the aim of providing a comprehensive view of the subject and identifying its characteristics and trends, the following research objective was established:

- Investigate the meta-heuristics employed in optimizing the mechanical properties of steels.

Additionally, the following research questions are proposed to contribute to the understanding and synthesis of the research objective:

1. What data are used as inputs for the optimization algorithm?
2. Which meta-heuristic algorithms are employed in the optimization of steels?
3. What parameters (quantitative or qualitative) are presented to ensure the performance of the optimization?

3.2 PLANNING THE REVIEW

In order to achieve the Objective and address the proposed research questions, the planning phase begins with formulating the search query to be used in Academic Search Engines (ASEs). In this context, the PICO method was adopted, which necessitates defining the elements of Population, Intervention, Comparison, and Outcomes based on the research questions. For each component of this process, the selected terms were delineated as follows:

- Population: *Steel*
- Intervention: *Genetic Algorithm, Particle Swarm*

- Outcomes: *Elongation, Tensile strength, Yield*

In this way, it was possible to formulate the search query considering terms derived from the PICO method, along with variations commonly employed in the field of meta-heuristics. We chose to use nine distinct keywords, requiring only eight logical operators to compose the search query. This made it compatible with all selected Academic Search Engines (ASEs). Thus, the decision was made to focus the research exclusively on genetic algorithms and particle swarm optimization, excluding other less common meta-heuristics and their variations from the search process. The search query was entered into the search fields, including Abstract and Title, when available. Finally, the formulation of the search query was established as follows:

- *steel AND optimization AND (genetic algorithm OR GA OR "Particle swarm" OR PSO) AND (elongation OR "tensile strength" OR yield)*

Due to the interdisciplinary nature of the topic, we chose to select relevant Academic Search Engines (ASEs) in engineering and computer science. The chosen ones include Digital Library (ACM DL), IEEEExplore, Science Direct, Scopus, Web of Science, and CAPES Catalog of Theses and Dissertations for a more specific look at theses and dissertations.

3.3 CONDUCTING THE REVIEW

After selecting the ASEs and formulating the search query, the subsequent step involves defining objective criteria, inclusion criteria, and exclusion criteria that will be used to determine which studies will be considered in the review. The criteria were applied in the sequence of objectives and exclusion. Below, these criteria are presented:

- Objective Criteria
 - Year Range: 2010 - 2024
 - Document Type: Articles, dissertation, and thesis
 - Language: English
 - Availability: Open Access
 - Size: Full or Short
- Exclusion Criteria
 - Exclude studies not utilizing meta-heuristic algorithms for optimizations
 - Exclude studies optimizing only non-mechanical properties of steels
 - Exclude studies optimizing non-metallic materials
 - Exclude studies optimizing steels in practical engineering contexts, such as welding and load-bearing support structures.

The article selection process was carried out by two assessors, with each being responsible for reviewing all chosen articles from the ASEs. In cases where there was disagreement regarding the acceptance of articles, a third assessor was consulted to resolve the conflict.

In addition to the selection criteria, quality criteria were established to evaluate the chosen articles. These criteria are outlined below:

- Quality Criteria

- The article presents the multi-objective optimizer used.
- The article presents the input variables for the optimizer.

Thus, for articles to be selected, they must meet both criteria, and the evaluation is conducted by both assessors, with each being responsible for examining the filtered articles from the ASEs. In cases of disagreement, a third assessor is involved in resolving the conflict.

The number of articles chosen from each ASE is illustrated in Table 1. The first column represents the number of articles retrieved using only the search query. The second column indicates the number of articles after the application of selection criteria. Finally, the third column highlights the number of articles selected for a more in-depth analysis after the application of quality criteria.

Table 1 – Table referring to the number of studies found, filtered, and selected in the search.

| ASE | Found | Filtered | Selected |
|----------------|--------------|-----------------|-----------------|
| CAPES | 15 | 1 | 1 |
| ACM DL | 193 | 0 | 0 |
| IEEEExplore | 15 | 4 | 0 |
| Science Direct | 48 | 3 | 2 |
| Scopus | 149 | 6 | 4 |
| Web of Science | 286 | 8 | 5 |

In the data collection process, the selected studies are divided into two groups, with each assessor tasked with gathering the information. Subsequently, the assessors cross-verify the data collected by each other. The collected information from the selected works includes:

- Optimization variables
- Optimization algorithm used to model the problem
- Presence of qualitative analysis
- Presence of quantitative analysis

3.4 DISCUSSIONS

From the selected studies, Table 2 is generated, containing a summary of the collected information that will be discussed in the following sections. The values presented in the input variables represent the respective numbers found for each element in each study.

3.4.1 INPUT VARIABLES FOR OPTIMIZATION

Based on the data in Table 2, it is noted that the chemical composition and process parameters are of great relevance when modeling the optimization of steel. This makes sense as they define which elements will be present in the steel and how its microstructure will be formed. In the case of chemical composition, even when it is not considered as an input for the optimizer, as in the cases of Resendiz-Flores et al. (2021) and Kumar, Chakrabarti e Chakraborti (2012), its values are essential constants in the system.

Although the use of chemical composition and process parameters is every day in studies, for each case, different elements may be considered, varying according to the optimization objective, required properties, and the steel manufacturing process. For instance, Mohanty, Bhattacharjee e Datta (2011) considers a cold rolling process, and Wu et al. (2017) focuses on hot rolling.

Different variables can be used to express the formation of steels in Kumar, Chakrabarti e Chakraborti (2012); for example, the grain size of the microstructure is used as an input variable, however even though it is efficient because it is a variable that relates directly to the properties of the steel, it is not so common to use because it involves metallographic analysis of each sample, which can become very costly.

In industrial-focused studies, dimensional information is typically included as input variables, as seen in Song et al. (2020) and Wu et al. (2017). For the final application, it is crucial to know the thickness and width of the sheet, as these factors significantly affect the strength, manufacturability, and stiffness, which are essential aspects to consider.

Furthermore, as the model becomes more generalized without specificity for a particular type of steel, the chemical composition and its settings become even more critical in the process, incorporating a more significant number of elements into the model. In this regard, Sgrott (2022) generalizes five types of steel, and as the study is focused on the production line of a company, the number of process parameters and chemical elements increases since the objective is to understand the specific characteristics of that production line and subsequently the development of new steels.

3.4.2 META-HEURISTIC ALGORITHMS

Optimization algorithms are used to generate new possible steel configurations with the desired properties, reducing the use of alloying elements. From the studies presented in Table 2, all authors use regression techniques to predict the desired properties as fitness functions for

meta-heuristic algorithms. In Lee et al. (2021) study, a test and comparison of 16 regression models are performed, followed by optimization with these prediction models.

Various types of algorithms were used in the selected studies. The Non-dominated Sorting Genetic Algorithm II (NSGA-II) is the most commonly used algorithm among the selected works. In other cases, the Non-dominated Sorting Genetic Algorithm III (NSGA-III), Predator-Prey Genetic Algorithm (PPGA), and Strength Pareto Evolutionary Algorithm II (SPEA2) were utilized to optimize tensile strength, yield strength, and elongation in Liu et al. (2023), Kumar, Chakrabarti e Chakraborti (2012), and Wu et al. (2017), respectively. Gurav, Patil e Solanki (2018) employed the Enhanced Parallel Cat Swarm Optimizer (EPCSO) to optimize yield strength and tensile strength. An Improved Particle Swarm Optimizer (PSO) was used in Song et al. (2020) to optimize tensile strength and plasticity. Lastly, a Multi-Objective Particle Swarm Optimization (MOPSO) was used in Shah et al. (2017) to optimize tensile strength and elongation.

3.4.3 QUANTITATIVE ANALYSIS

In numerous studies, qualitative performance analyses often prioritize the regressor, which predicts properties, over the optimization process itself. Song et al. (2020) transforms a multi-objective Particle Swarm Optimization (PSO) into a single-objective PSO by employing linear and non-linear inertial weights to balance exploration and exploitation abilities. The convergence speed for each inertial weight is meticulously measured.

Meanwhile, Kumar, Chakrabarti e Chakraborti (2012) compares the best compositions discovered with experimental and traditional steels from the literature to assess similarities and improvements in proposed designs. Similarly, Liu et al. (2023) adopts this approach but solely compares final property values. Additionally, Resendiz-Flores et al. (2021) validate the optimizer's results through experimental tests with three configurations, where the maximum observed error in optimized properties is 9.9%. This validation process is facilitated by maintaining a constant chemical composition of the alloy, with only variations in heat treatment parameters.

Furthermore, Sgrott (2022) conducts a series of study cases with NSGA-II, stressing and testing the Multi-Objective Evolutionary Algorithm (MOEA) with industrial parameters. They obtain performance metric values such as HV and IGD and apply an online control technique for mutation and recombination parameters, improving convergence and diversity in results, as evidenced by IGD and Diversity Comparator Indicator (DCI) metrics when compared to fixed parameter values.

3.4.4 QUALITATIVE ANALYSIS

Qualitative analyses can be used to underpin the optimization algorithm's results and performance, comparing them with theoretical and practical foundations. This is crucial for a practical understanding of the algorithms' limitations, enabling cross-referencing between different models, empirical observations, physical laws, etc.

Authors such as Mohanty, Bhattacharjee e Datta (2011), Dutta et al. (2019), Kumar, Chakrabarti e Chakraborti (2012), and Song et al. (2020) conduct qualitative analyses, showcasing the Pareto frontier resulting from optimization. Similarly, Shah et al. (2017) follows a similar process, albeit comparing results from various regression models. While practically beneficial, these analyses offer limited insight into explaining or quantifying the optimizer's performance, especially since the true Pareto frontier remains to be discovered, except for cases where comparing optimizers or regression models is pertinent.

In contrast, Lee et al. (2021) surpasses merely presenting non-dominated points of the Pareto frontier by also incorporating dominated points resulting from optimization, employing a range of regression models.

Furthermore, Lee et al. (2021) depicts properties within the solution space, contrasting the diverse types of regressor models utilized in the study. Meanwhile, Wang et al. (2020) illustrates the degrees of correlation between the original composition and the optimized compositions with the best property values. Additionally, Wu et al. (2017), after refining the database, scrutinizes fluctuations in optimized properties in the conventional hot rolling process compared to the optimized process.

In another vein, Sgrott (2022) conducts optimizations based on a reference steel. The outcomes delineate properties within the solution space achieved and the distributions of values obtained for each feature, showcasing the divergence observed in the optimizations.

3.4.5 CONSIDERATIONS

Through the literature review, it becomes apparent that given the complexity of steel alloy development, each project must be analyzed as a unique case, considering the desired properties and defining the chemical elements to be included in the model. Each steel grade has its characteristics and, therefore, will be better suited to different parameters. Additionally, the manufacturing process, along with machinery limitations, must be considered to define the variable ranges, requiring knowledge of metallurgical principles to guide the process and result in feasible composition values.

Among all optimization algorithms, NSGA-II stands out as the most widely used among authors. Moreover, the everyday use of artificial neural networks or other regression methods for modeling mechanical properties is observed. These models are subsequently employed as fitness functions within the optimization algorithm. However, the consolidation of the database for model training is crucial. This requirement is necessary to assess the quality of the optimizer's responses and make meaningful comparisons between them.

Considering the convergence analyses related to the optimization algorithm, the authors have primarily focused on the quality of the property prediction model. Only some studies use quality metrics to ensure the diversity or performance of the solutions found. This choice may be justified by the fact that each study has its desired property values. As the optimizer successfully finds these values, no further analysis is conducted. However, in practical contexts, achieving

desired property results with variations in chemical compositions is crucial. It provides the expert with options that best align with industrial settings in the manufacturing process and possible client constraints.

Finally, given the complexity of the problem, numerous challenges may hinder the development of new steels through computational methods, with most involving property modeling methods, whether empirical or prediction methods. With continuous research and development in machine learning and various branches of metallurgy, there are many possibilities to explore new modeling models and optimization algorithms capable of increasing accuracy in achieving desired values with diversity in chemical compositions. This offers the expert multiple feasible implementation possibilities for new steels.

| Paper title | Author | Optimization Algorithm | Input Variables | | | Output Variables | Quantitative Analysis | Qualitative Analysis |
|---|--|------------------------|----------------------|--------------------|--------------------------|---|-----------------------|----------------------|
| | | | Chemical Composition | Process Parameters | Dimensional Informations | | | |
| A machine-learning-based alloy design platform that enables both forward and inverse predictions for thermo-mechanically controlled processed (TMCP) steel alloys | Lee et al. (2021) | NSGA-II | [14] | [2] | | TS, YS | | X |
| A Multi-Objective Data-driven Evolutionary Algorithm Applied to Steel Modeling | Sgroffo (2022) | NSGA-II | [13] | [14] | [2] | TS, YS, EL | X | X |
| A steel property optimization model based on the XGBoost algorithm and improved PSO | Song et al. (2020) | Improved PSO | [22] | [3] | [2] | TS, Plasticity | X | X |
| Data-driven pareto optimization for microalloyed steels using genetic algorithms | Kumar, Chakrabarti, Chakraborti (2012) | PPGA | | [13] | | TS, YS, EL | X | X |
| Designing cold rolled IF steel sheets with optimized tensile properties using ANN and GA | Mohanty, Bhattacharjee e Datta (2011) | NSGA-II | [10] | [7] | | TS, YS, EL | | X |
| Designing dual-phase steels with improved performance using ANN and GA in tandem | Dutta et al. (2019) | NSGA-II | [10] | [3] | | TS, YS, EL, Uniform EL, Yield rate, Yield hardening | | X |
| Design of comprehensive mechanical properties by machine learning and high-throughput optimization algorithm in RAFM steels | Wang et al. (2020) | NSGA-II | [9] | [1] | | YS, Impact energy | | X |
| High Dimensional Data-driven Optimal Design for Hot Strip Rolling of C-Mn Steels | Wu et al. (2017) | SPEA-II | [3] | [3] | [2] | TS, YS, EL | | X |
| Optimal design of hot-dip galvanized dp steels via artificial neural networks and multi-objective genetic optimization | Resendiz-Flores et al. (2021) | NSGA-II | | [3] | | TS, YS, EL | X | |
| Optimal Design of the Austenitic Stainless-Steel Composition Based on Machine Learning and Genetic Algorithm | Liu et al. (2023) | NSGA-III | [3] | [16] | | TS, YS, EL, Reduction of area | X | |
| Optimization of annealing cycle parameters of dual phase and interstitial free steels by multiobjective genetic algorithms | Shah et al. (2017) | Knear-MOPSO | [3] | [15] | | TS, EL | | X |
| Optimizing Tensile Strength and Yield Point of Steel Bar with Artificial Neural Network with Enhanced Parallel Cat Swarm Optimizer | Gurav, Patil e Solanki, (2018) | EPCSO | [10] | | | TS, YS | | X |

Table 2 – Selected papers/theses

4 PROPOSED APPROACH

In this chapter, we present the proposed methodology for predicting the mechanical properties of steel and explain how this model is subsequently used in the optimization phase.

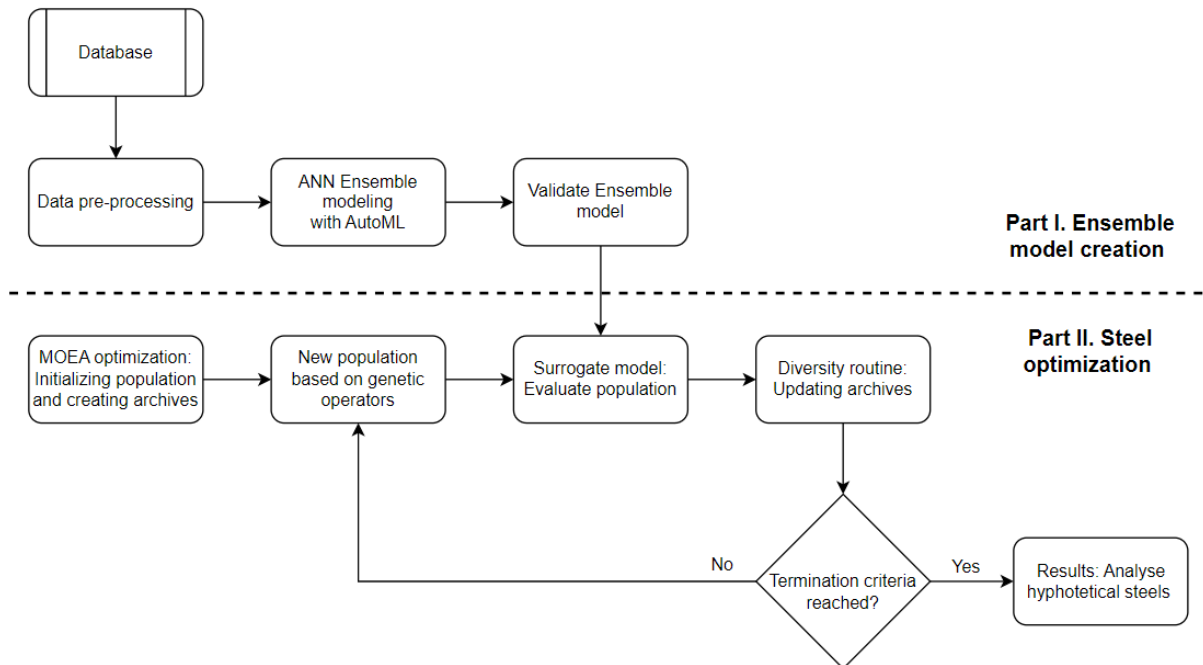


Figure 10 – Proposed computational system. Source: Own authorship.

Figure 10 shows a simplified flowchart coupling the prediction model creation and its application in steel optimization. The process begins with the creation of a regression model, an Artificial Neural Network (ANN) trained on the dataset within the problem domain, subsequently used as a surrogate model. The inputs to the model include chemical composition, processing parameters, and dimensional information, while the outputs consist of evaluations of three mechanical properties: EL, TS, and YS.

The development of this model begins with the collection of data from the steel factory's historical records, followed by data cleaning and preprocessing to prepare the data for Artificial Neural Network (ANN) training. The model training is automated through Neural Architecture Search (NAS), from which the five best models are selected and combined to create an ensemble model. This model is then validated.

In the optimization phase, the ensemble model is integrated with a Multi-Objective Evolutionary Algorithm (MOEA) as a surrogate model, using its predictions in the fitness calculation. Additionally, a diversity routine is implemented, involving the creation of two archives: one focused on convergence and the other on diversity of results. These archives communicate with the MOEA population to maintain high genotypic diversity. At the end of the process, due to the multi-objective nature of the problem, a list of the most promising solutions is generated for the user.

4.1 REGRESSOR MODELING

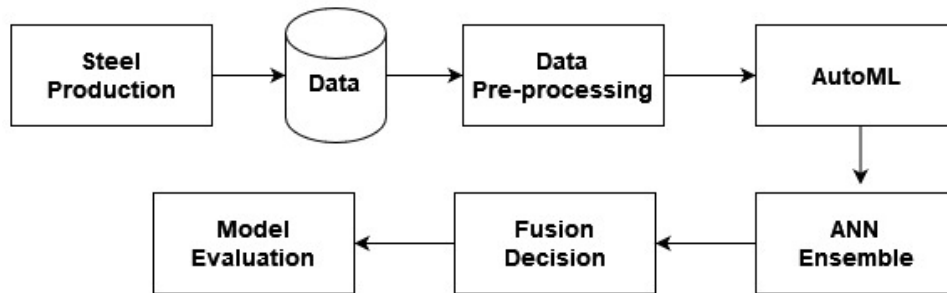


Figure 11 – Proposed surrogate modeling flowchart. Source: (SILVA et al., 2023).

Figure 11 provides an overview of the proposed model. Initially, data is extracted from the steel production process and organized in a comprehensive database that encompasses all pertinent data points, with input and output variables inherently represented as integers or floating-point numbers. Following data extraction, procedures for processing and balancing are implemented to ensure a well-rounded representation of each steel type in the dataset.

Subsequent to data preprocessing, hyperparameter tuning is executed through the application of Automated Machine Learning (AutoML). This iterative process results in the development of a multivariate ensemble regression model comprising the top 5 Artificial Neural Networks (ANNs) generated. Once the ensemble model is established, the subsequent step involves formulating the methodology for consolidating individual predictions into a singular value for each mechanical property. Finally, the model's accuracy is evaluated, and this iterative process is repeated until a precise and replicable model is attained.

The Ensemble model takes input from a total of twenty-seven variables. Among these, fourteen represent chemical elements, eleven are associated with various processing parameters across different manufacturing stages, and two are related to dimensional parameters. The model generates predictions for three output variables, precisely the mechanical properties of Yield Strength (YS), Tensile Strength (TS), and Elongation (EL).

4.1.1 NEURAL ARCHITECTURE SEARCH

The choice and optimization of hyperparameters in the training of an artificial neural network constitute a complex process. Depending on the number of required possibilities, an exhaustive search becomes impractical in terms of time, while overly limiting the options may lead to a configuration far from ideal, compromising the model's performance.

To address these issues, Auto-Keras(JIN; SONG; HU, 2019), a Neural Architecture Search (NAS) framework, was employed as AutoML to optimize the process of selecting hyperparameters for the generated artificial neural networks. Table 3 outlines the search space utilized by NAS for parameters such as the number of layers, number of neurons, and regularization.

Table 3 – Search space for the NAS parameters.

| Parameter | Values |
|----------------------------------|--|
| Number of layers | [1, 2, 3] |
| Number of neurons | [16, 32, 64, 128, 256, 512, 1024] |
| Use of drop-out in hidden layers | [Yes, No] |
| Drop-out value for hidden layers | [0, 0.25, 0.5] |
| Use of drop-out in output layer | [Yes, No] |
| Drop-out value for output layer | [0, 0.25, 0.5] |
| Use of batch-regularization | [Yes, No] |
| Optimizer | [stochastic gradient descent, adam, adam weighted decay (adam WD)] |
| Learning rate | [0.1, 0.01, 0.001, 0.0001, 0.00001, 0.00002] |

Auto-Keras uses Bayesian optimization, a probabilistic model-based optimization technique, to guide the network morphism during the development of a neural network kernel. This approach allows Auto-Keras to make informed decisions about the architecture's hyperparameters and configuration. Furthermore, Auto-Keras employs a tree-structured acquisition function optimization algorithm, enhancing its efficiency in exploring the extensive search space associated with artificial neural network architectures. The combination of Bayesian optimization and the tree-structured acquisition function contributes to the robustness and effectiveness of the Auto-Keras framework in automatically tuning and adapting neural network architectures (JIN; SONG; HU, 2019).

The evaluation of the model's performance on the validation dataset involved the calculation of two performance metrics: Mean Absolute Error (MAE) and Mean Squared Error (MSE). MAE measures the average absolute difference between predicted and actual values, offering insight into the average magnitude of errors. Conversely, MSE calculates the average squared difference between predicted and actual values, assigning more weight to more significant errors.

The E-ANN model constitutes an ensemble of the top five neural networks selected from a pool of one hundred neural networks generated by the NAS framework. The selection of these five neural networks was based on their MAE performance.

A cross-validation procedure was implemented to ensure an unbiased comparison of different artificial neural network models. This involved randomly dividing the dataset into ten parts, or "folds," with each iteration using one fold as the test set and the remaining folds as the training set.

4.2 MOEA FOR STEEL DESIGN OPTIMIZATION

After creating the regression model, which models the relationship between IF, BH, HSLA, DP, and TRIP steel grades, it is integrated into the MOEA as a surrogate model and used to compose the fitness function. As suggested by Sgrott (2022), the optimization objective is not to minimize or maximize the mechanical properties but rather to optimize the error between

the generated individuals and the target property values defined before the optimization process begins.

4.2.1 MOEA

The MOEA plays a pivotal role in the quest for new steel configurations. Naturally, each utilized algorithm possesses distinct characteristics, resulting in solutions with varying levels of accuracy and variance concerning the proposed objective.

As indicated by the SLR, NSGA-II stands out as the most prevalent algorithm for optimizing mechanical properties. The work conducted by Sgrott (2022) also employs this optimizer. To assess the performance of new algorithms within this problem context and compare them with NSGA-II, a study was conducted to identify potential MOEA. In this process, specific criteria were established for selection. Firstly, the MOEA must be many-objectives rather than multi-objectives, meaning they should optimize three or more objectives to accommodate potential future project expansions with the company. Secondly, the decision was made to work with recent algorithms (considering those developed after 2015), thereby excluding alternatives identified in the SLR. The third and final criterion was that the selected algorithms should exhibit superior performance to NSGA-II in recognized benchmark tests.

Based on these criteria, three MOEA were chosen for subsequent comparison with NSGA-II in the context of steel design. Below are the names of these algorithms:

- NSGA-III (DEB; JAIN, 2013)(JAIN; DEB, 2013)
- AGE-MOEA (PANICHELLA, 2019)
- RVEA (CHENG et al., 2016)

The NSGA-III was chosen due to its similar foundation to NSGA-II but with the additional capability of handling three or more objectives. Both the RVEA and AGE-MOEA, being relatively recent approaches, have shown superior results compared to NSGA-II and NSGA-III among others MOEAs across various real-world problems and benchmarks (RAHIMI et al., 2023) (TANABE; ISHIBUCHI; OYAMA, 2017) (TIWARI et al., 2022) (Kouider Amar et al., 2023).

For all MOEA, the initialization of the population and the genetic operators follow a consistent pattern. The initial population is generated randomly, following a uniform distribution. This ensures that the initial solutions are evenly distributed across the search space, providing good coverage of the space of possible solutions and increasing the chances of finding optimal solutions.

The selection of individuals over generations is done through random selection, where each individual has an equal probability of being chosen to generate the next population. The

mutation operator used is a polynomial mutation, which alters the values of genes in an individual in a controlled manner based on a probabilistic distribution that resembles a polynomial probability density function (DEB, 2001).

For the recombination operator, the Simulated Binary Crossover (SBX) is used, which simulates the behavior of binary crossover in the context of continuous variables (DEB; AGRAWAL et al., 1995). This operator promotes the exploration of the search space and the efficient creation of new individuals.

The distribution parameter (η_m) for polynomial mutation, which controls the shape of the distribution, is set to 20. The distribution parameter (η_c) for recombination, which controls the diversity of offspring, is set to 15. Additionally, an online parameter control for recombination and mutation is utilized. This means that the probability of these operations being performed varies throughout the optimization process based on deterministic rules, as shown in Figure 12. The implementation of parameter control and genetic operators, along with their distribution values, is based on the tests conducted by Sgrott (2022).

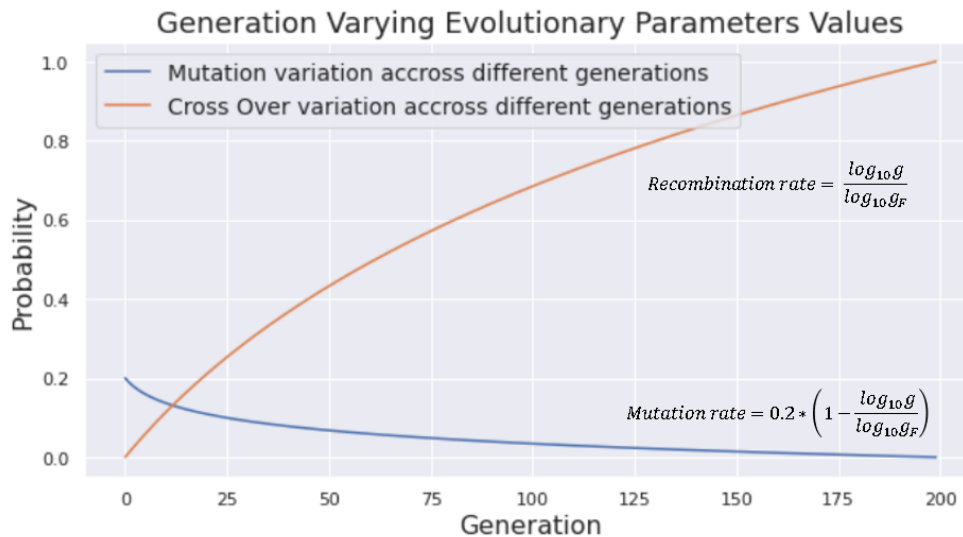


Figure 12 – Online parameter control using deterministic rules for Recombination and Mutation. Source: Adapted from Sgrott (2022).

4.2.2 TWO-ARCHIVE STRATEGY

Archives, or external repositories, have been a focal point of study in MOEA, mainly when aiming to preserve solution diversity throughout the optimization process. The concept behind this method is that, through predefined criteria, we can determine which solutions will be included in the archive. From there, decisions such as showcasing specific solutions to the user or performing operations with these repositories to modify the optimization can be made.

In the investigation led by (LI et al., 2014), dominance relations are employed to examine and manipulate solutions as they enter and exit two distinct archives. The convergence archive stores solutions that are not dominated, while the diversity archive houses individuals that do

not dominate any solution. Another strategy, presented by (DING et al., 2019), involves the management of two archives: a uniform archive designed to sustain solutions across the search space using distance metrics relative to the reference points employed in optimization and a single elite archive that retains solutions with the shortest distance to the NSGA-III reference point. Furthermore, (KUMAR et al., 2023) introduces archive-1, focused on convergence, utilizing auxiliary functions reliant on fitness metrics to incorporate solutions. Concurrently, archive-2, which is dedicated to diversity, employs auxiliary functions that capture the diversity of solutions through fitness values.

While the methods for updating archives may vary, they share a common objective: establishing two archives as the basis for generating the next optimization generation. However, upon closer examination of the diversity archive, it becomes apparent that all proposed approaches primarily focus on enhancing the phenotypic diversity of the solutions. However, this falls short of our requirements, given that our objective pertains to steel with specific properties. Our goal is to achieve the highest diversity in input configurations, effectively maximizing genotypic diversity.

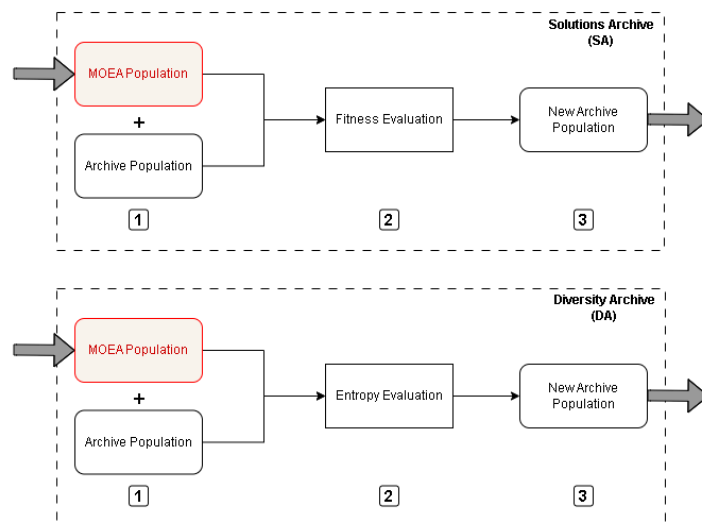


Figure 13 – Flowchart of solution and diversity archives. Source: Own authorship.

The proposed methodology integrates two external archives within the MOEA framework: the solution archive (SA) and the diversity archive (DA). The sequence of activities within each archive is depicted in Figure 13. Initially, the population of the genetic algorithm is combined with the archive population. In the first generation, the archive is devoid of entries. Following this, Entropy/fitness is computed for the population, and subsequently, the population is arranged by entropy/fitness. Individuals are then excluded until the maximum archive size is adhered to.

The primary focus of the solution archive (SA) is to store promising solutions in terms of fitness, highlighting optimal or near-optimal solutions identified at the end of the optimization. Conversely, the diversity archive (DA) is exclusively dedicated to preserving the most genotypically diverse solutions uncovered across generations, ensuring the diversity of steel con-

figurations in the optimization. In each generation, the genetic algorithm transfers the population to both archives to update their respective sets of solutions.

The only difference between the two archives is the calculation performed during the second step. Given that the SA is exclusively focused on the most promising solutions close to the target, we use fitness as the inclusion criterion for this archive. As for the DA, we aim to capture the most diverse solutions throughout the optimization process. Therefore, the inclusion criterion for this archive is based on a diversity metric using Shannon entropy, as defined by Equation 4.

4.2.2.1 MOEA REINTRODUCTION OF SOLUTIONS

When dealing with MOEA, several techniques are proposed to ensure an optimal set of solutions at the end. The use of an external repository, combined with the reintroduction of these solutions into the main population, is every day and has already been implemented in renowned algorithms such as SPEA(ZITZLER; THIELE, 1998) and SPEA2(ZITZLER, 1999). In both cases, the archive is a list of non-dominated solutions found during evolution, which can be reintroduced to maintain diversity and preserve solutions that were effective in previous iterations. This helps prevent premature convergence to a specific set of solutions, allowing the algorithm to explore the search space more comprehensively.

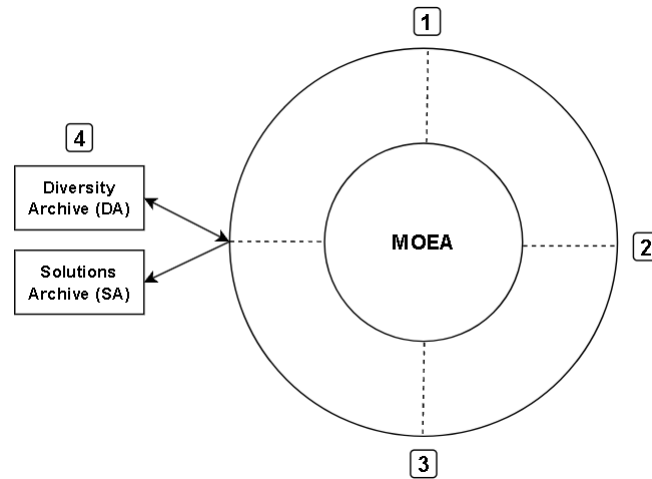


Figure 14 – Flowchart of the genetic algorithm with solution and diversity archives, and reintroduction of solution. Source: Own authorship.

Figure 14 illustrates the system with reintroduced variables, representing the reintroduction of solutions from the diversity archive into the optimization process. The circular symbol represents the generations of the genetic algorithm, focusing solely on the primary operators. The steps are described below:

1. Initiating the generation is represented
2. Fitness calculations

3. Selection, recombination, and mutation of steel configurations
4. Populations of the solution and diversity archives are updated

The parameter *reintro* ultimately determines the number of steels ('n') to be reintroduced into the optimization. For this purpose, 'n' steels are randomly chosen from the diversity archive population and incorporated into the genetic algorithm population, displacing the 'n' steels with the worst fitness sum values.

4.2.3 STAGGERED OPTIMIZATION

When performing optimization, due to the stochastic nature of the MOEA, there is no guarantee that all or a large part of the range of possibilities of the input variables will be explored and represented in the final solutions presented by the solution archive. However, discretizing the range of values for certain variables can be important in the metallurgical context, as small changes can result in different types of steel. Additionally, for specialists, it may be essential to have results in a smaller and more specific range better to understand the influence of the variable in question.

Typically, such experiments can be carried out by restricting the initial bounds of the optimization to the desired range with the desired variables and performing a series of optimizations with the desired modifications. To facilitate the process and give the specialist the option of which variables will be tested and what increment of the range of values for each variable, a staggered optimization is proposed.

| | | X_{01} | X_{02} | X_{03} | X_{04} | X_{05} | X_{06} | X_{07} | X_{08} | ... | X_{27} |
|-------------------|------|----------|----------|----------|----------|----------|----------|----------|----------|-----|----------|
| Base Optimization | Mín. | 1 | 50 | 1100 | 870 | 550 | 0.05 | 0.50 | 0.004 | ... | 300 |
| | Máx. | 2 | 65 | 1200 | 930 | 680 | 0.20 | 2.50 | 0.020 | ... | 460 |
| | Step | | 5 | | | | 0.01 | | | ... | |

| Additional Opt due to scaling X_{02} | | X_{01} | X_{02} | X_{03} | X_{04} | X_{05} | X_{06} | X_{07} | X_{08} | ... | X_{27} |
|--|---|----------|----------|----------|----------|----------|----------|----------|----------|-----|----------|
| 1 | 1 | 50 | 1100 | 870 | 550 | 0.05 | 0.50 | 0.004 | ... | 300 | |
| | 2 | 55 | 1200 | 930 | 680 | 0.20 | 2.50 | 0.020 | ... | 460 | |
| 2 | 1 | 60 | 1100 | 870 | 550 | 0.05 | 0.50 | 0.004 | ... | 300 | |
| | 2 | 65 | 1200 | 930 | 680 | 0.20 | 2.50 | 0.020 | ... | 460 | |

| Additional Opt due to scaling X_{07} | | X_{01} | X_{02} | X_{03} | X_{04} | X_{05} | X_{06} | X_{07} | X_{08} | ... | X_{27} |
|--|---|----------|----------|----------|----------|----------|----------|----------|----------|-----|----------|
| 1 | 1 | 50 | 1100 | 870 | 550 | 0.05 | 0.50 | 0.004 | ... | 300 | |
| | 2 | 65 | 1200 | 930 | 680 | 0.06 | 2.50 | 0.020 | ... | 460 | |
| ⋮ | | | | | | | | | | | |
| 2 | 1 | 50 | 1100 | 870 | 550 | 0.19 | 0.50 | 0.004 | ... | 300 | |
| | 2 | 65 | 1200 | 930 | 680 | 0.20 | 2.50 | 0.020 | ... | 460 | |

Figure 15 – Example of the staggered optimization process, 3 additional optimizations are made due to the staggering of X_{02} and 15 additional optimizations due to the staggering of X_{07} . Source: Own authorship.

Figure 15 shows an example of the process. Initially, the broader initial bounds are provided. In this case, two input variables are chosen for the stagerring, X_{02} and X_{07} . From the informed step values, the initial range of values is divided to form a set of bounds for each variable chosen. The set of bounds is formed by the sum of the possibilities generated by each staggered variable plus the informed initial bounds. For each of the bounds, an optimization is performed, and in the end, the results are grouped in the solution archive.

5 RESULTS AND ANALYSIS

This chapter presents the results with the corresponding analyses of the changes and methods applied.

5.1 REGRESSOR ANALYSIS

In this section, we provide an overview of the dataset utilized for regressor modeling, along with the outcomes obtained through the application of more balanced data and advanced regressor modeling techniques. The impact of data modeling on the regressor is emphasized, and insights are gleaned using xAI techniques.

5.1.1 DATABASE

The database was collected using actual data from the steel production process. To ensure that every type of steel had adequate representation in the dataset, the authors utilized an ad-hoc filter method suggested by steel specialists. Despite the unequal distribution of steel grades, the ANNs should be capable of generalizing the data, given that each steel grade has a sufficient amount of representative data.

The initial consolidated dataset contains 123608 rows and 27 columns, including process parameters and chemical composition that have a direct impact on the prediction outcomes and are shown in detail in Table 4.

Table 5 offers an overview of the current data distribution for each steel grade post-consolidation. Our effort is directed towards balancing the total number of samples for most steel types. However, achieving balance for TRIP steel proves challenging due to its low production volume on the production line. Despite its limited representation, data for TRIP steel, with its crucial characteristics for attaining high mechanical property values, is included in the dataset.

Table 4 – Description from the model’s variables, where CE, PP, DIM, and MP stand for Chemical Element, Process Parameter, Dimension, and Mechanical Property, respectively.

| Name | Description | Type | Unit | Origin |
|-------------|--|-------------|-------------|---------------|
| X_{01} | Carbon content | CE | ppm | SM |
| X_{02} | Manganese content | CE | ppm | SM |
| X_{03} | Phosphorus content | CE | ppm | SM |
| X_{04} | Silicon content | CE | ppm | SM |
| X_{05} | Sulfur content | CE | ppm | SM |
| X_{06} | Nickel content | CE | ppm | SM |
| X_{07} | Aluminium content | CE | ppm | SM |
| X_{08} | Chrome content | CE | ppm | SM |
| X_{09} | Niobium content | CE | ppm | SM |
| X_{10} | Molybdenum content | CE | ppm | SM |
| X_{11} | Titanium content | CE | ppm | SM |
| X_{12} | Vanadium content | CE | ppm | SM |
| X_{13} | Boron content | CE | ppm | SM |
| X_{14} | Nitrogen content | CE | ppm | SM |
| X_{15} | Coil width | DIM | mm | HDG |
| X_{16} | Coiling temperature | PP | °C | HSM |
| X_{17} | Heating temperature before hot rolling | PP | °C | HSM |
| X_{18} | Heating temperature after hot rolling | PP | °C | HSM |
| X_{19} | Cold rolling reduction | PP | % | CRM |
| X_{20} | Thickness after hot rolling | DIM | mm | CRM |
| X_{21} | Line speed | PP | m/s | HDG |
| X_{22} | Mean Skin Pass Mill elongation | PP | % | HDG |
| X_{23} | Temperature from Pyrometer 03 | PP | °C | HDG |
| X_{24} | Temperature from Pyrometer 04 | PP | °C | HDG |
| X_{27} | Temperature from Pyrometer 16 | PP | °C | HDG |
| Y_{01} | Yield Strength | MP | MPa | LAB |
| Y_{02} | Ultimate Tensile Strength | MP | MPa | LAB |
| Y_{03} | Elongation | MP | % | LAB |

| Steel Type | Count (%) |
|-------------------|------------------|
| BH | 20.16% |
| IF | 38.37% |
| HSLA | 20.13% |
| DP | 18.92% |
| TRIP | 2.42% |

Table 5 – Distribution of Steel Types

5.1.2 ENSEMBLE MODELING

As presented in Chapter 4, this section aims to present the performance results of the proposed approach, as well as to analyze the interpretability and sensitivity of the model. This is intended to provide a deeper understanding of the developed model.

The proposed model undergoes evaluation alongside two other models, all generated using AutoML. The B-ANN model selects the best neural network from the one hundred generated by Auto-Keras based on its performance using the MAE metric. The ANN model, on the other hand, is constructed for each fold of the cross-validation and represents the first neural network generated by Auto-Keras.

In each fold, the compared models are created, and the results are used to assess the robustness of observed differences between the models. All results were obtained from the exact same test dataset for consistency. Analyzing these metric results provides a comprehensive evaluation of the E-ANN model's performance compared to the others.

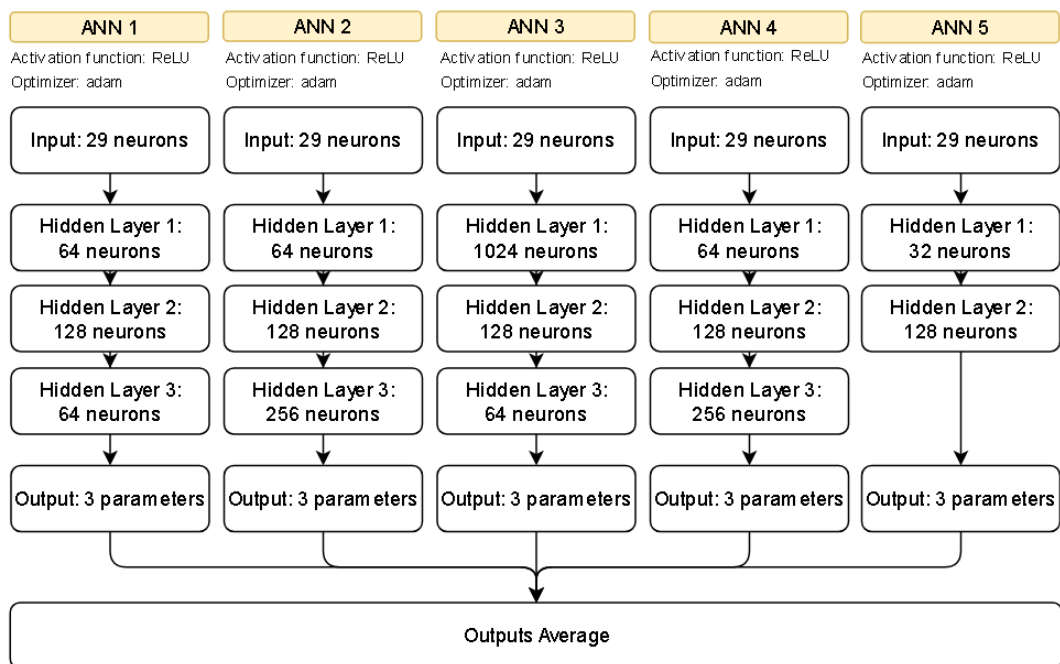


Figure 16 – Best five ANNs found using the NAS architecture.

Figure 16 depicts the final configurations for the Artificial Neural Networks (ANNs) that constitute the ensemble. It is observed that the Neural Architecture Search (NAS) yields five distinct models with varying sizes and layers. The activation function employed for all models is ReLU, chosen based on the outcomes reported by Sgrott (2022).

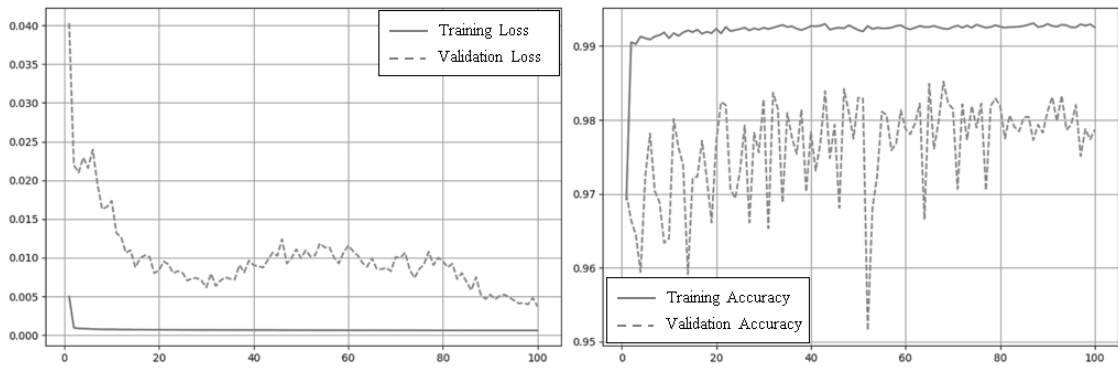


Figure 17 – Training and validation loss of training epochs using the NAS architecture.

Regarding the model loss of the Artificial Neural Network (ANN) for the training and validation data, Figure 17 demonstrates that the optimal ANN does not experience overfitting or underfitting. While Figure 17 presents explicitly the performance of the B-ANN model, it is crucial to emphasize that the remaining ANNs employed to construct the ensemble display analogous behavior.

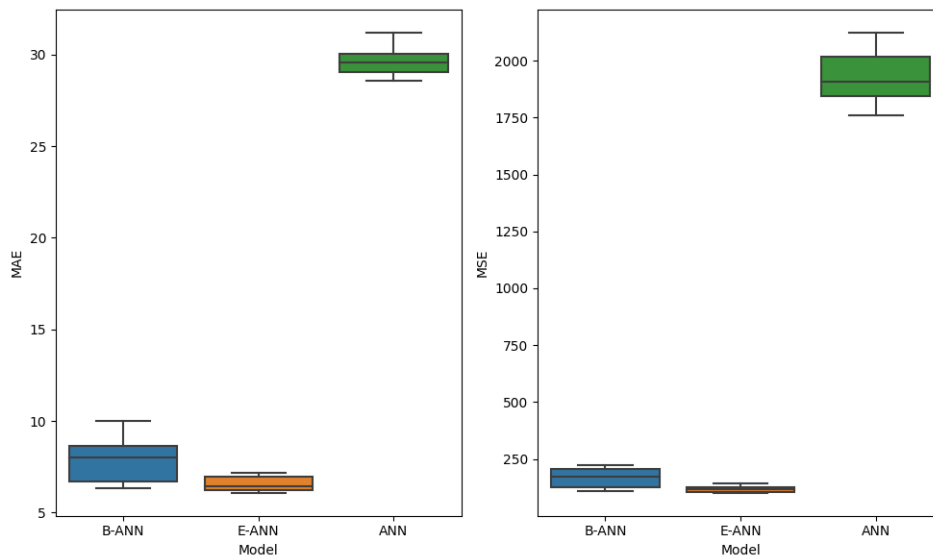


Figure 18 – Performance Comparison of Models in 10-Fold Cross-Validation.

Table 6 – Dunn’s test P-values for the model performance comparison dataset (values above the main diagonal represent the values for the MAE metric, and values below the main diagonal indicate the values for the MSE metric).

| Models | B-ANN | E-ANN | ANN |
|--------------|---------------|---------------|---------------|
| B-ANN | 1.0000 | 3.73e-02 | 5.63e-03 |
| E-ANN | 2.71e-02 | 1.0000 | 1.00e-06 |
| ANN | 6.82e-03 | 8.86e-07 | 1.0000 |

By applying cross-validation to the three evaluated models, aiming to ensure reproducibility, we can see in Figure 18 that the E-ANN model outperforms the other two. The results demonstrate a significant decrease in Mean Absolute Error (MAE) and Mean Squared Error (MSE) for the E-ANN.

To ensure the test's statistical significance, the Dunn test was conducted with a significance level of 5%. The results are presented in Table 6, where values above the main diagonal represent the values for the MAE metric, and values below the main diagonal indicate the values for the MSE metric. The results indicate a statistically significant difference among the tested data. Thus, the improved performance of the E-ANN model compared to others is clearly demonstrated.

This improvement in performance can be attributed to the combination of the results of the five main ANNs in the E-ANN model. One of the advantages of using ensembles is that they allow for better capture of the nuances and patterns in the data (KROGH; VEDELSBY, 1994).

On the other hand, the ANN model, which is based on a single execution of Auto-Keras, proves to be unquestionably inferior to the other two models. The E-ANN and B-ANN models are created from multiple runs, showing the importance of performing multiple runs of the NAS and exploring different possibilities to obtain a more reliable and generally better result.

5.1.2.1 INTERPRETABILITY TECHNIQUES

Explainable Artificial Intelligence (xAI) refers to a set of techniques and approaches aimed at making artificial intelligence models more understandable and explainable for humans. There are several reasons why we should use xAI. Firstly, transparency and explainability are crucial to ensure trust and acceptance from users and stakeholders in AI models (DAS; RAD, 2020). By understanding how a model makes decisions, users can assess its reliability and make informed decisions based on its predictions.

A sensitivity analysis was conducted to delve deeper into the workings of the model. The objective of model sensitivity analysis is to quantify the relative importance of each input parameter in influencing the value of a designated output variable (HOMMA; SALTELLI, 1996). By systematically altering one parameter while keeping all other variables constant, the effects of different combinations of input parameters can be compared across various models. This approach allows for a more comprehensive evaluation of how individual variables impact the overall mechanical behavior of the materials under investigation.

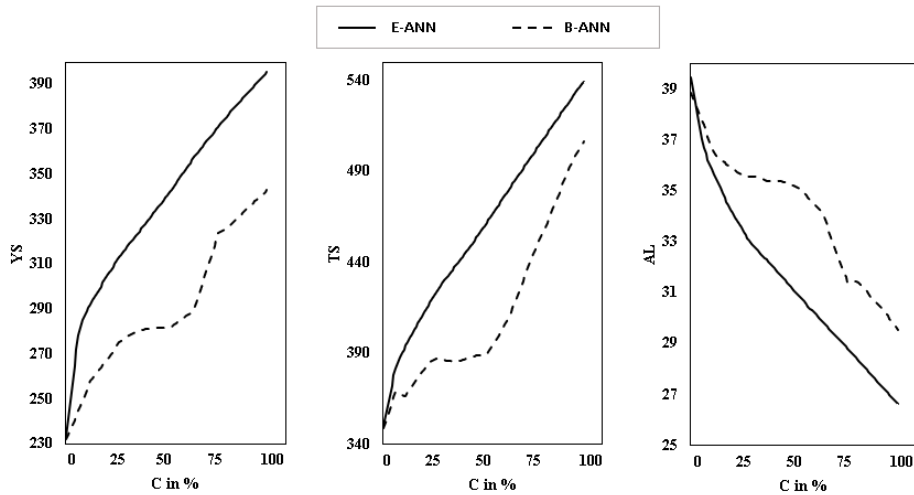


Figure 19 – Sensitivity analysis of 'C' for the E-ANN and B-ANN models.

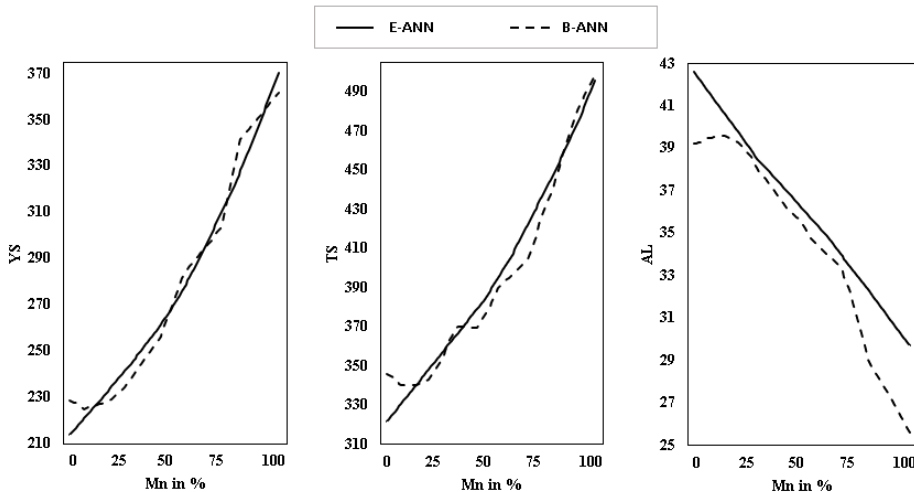


Figure 20 – Sensitivity analysis of 'Mn' for the E-ANN and B-ANN models.

Figure 19 illustrates a distinct trend wherein an elevation in the carbon percentage leads to higher values of tensile strength and yield strength, consequently enhancing the overall strength of the steel. Conversely, there is a decrease in elongation. This property behavior aligns with expectations outlined in Schweitzer et al. (2003) for increases in carbon. Likewise, in Figure 20, it is evident that as the percentage of manganese in the steel composition increases, the mechanical properties exhibit a similar trend as observed with carbon. This aligns with expectations outlined in Sarkar et al. (2010b).

For both evaluated models, the analysis demonstrated the attainment of the desired behavior, showcasing consistent patterns across the majority of the considered value range. However, as this is a local analysis, the magnitude of variations for each chemical element depends significantly on the presence of other chemical elements and process parameters within the system. Nevertheless, this analysis remains valid and valuable for comprehending the relationships between chemical elements and mechanical properties, particularly for decision-makers who

can place more confidence in the model's ability to depict relationships among crucial features accurately.

To acquire a more profound insight into the collective impact of input parameters on the mechanical properties, SHAP (LUNDBERG; LEE, 2017) was employed to calculate the distribution of the impact of each feature on the model's output. The results can be seen in Figure 21.

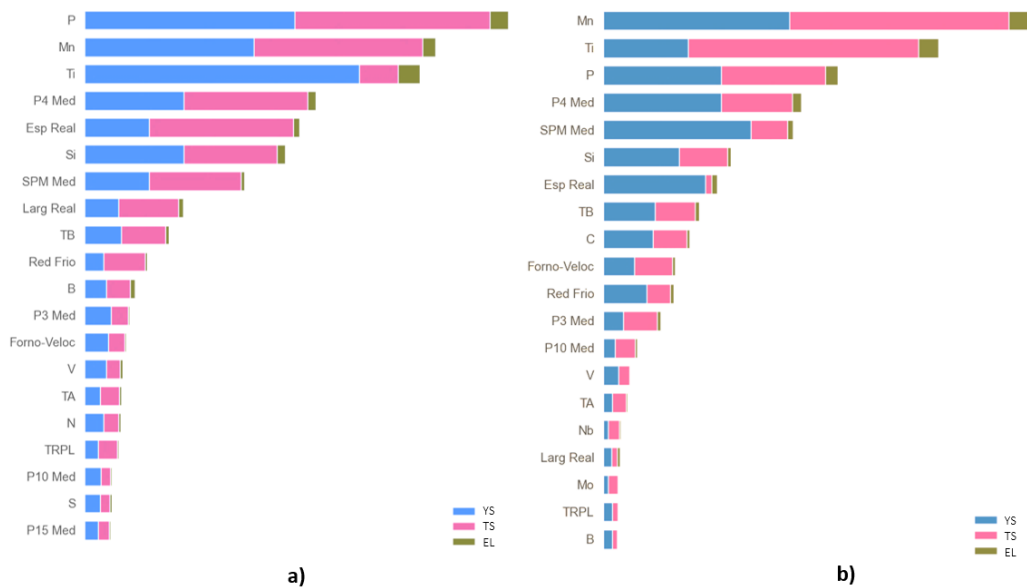


Figure 21 – SHAP values for a) B-ANN Model, b) E-ANN Model.

In Figure 21, it is evident that manganese emerges as one of the most influential elements in the B-ANN model, whereas carbon does not rank among the most influential features. However, in the E-ANN model, manganese maintains its significant importance, and carbon is now recognized among the most influential characteristics. Considering the metallurgical context described in Krauss (2017), both chemical elements play crucial roles in influencing the mechanical properties under study. Thus, the E-ANN model aligns more consistently with the metallurgical reality.

When comparing these findings with those presented in Sgrott et al. (2021), a notable decrease in the significance of carbon is observed in both models. This decline can be attributed to the incorporation of additional steel types, including DP, BH, TRIP, and HSLA, alongside IF. Consequently, the combination of steels with varying levels of complexity assigns heightened importance to alloy elements and process temperatures. These factors play a crucial role in hardening and phase transformation, ultimately defining the specific steel grade under consideration. Thus, alloy elements and process temperatures exert a more significant influence on the model, surpassing the relative importance of carbon.

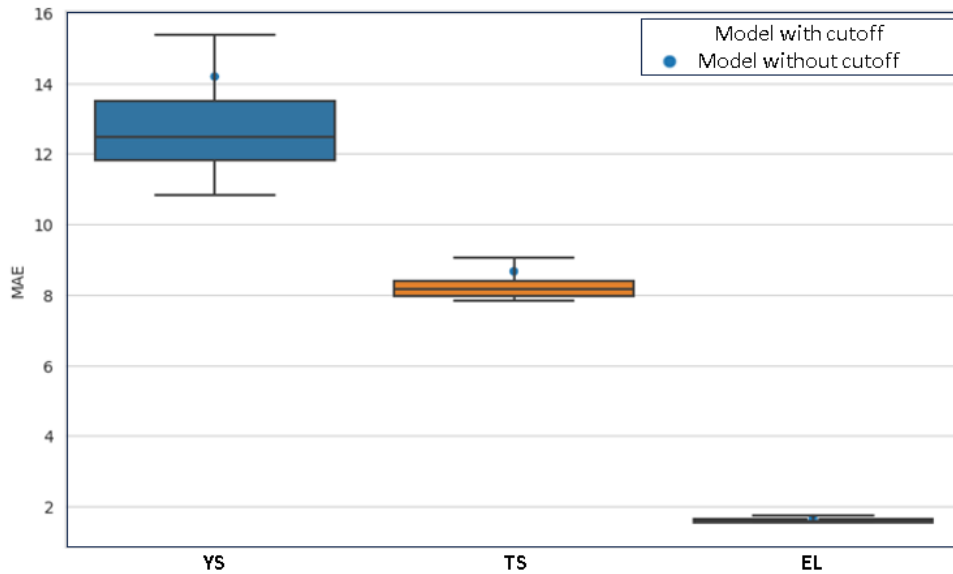


Figure 23 – Box plot of MAE values per mechanical properties, using the database and its limited version for each model.

Table 7 – Dunn’s test P-values comparing the original and cutted dataset for MAE values per mechanical properties.

| Properties | P-value |
|------------|----------|
| YS | 3.43e-01 |
| TS | 5.27e-01 |
| EL | 7.52e-01 |

In Figure 23, a box plot is displayed with the MAE values corresponding to each mechanical property. In the plot, we can also see a data point representing the E-ANN with the dataset without data reduction. It is noticeable that only for YS is there a difference of 4 MPa between the old dataset and the median value of the new dataset. This error, according to experts, does not raise significant concerns regarding prediction accuracy.

Furthermore, in alignment with the previous points, Table 7 presents the results of the Dunn test comparing the outcomes achieved with the original dataset and the dataset with data cutoff. It can be observed that the results indicate no statistically significant difference between the outcomes, demonstrating that the model was not adversely affected by the data cutoff.

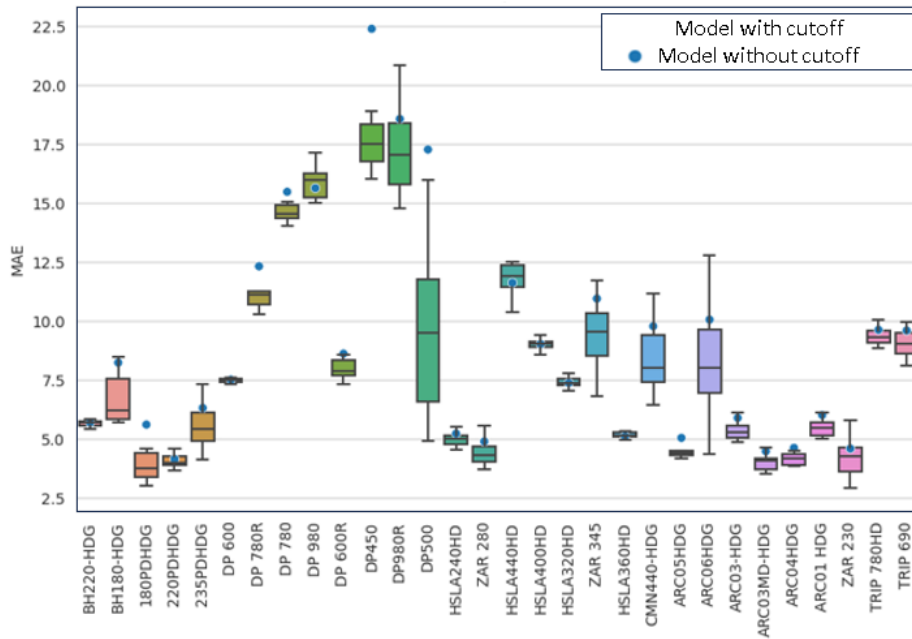


Figure 24 – Box plot of MAE values per subtypes of steel grade, using the database and its limited version for each model.

In Figure 24, the analysis follows the same idea as the previous plot, but in this case, comparisons with the subtypes of each steel grade are shown. Again, in cases where the new E-ANN model exhibits larger errors, they are not significant enough to pose any issues in predicting the properties from a metallurgical perspective.

After the changes, the updated distribution for each steel grade in the database is presented in Table 8. In comparison with the original distribution shown in Table 5, some of the steel grades with higher representation experienced a reduction in proportion. Although the database is not entirely balanced, approximately thirty-six thousand data points were removed, resulting in a total of 86,785 steel samples. This reduction did not significantly compromise the predictive capacity of the mechanical properties.

| Steel Type | Count (%) |
|------------|-----------|
| BH | 19.73% |
| IF | 31.61% |
| HSLA | 27.34% |
| DP | 18.41% |
| TRIP | 2.91% |

Table 8 – Distribution of Steel Types after the limitation of the database

5.2 OPTIMIZATION ANALYSIS

In this section, we present the results obtained from analyzing different MOEAs, along with the implementation of a second archive specifically designed to capture the genotypic diversity of the generated solutions.

5.2.1 MOEA ALGORITHM

As discussed in Chapter 4, three MOEAs have been chosen to have their performances compared with NSGA-II. Thus, the experimental plan involves selecting ten random steels for testing, ensuring that none of these steels were used in the training of the E-ANN. One hundred runs will be conducted for each MOEA, and each of the selected steels, and the values of HV and IGD for each optimization will be recorded.

Both performance indicators highlight the convergence of MOEA optimization. With a significant number of experiments conducted for each steel grade, it is possible to establish a statistical foundation to understand which MOEA exhibits the best behavior regarding the problem.

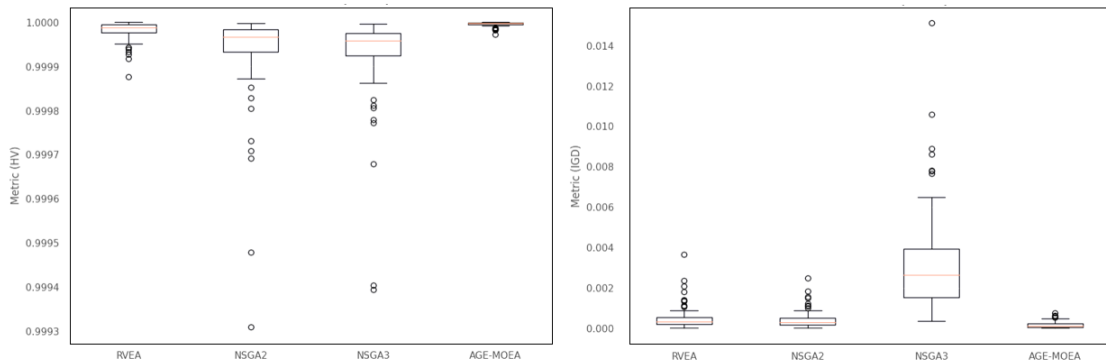


Figure 25 – Final HV and IGD values for all MOEA tested and IF steels.

Table 9 – Dunn’s test P-values for Final HV and IGD values for all MOEA tested and IF steels (values above the main diagonal represent the values for the HV metric, and values below the main diagonal indicate the values for the IGD metric).

| MOEA | NSGA-II | NSGA-III | RVEA | AGE-MOEA |
|----------|----------|----------|----------|----------|
| NSGA-II | 1.0000 | 7.57e-03 | 2.42e-15 | 1.16e-42 |
| NSGA-III | 7.97e-24 | 1.0000 | 1.54e-07 | 3.06e-28 |
| RVEA | 7.21e-24 | 9.92e-01 | 1.0000 | 7.82e-09 |
| AGE-MOEA | 3.53e-48 | 6.17e-06 | 6.46e-06 | 1.0000 |

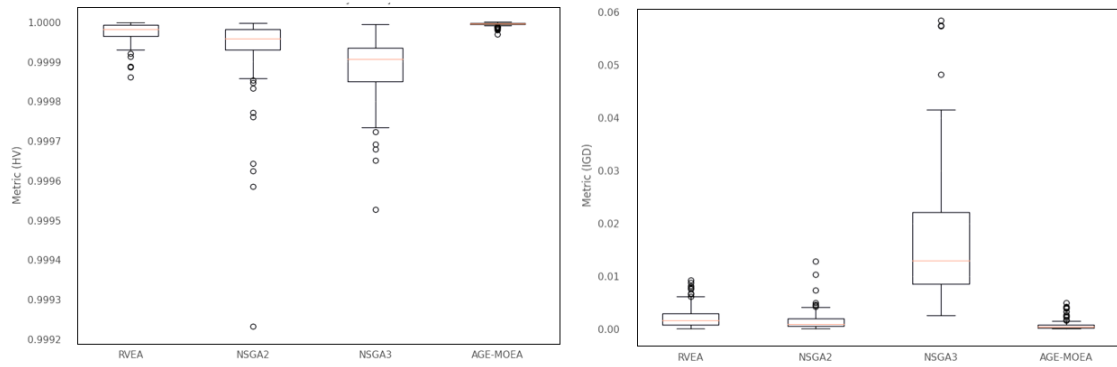


Figure 26 – Final HV and IGD values for all MOEA tested and BH steels.

Table 10 – Dunn’s test P-values for Final HV and IGD values for all MOEA tested and BH steels (values above the main diagonal represent the values for the HV metric, and values below the main diagonal indicate the values for the IGD metric).

| MOEA | NSGA-II | NSGA-III | RVEA | AGE-MOEA |
|-----------------|---------------|---------------|---------------|---------------|
| NSGA-II | 1.0000 | 5.68e-04 | 2.69e-15 | 5.28e-49 |
| NSGA-III | 1.24e-20 | 1.0000 | 8.27e-06 | 1.91e-29 |
| RVEA | 9.44e-20 | 8.28e-01 | 1.0000 | 9.83e-12 |
| AGE-MOEA | 2.32e-51 | 8.25e-09 | 2.22e-09 | 1.0000 |

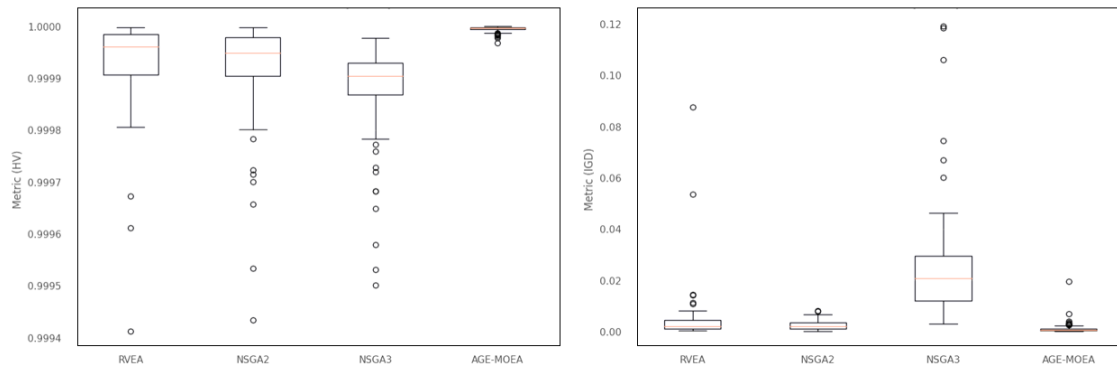


Figure 27 – Final HV and IGD values for all MOEA tested and HSLA steels.

Table 11 – Dunn’s test P-values for Final HV and IGD values for all MOEA tested and HSLA steels (values above the main diagonal represent the values for the HV metric, and values below the main diagonal indicate the values for the IGD metric).

| MOEA | NSGA-II | NSGA-III | RVEA | AGE-MOEA |
|-----------------|---------------|---------------|---------------|---------------|
| NSGA-II | 1.0000 | 4.61e-04 | 1.09e-09 | 1.47e-45 |
| NSGA-III | 2.78e-23 | 1.0000 | 9.49e-03 | 1.49e-26 |
| RVEA | 8.86e-24 | 9.10e-01 | 1.0000 | 6.98e-16 |
| AGE-MOEA | 5.76e-50 | 8.56e-07 | 1.52e-06 | 1.0000 |

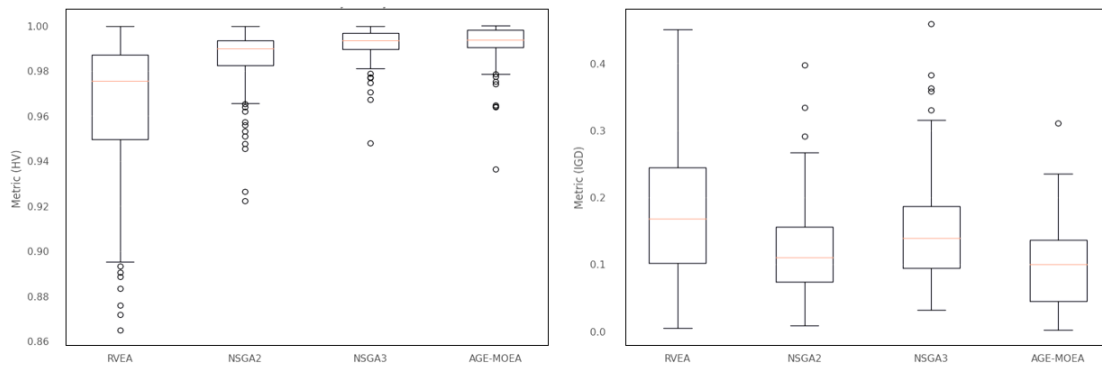


Figure 28 – Final HV and IGD values for all MOEA tested and DP steels.

Table 12 – Dunn’s test P-values for Final HV and IGD values for all MOEA tested and DP steels (values above the main diagonal represent the values for the HV metric, and values below the main diagonal indicate the values for the IGD metric).

| MOEA | NSGA-II | NSGA-III | RVEA | AGE-MOEA |
|-----------------|---------------|---------------|---------------|---------------|
| NSGA-II | 1.0000 | 4.08e-04 | 1.07e-09 | 6.10e-46 |
| NSGA-III | 5.19e-25 | 1.0000 | 1.04e-02 | 1.09e-26 |
| RVEA | 5.31e-17 | 5.12e-02 | 1.0000 | 4.31e-16 |
| AGE-MOEA | 2.75e-48 | 1.94e-05 | 4.91e-10 | 1.0000 |

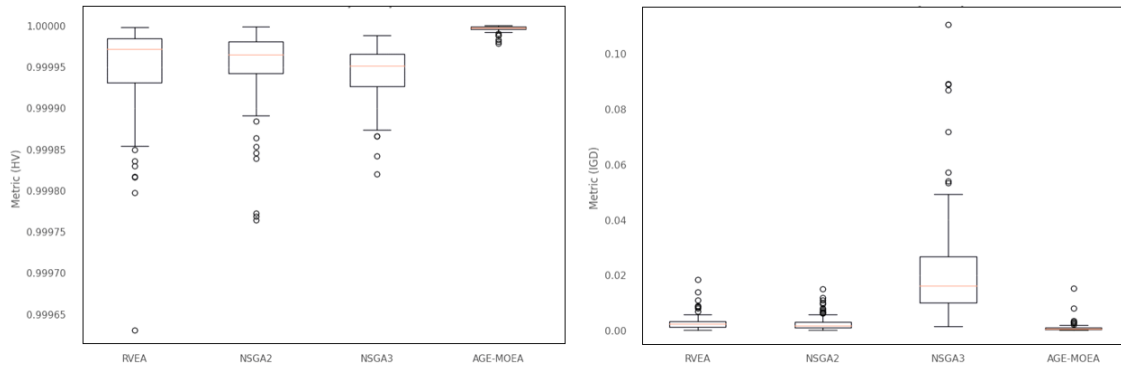


Figure 29 – Final HV and IGD values for all MOEA tested and TRIP steels.

Table 13 – Dunn’s test P-values for Final HV and IGD values for all MOEA tested and TRIP steels (values above the main diagonal represent the values for the HV metric, and values below the main diagonal indicate the values for the IGD metric).

| MOEA | NSGA-II | NSGA-III | RVEA | AGE-MOEA |
|-----------------|---------------|---------------|---------------|---------------|
| NSGA-II | 1.0000 | 1.29e-24 | 8.81e-22 | 9.84e-55 |
| NSGA-III | 1.44e-04 | 1.0000 | 5.15e-01 | 9.33e-08 |
| RVEA | 3.15e-05 | 7.18e-01 | 1.0000 | 2.09e-09 |
| AGE-MOEA | 1.27e-45 | 3.19e-25 | 1.31e-23 | 1.0000 |

Figures 25 to 29 depict the results obtained for a total of one thousand optimizations for each MOEA, and the final values of the HV and IGD performance indicators are presented in boxplots. From the results, we can observe the trend and consistency of AGE-MOEA in reaching optimal values for the indicators.

Tables 9 to 13 show the statistical tests involving each MOEA and steel grade for both performance metrics. The values above the main diagonal represent the values for the HV metric, and values below the main diagonal indicate the values for the IGD metric.

When examining the scales achieved in the plots, it becomes evident that the variation is minimal. However with the analyses shown in the tables, there is statistical difference between the values reached by the four MOEAs in the vast majority of cases. The exceptions are tests comparing RVEA with NSGA-III, which show a slight no statistical difference between the data sets.

Even with significant differences in performance indicators in the conducted optimizations, it is crucial to analyze how each MOEA generates solutions around the three objective mechanical properties and how these solutions are distributed concerning the desired target. Thus, steels with the worst HV and IGD values were chosen for an analysis of the distribution of property values found in the optimization for each MOEA. The selection of steels with worse indicators aims to assess and choose a MOEA based on its accuracy in finding solutions on or

near the target, even in the worst-case scenario for evaluated properties. Table 14 shows the mechanical properties corresponding to the critical steels used for the analysis.

Table 14 – Critical steel mechanical properties values used for distribution analysis.

| Steel Grade | TS (MPa) | YS (MPa) | EL (%) |
|-------------|----------|----------|--------|
| BH | 243 | 356 | 38.1 |
| IF | 292 | 356 | 42.7 |
| DP | 316 | 495 | 27.4 |
| HSLA | 497 | 597 | 20.3 |
| TRIP | 416 | 693 | 29.4 |

Figures 30 to 34 display plots for each MOEA, illustrating YS on the x-axis and TS on the y-axis, while the color bar represents EL. When comparing the results for the MOEAs in each steel grade, it becomes evident that NSGA-II, the default optimizer in the system, exhibits a widely dispersed solution cloud in relation to the targets. This is suboptimal, as maximizing the system's efficiency requires a set of solutions as close as possible to the targets, a collection of exact and accurate solutions. In contrast, RVEA demonstrates a more compact set of solutions, achieving superior precision and accuracy compared to other MOEAs across all steel grades.

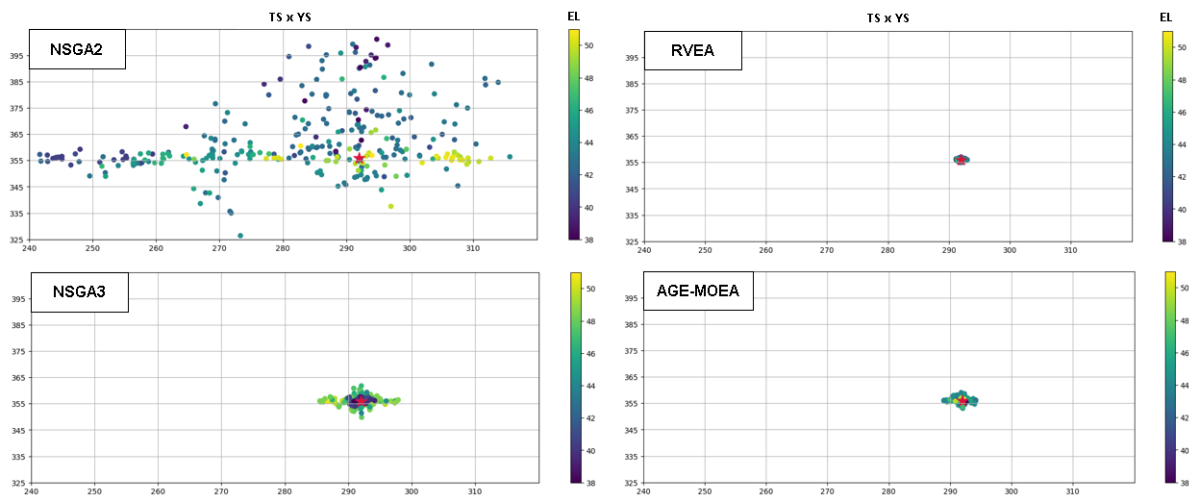


Figure 30 – Dispersion of mechanical properties for each MOEA for IF steel.

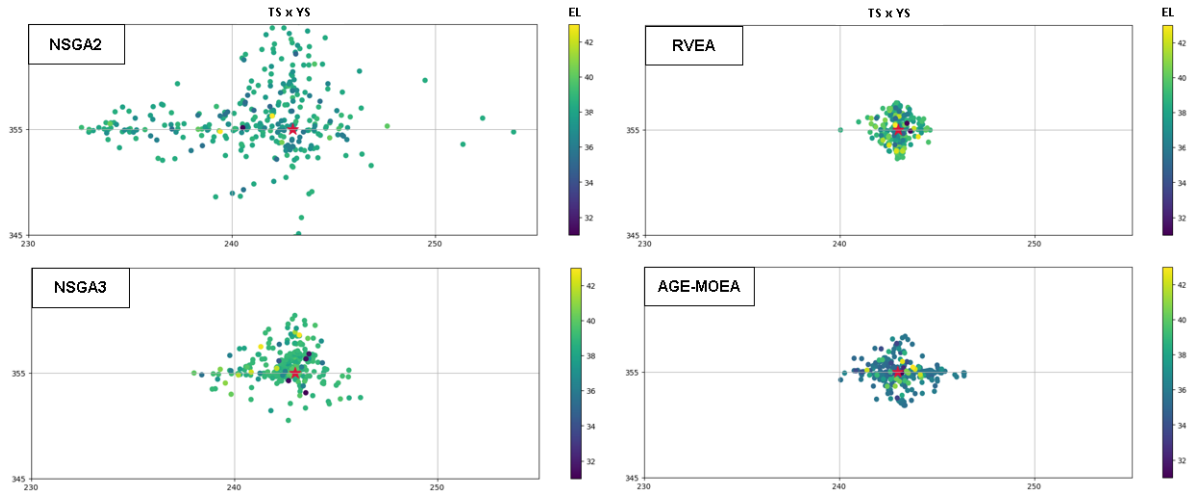


Figure 31 – Dispersion of mechanical properties for each MOEA for BH steel.

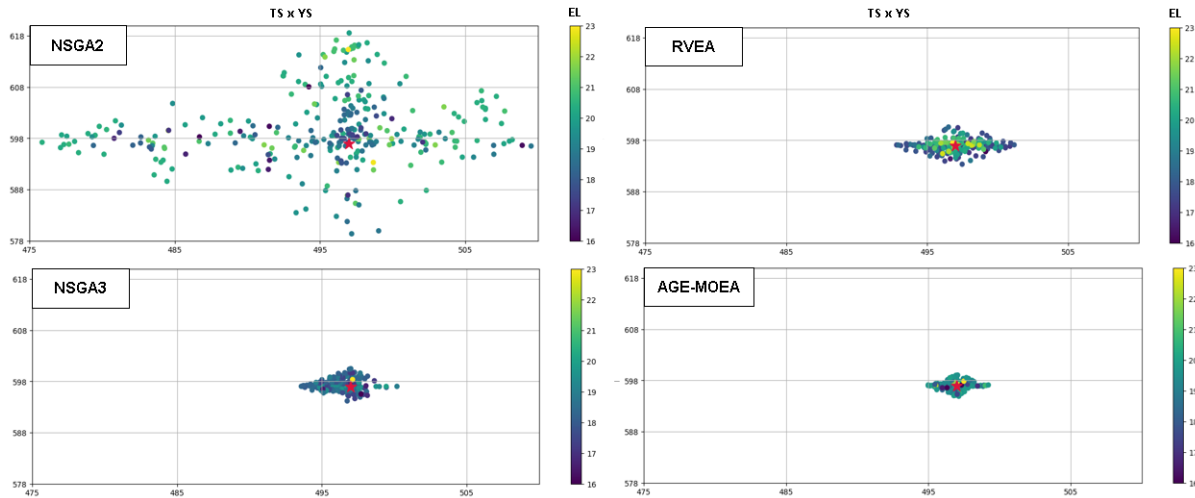


Figure 32 – Dispersion of mechanical properties for each MOEA for HSLA steel.

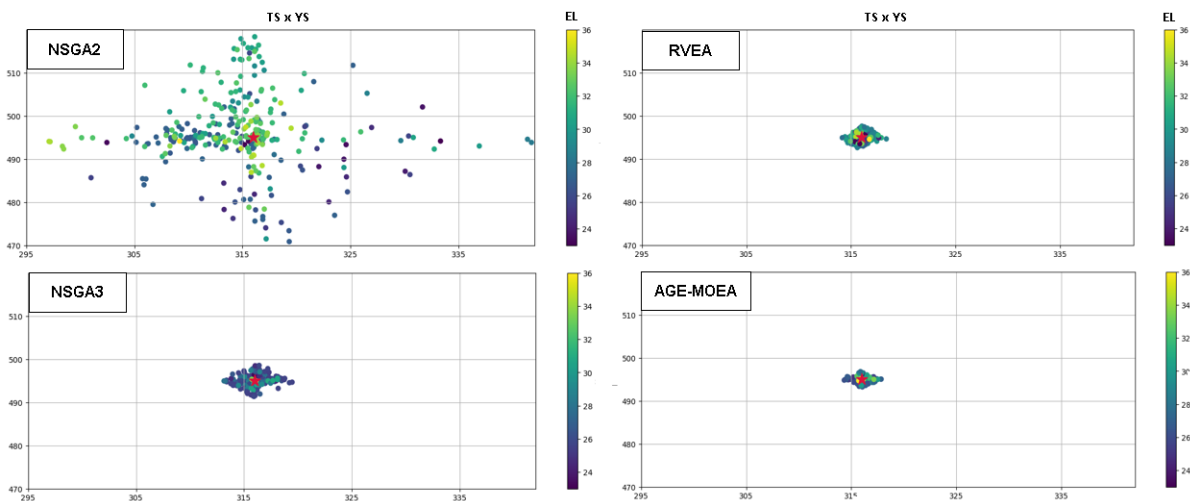


Figure 33 – Dispersion of mechanical properties for each MOEA for DP steel.

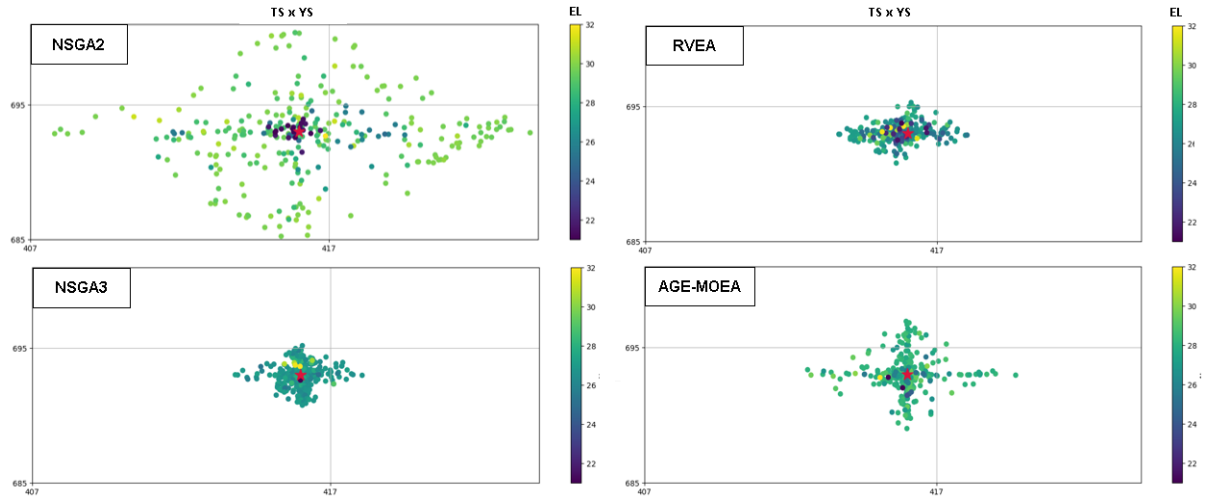


Figure 34 – Dispersion of mechanical properties for each MOEA for TRIP steel.

In addition to performance evaluation, analyzing the runtime of MOEAs is crucial, as a potential transition to another optimizer should not significantly increase the computational costs of the application. Table 15 provides the mean values and standard deviations for the execution times of each MOEA. It is noteworthy that the only optimizer deviating from the time pattern is AGE-MOEA, while the others exhibit very similar values.

Table 15 – MOEAs Mean time for each run.

| MOEA | Mean (sec) | Standart Deviation (sec) |
|----------|------------|--------------------------|
| NSGA-II | 20.3 | 1.98 |
| NSGA-III | 23.5 | 2.11 |
| RVEA | 20.7 | 2.36 |
| AGE-MOEA | 32.8 | 3.23 |

Consequently, based on these results, RVEA was chosen to replace NSGA-II as the system's default optimizer. This decision was influenced by RVEA's convergence capability, being one of the best MOEA in terms of performance indicators, and its high precision and accuracy concerning the proposed critical mechanical property targets, in addition to not adding any additional time to system execution. Ultimately, RVEA was adopted as the standard for subsequent subsections and conducted tests.

5.2.2 TWO-ARCHIVES STRATEGY

The configuration proposed in this work uses two archives in conjunction with the reintroduction of solutions in the optimization process.

Gene frequency metric (GF) will be calculated for each configuration, and the mean and standard deviation of each configuration will be evaluated. The optimization is shown in Table 16. We employ the following parameters:

Table 16 – Optimization parameters for the two-archive strategy evaluation.

| Parameter | Value |
|--------------|-------|
| Generations | 100 |
| Individuals | 50 |
| Archive size | 100 |
| Runs | 30 |

5.2.2.1 REINTRODUCTION PARAMETER

The parameter governing the reintroduction of solutions into the optimization process was subjected to testing using different values: 4%, 6%, 8%, and 10%. The purpose of this test is to identify the value that yields better GF values, thus increasing the genotypic diversity of the solutions found by the MOEA. Figure 35 presents box plots with the values obtained from 30 runs for different parameter values for all steel grades.

As the statistical tests shown in table 17 show, no statistically significant difference is observed among the tested values. Consequently, we opted for selecting the value of 4% as the most suitable, as it is the lowest among those examined.

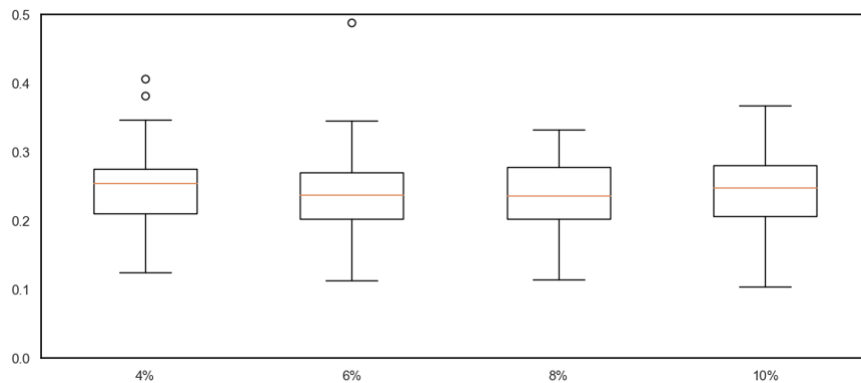


Figure 35 – Box plots of the GF values for different values of the solution reintroduction parameter.

Table 17 – P-values for reintroduction parameter using Dunn test.

| Parameter | 4% | 6% | 8% | 10% |
|-----------|--------|--------|--------|--------|
| 4% | 1.0000 | 0.1572 | 0.3644 | 0.8181 |
| 6% | | 1.0000 | 0.6117 | 0.2361 |
| 8% | | | 1.0000 | 0.4984 |
| 10% | | | | 1.0000 |

This choice is made because, given that the solutions in the DA may not necessarily exhibit superior fitness to those selected from the population, substituting fewer solutions minimizes the risk of negatively impacting the optimization process.

Furthermore, considering the elitism technique, widely used in genetic algorithms, when transferring many solutions with the best fitness values to the next generation, we may cause a decrease in the exploratory ability of the optimizer, thus reducing the diversity of the population (SELÇUKLU, 2023). Conversely, when transferring many solutions with high genotypic diversity to the next generations, we may interfere with the optimizer's ability to converge to progressively better solutions.

5.2.2.2 ARCHIVES PERFORMANCES

The MOEA configuration proposed will be referred to as "C2". To assess its performance, a comparison will be made with the configuration proposed by Sgrott (2022), which utilizes only the SA archive and does not include the reintroduction of solutions in the optimization process. This MOEA configuration will be referred to as "C1".

Table 18 shows the selected mechanical property targets. We chose these specific values using specialists' information.

Table 18 – Mechanical property values used for each steel.

| Steel Grade | TS (MPa) | YS (MPa) | EL (%) |
|-------------|----------|----------|--------|
| BH | 243 | 356 | 38.1 |
| IF | 292 | 356 | 42.7 |
| DP | 316 | 495 | 27.4 |
| HSLA | 497 | 597 | 20.3 |
| TRIP | 416 | 693 | 29.4 |

Using the optimization parameters from the 16 table, the C1 and C2 configurations were tested. Figure 36 shows box plots with the values of GF obtained from 30 runs for each grade of steel. The results show an increase when the DA is used.

Additionally, it is notable that the area representing the lower limit of the Diversity Archive (DA) tends to overlap with the region where the Solution Archive (SA) occurs most frequently. This implies that even in instances where the SA exhibits suboptimal performance, it is unlikely to perform worse than the DA. This correlation between the SA and DA is advantageous as it offers performance assurance for the DA.

Furthermore, Table 19 illustrates the results of the Dunn test for each type of steel comparing configurations C1 and C2. From the results, it is evident that there is a significant difference between the configurations for all steels except for TRIP steel. However, this lack of statistical significance does not necessarily imply a lack of practical significance. Therefore, further analyses were conducted to ensure the practical effects of the proposal.

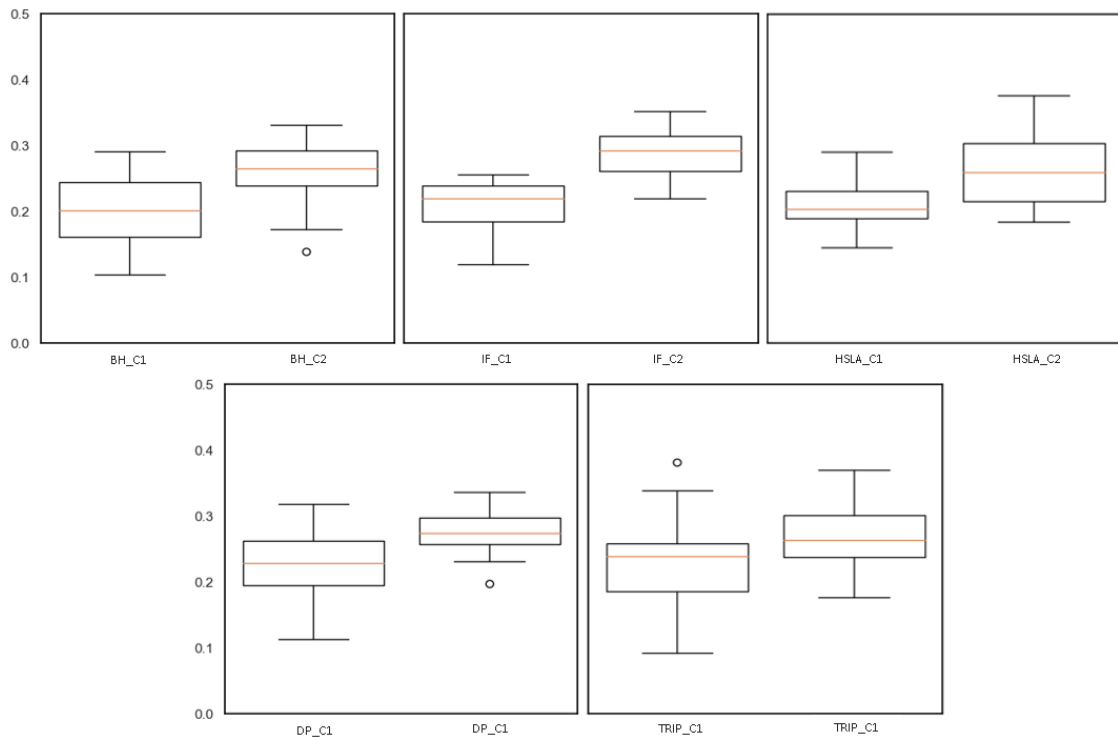


Figure 36 – GF results for each type of steel and 30 runs.

Table 19 – Dunn’s test P-values for each type of steel for comparing the two archives configurations.

| Steel | P-value |
|--------------|----------------|
| BH | 4.50e-03 |
| IF | 7.42e-07 |
| HSLA | 9.00e-04 |
| DP | 1.70e-03 |
| TRIP | 6.59e-02 |

Even with the noticeable increase when using the Diversity Archive (DA), additional analyses were conducted to ensure that the enhancement of genotypic diversity was significant for each optimization variable. This fulfills the goal of providing more steel design options for decision-makers. Figures 37 and 38 show histograms comparing the two configurations; each column represents the count of occurrences of a given value within the analyzed range.

For this analysis, the TRIP steel was chosen due to its complexity and high mechanical strength values, presenting more challenges for the MOEA. Ensuring that an increase in genotypic diversity is achieved for this grade of steel is crucial.

In both Figures 37 and 38, we can observe that, in all six cases shown, the C2 configuration managed to expand the range of values for the solutions discovered in the optimization, filling gaps in regions where C1 fails to find steel options. This indicates greater diversity in the data distribution when using C2.

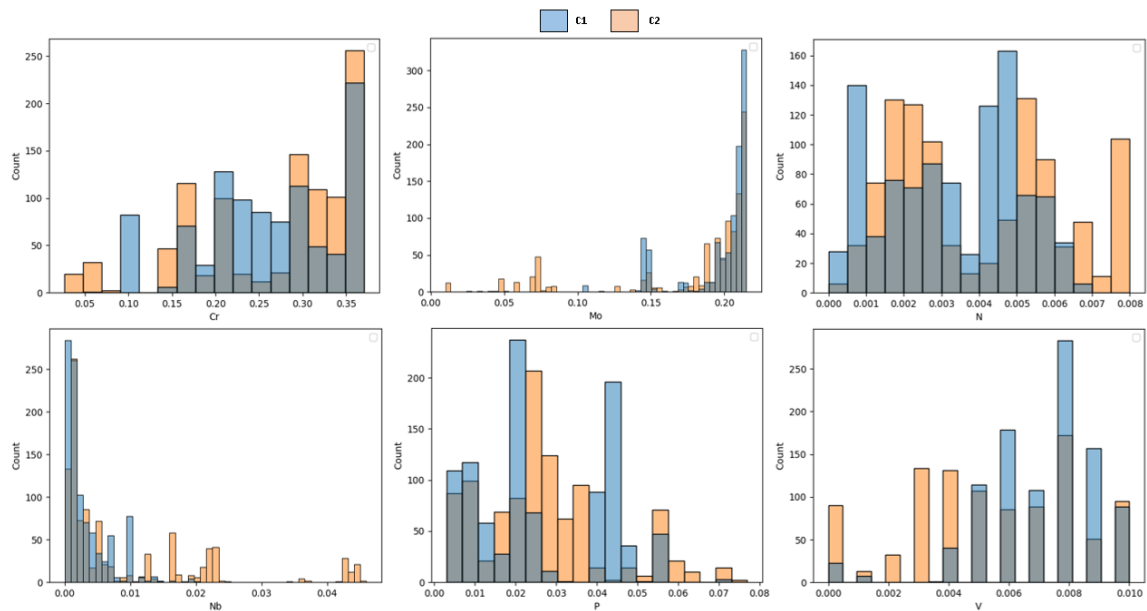


Figure 37 – Histogram of the configurations for six chemical input variables.

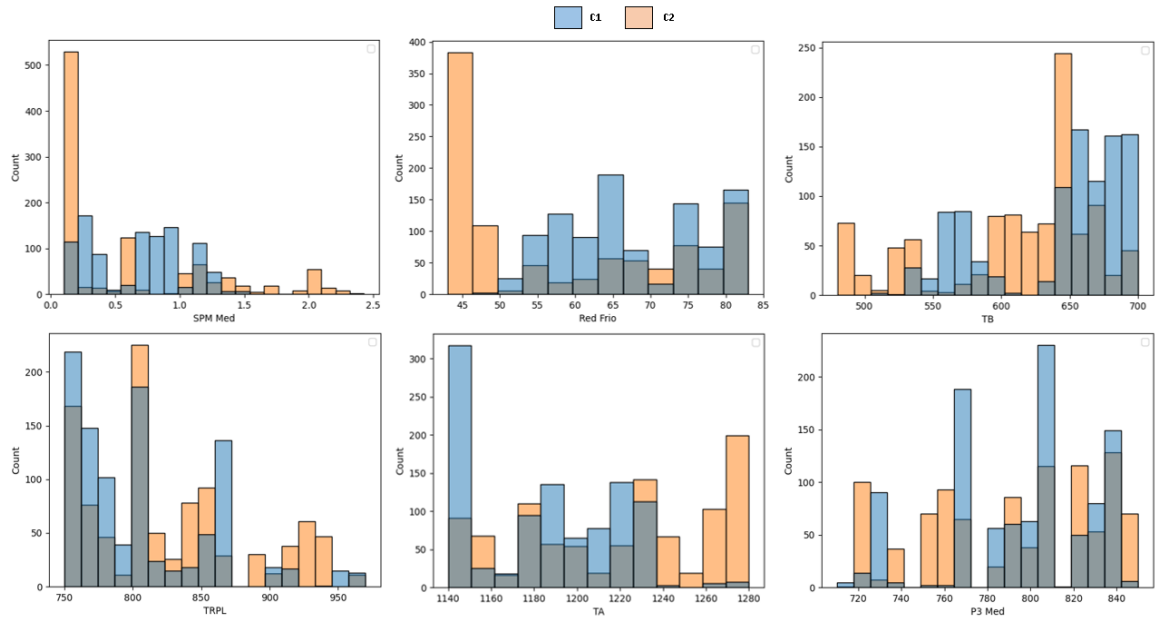


Figure 38 – Histogram of the configurations for six process parameters input variables.

Overall, only two chemical composition variables showed cases where the use of C1 was not effective, namely Nickel and Sulfur. Regarding the process parameter variables, only Real Width exhibited a slight disadvantage when using C1. Nevertheless, given that this occurred in only three out of twenty-seven cases, we can conclude that the use of C1 was beneficial for the genotypic diversity of the optimization, proving to be effective, particularly in variables with a greater impact on the results of the E-ANN.

To ensure that, even with the increased genotypic diversity, the accuracy and precision of the MOEA in finding solutions close to the targets were not compromised, an analysis of the Dispersion of mechanical properties was conducted for each configuration. Figure 39 shows the Dispersion of mechanical properties for TRIP steel; the stars in the plots represent the target values.

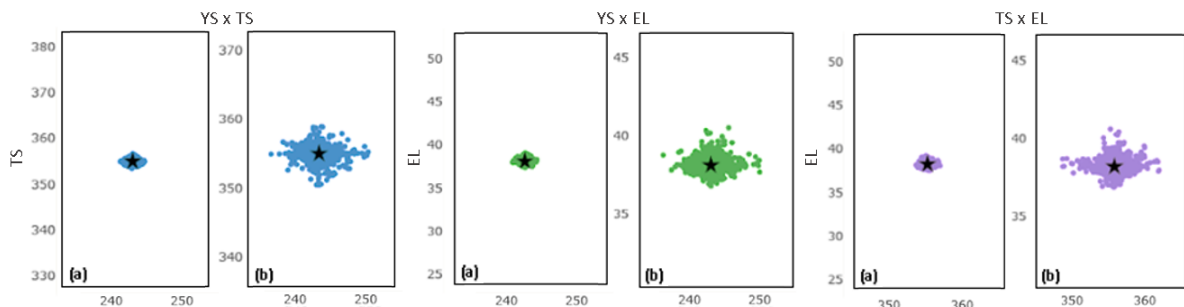


Figure 39 – TRIP steel dispersion of mechanical properties for (a) C1, (b) C2.

There is a noticeable increase in the Dispersion of points around the target values, indicating a rise in phenotypic diversity resulting from greater genotypic diversity. However, this variation does not exceed 10 MPa for YS and TS and 5% for EL. For these properties, such variations do not denote a significant change, given that the measurement processes throughout

the factory can introduce similar errors. From a metallurgical standpoint, focusing solely on the properties, the steels are practically indistinguishable due to the precision of the manufacturing process and steel measurements. Although only the results for TRIP steel are shown, the behavior is repeated for all the other types of steel studied.

5.2.3 CASE STUDY: ROTA 2030

A case study was conducted to test the functionality and capability of staggered optimization. This case study represents a real-world scenario where the client purchases steel. Given the mechanical property requirements, the company opts to increase the yield strength (YS) of the steel to ensure a greater safety margin. For comparison purposes, standard optimization without staggering will also be performed.

The variables selected by the experts for the staggering, along with the bounds and increments, are shown in Table 20; all the other variables are constants. The mechanical properties targets are shown in Table 21.

Table 20 – Description from the staggered variables.

| Name | Description | Unit | Bounds | Increment |
|-------------|--|-------------|---------------|------------------|
| X_{16} | Coiling temperature | °C | [800, 920] | 20 |
| X_{17} | Heating temperature before hot rolling | °C | [550, 700] | 20 |
| X_{21} | Line speed | m/s | [60, 160] | 20 |
| X_{22} | Mean Skin Pass Mill elongation | % | [0.2, 1.8] | 0.2 |
| X_{23} | Temperature from Pyrometer 03 | °C | [750, 830] | 20 |
| X_{24} | Temperature from Pyrometer 04 | °C | [750, 830] | 20 |

Table 21 – Mechanical property values used for each steel.

| TS (MPa) | YS (MPa) | EL (%) |
|-----------------|-----------------|---------------|
| 230 | 310 | 43 |

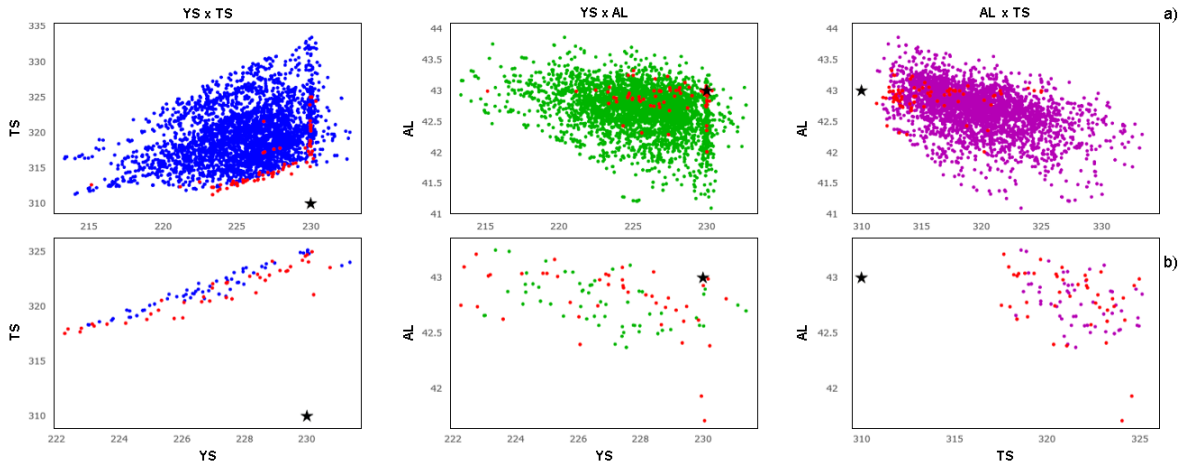


Figure 40 – Dispersion of mechanical properties for the a) staggered optimization b) standart optimization.

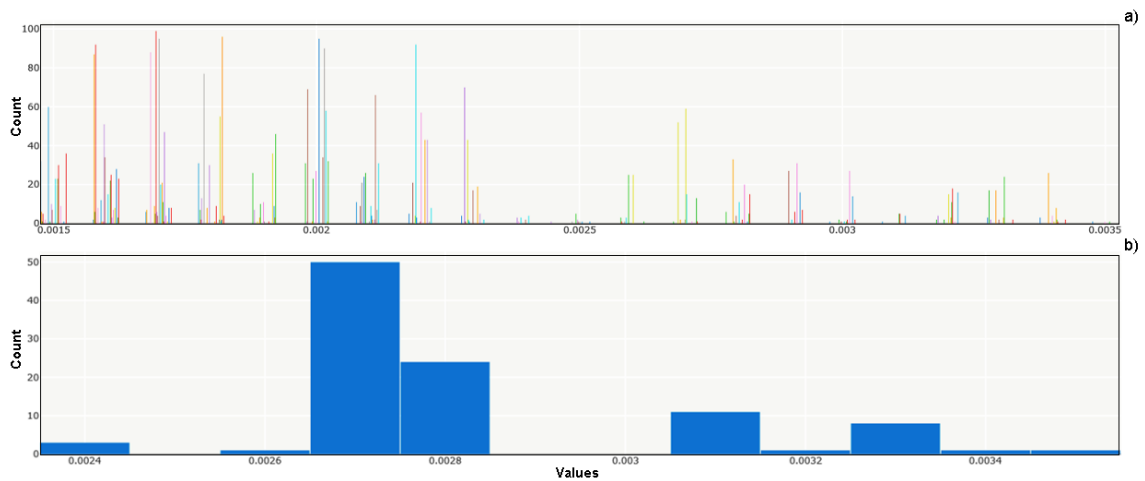


Figure 41 – Carbon histogram for the a) staggered optimization b) standart optimization.

Even without analyzing the results, some conclusions can be drawn regarding the differences between the two methods. Due to the use of multiple optimizations with different bounds, staged optimization may exhibit segments better than standard optimization, with a higher concentration of solutions near the target, as well as segments worse than standard optimization, with a higher concentration in regions distant from the target, since not all generated bounds will be conducive to good results. This behavior can be seen in Figure 40, where the red dots represent the non-dominated solutions. Furthermore, analyzing the histograms in Figure 41, we can see that even for variables that were not staged in the optimization, their operating range increased compared to standard optimization.

In both cases, the generated results only reach the target for some properties. However, it is essential to consider that the study aims to improve the properties by modifying only six out of 27 possible variables, which are primarily process parameters while keeping the chemical composition constant. Thus, the optimizer is still able to identify possibilities that come close to

the desired extreme composition, fulfilling its role of guiding a direction rather than delivering a finished steel product.

5.2.3.1 STAGGERED OPTIMIZATION PARALLELIZATION

Given the characteristics of staggered optimization, which creates multiple additional optimizations, parallelism emerges as an alternative to reduce the total execution time. Unlike typical parallelization processes in MOEA, where the fitness function or genetic operators are parallelized due to being the optimization bottleneck, in this case, each subprocess created and assigned to a processor thread represents an optimization with one of the possibilities from the total set of bounds. The specifications of the system used for the experiment are shown below:

- Operating System: Debian GNU/Linux 12
- Processor: Intel Core i7 with six cores and a base frequency of 2.2 GHz
- Memory: 16 GB RAM
- Storage: 1 TB of available space

To standardize the test, the increment for each variable chosen for staggering is selected so that its range is divided to create five additional optimizations. Figure 42 shows the execution times for stepped optimizations with and without the use of parallelism for different numbers of stepped variables. From the results, we can clearly see the reduction in execution time achieved with parallel optimization. Table 22 shows the speedup values achieved for each number of staggered variables.

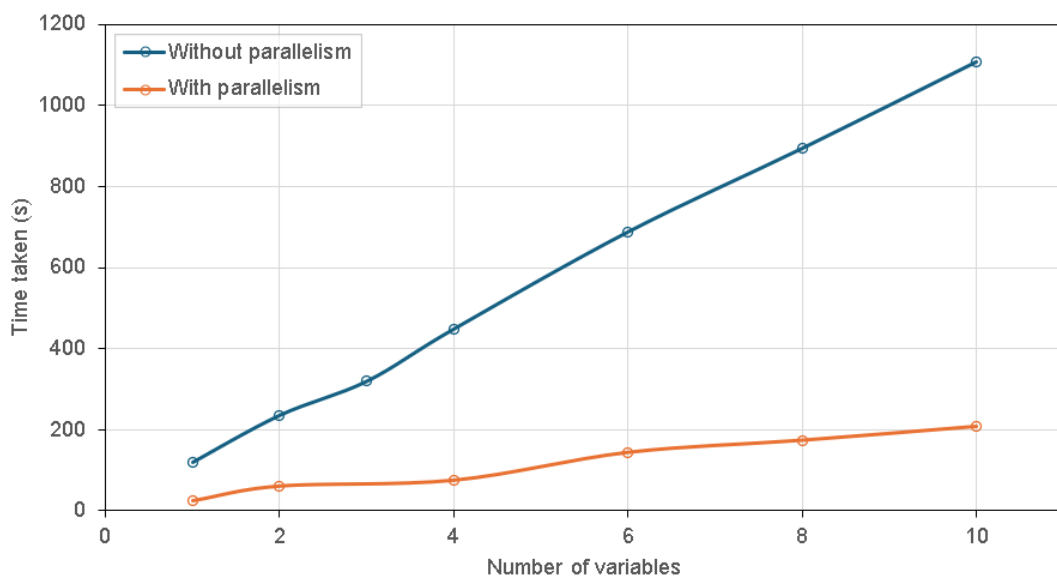


Figure 42 – Time Taken to Display the Plots plot.

Table 22 – Speedup values for each case.

| Number of variables | 1 | 2 | 4 | 6 | 8 | 10 |
|---------------------|-----|-----|-----|-----|-----|-----|
| Speed up | 4.6 | 3.8 | 5.9 | 4.8 | 5.2 | 5.4 |

As the complete system is used through a local web server, it is essential to test the performance of parallelization in conjunction with the browser, as well as to make comparisons between browsers to determine the recommended browser for the system. To this end, an experiment was conducted to identify the best among three options: Google Chrome, Firefox, and Microsoft Edge. Other browsers were excluded from this comparison for the following reasons: either the app does not support them (such as Safari), or they are based on one of the three main browsers (for example, Opera and Brave are Chrome-based browsers).

The experiment involved two main comparisons: the Time taken to complete the optimization and display the graphs of its results and the Memory consumed to display the results. As before, for each scaled variable, the increment is set so that the number of additional optimizations is 5.

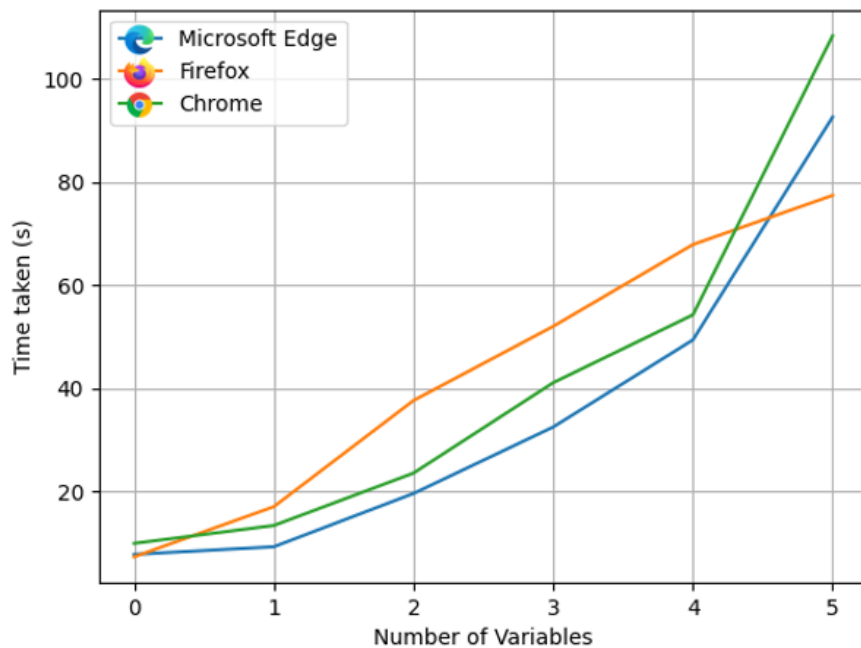


Figure 43 – Time taken to complete the optimization and display the results plots.

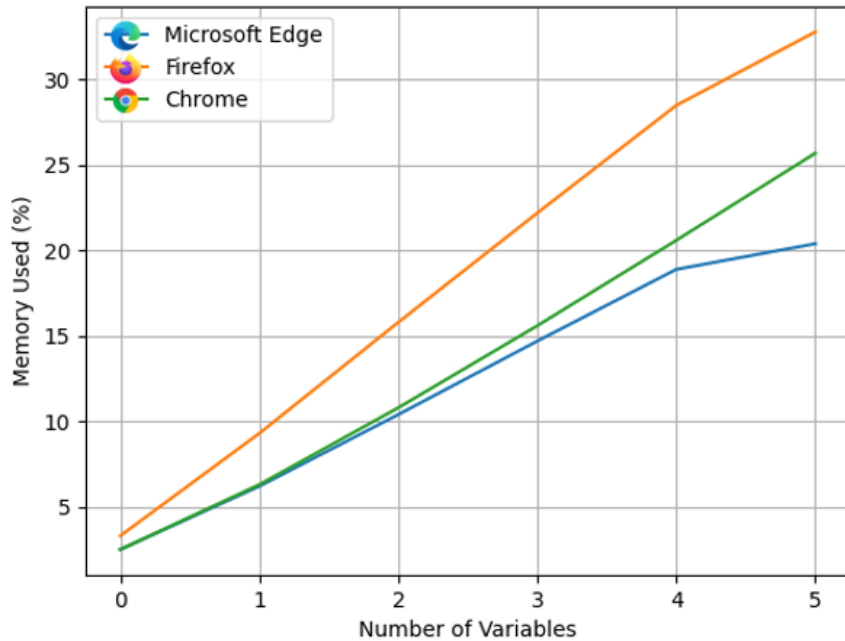


Figure 44 – Memory Consumed to Display the results plots.

As indicated by the data presented above, there is not a substantial difference between the browsers in either plot. Nevertheless, it is worth noting that Firefox, although it takes up more Time and Memory than the other two, exhibits periods where the gaps narrow. In the time plot, Firefox even falls below the others. Given that there is no evident advantage, users can freely choose any of the three browsers, as the differences between them are minimal. Last but not least, it is essential to acknowledge that despite the observations above, the app encountered occasional issues when used with Chrome-based browsers. Therefore, if a recommendation were to be made, opting for *Firefox* would be advisable, considering that the app is primarily developed for compatibility with it.

6 FINAL CONSIDERATIONS AND FUTURE WORK

In pursuit of enhancing the outcomes derived from the system proposing novel chemical compositions and processing parameters for steel production with desired mechanical properties, this study has diligently focused on two pivotal objectives within the optimization procedure's search mechanism. Our primary goal has been to elevate the precision of the solutions generated in relation to the targeted mechanical properties, with the overarching aim of rendering a majority of results more pertinent and representative as viable solutions for decision-makers.

Concurrently, we have strived to attain greater genotypic diversity in the solutions unearthed by the optimizer. This deliberate pursuit allows for the exploration of diverse steel configurations exhibiting the desired mechanical properties, thereby substantially enriching the spectrum of options available to decision-makers. The convergence of these objectives signifies a substantial step forward in the efficacy of the system, presenting a more robust and versatile tool for decision-makers in the realm of steel production optimization.

The adoption of AutoML structures, exemplified by NAS tools, has brought about a paradigm shift in machine learning applications. These structures allow users to navigate the vast search space of neural network architectures efficiently. From this, our research establishes convincing evidence of the effectiveness of employing an ensemble of ANNs in predicting the mechanical properties of various types of steel. Demonstrating superiority in performance metrics on the test dataset, the ensemble model outperformed its single ANN counterpart.

Moreover, the ensemble methodology yielded profound insights into the intricate relationships between input parameters and mechanical properties. This revealed the model's sensitivity to incorporating diverse types of steels, ranging from simple to complex, each characterized by distinct hardening mechanisms.

From the point of view of optimization, the utilization of an archive targeting solution diversity, coupled with reintroducing these solutions into the optimizer, proves highly advantageous in implementing multi-objective evolutionary algorithms. This practice fosters an augmentation in genotypic diversity among solutions.

Analyzing variable histograms substantiates the practicality of verifying diversity through the frequency metric, ensuring diversity is maintained in the Diversity Archive (DA). This broadens the scope of values covered by the DA, contributing to a more comprehensive exploration of the search space. This approach exhibits promise for optimizing complex problems with multiple objectives, where diversity plays a pivotal role in preventing premature convergence and locating more diverse solutions proximate to the global optimum.

Noteworthy enhancements in the diversity metric, coupled with an expanded range of variable use, are complemented by positive feedback from experts. This attests to the efficacy of increased diversity, enabling a more thorough exploration of alternatives for the proposed mechanical property targets.

Besides the dual-archive strategy, the staggered optimization applied in the Rota 2030 case

study also provided experts with a broader view of the possibilities for chemical compositions and process parameters. Finding the ideal boundary values for optimization can be challenging, and by using staggered optimization, this process can be accelerated.

Finally, the work encounters several challenges, notably in understanding how the distinct characteristics of different types of steel impact the system's ability to propose innovative solutions, avoiding associations with potential biases. Despite this, the applied techniques have proven effective in achieving the proposed objective, providing the industry with the capacity for innovation and readiness to tackle new challenges in the metallurgical sector.

Future works can involve the use of better data processing techniques, modeling new data such as microstructure, and revisit the division of the database and data slicing, a deeper investigation, explanation and interpretation of the prediction model by using new xAI tools, and finally, revamping the optimization algorithm such that it maintains a more diversified population across its evolution, by implementing adaptive controls.

6.1 ACKNOWLEDGMENTS

The authors thank the ArcelorMittal Brazil R&D Group for its financial and technical support.

BIBLIOGRAPHY

- ABIODUN, Oludare Isaac et al. State-of-the-art in artificial neural network applications: A survey. **Heliyon**, Elsevier, v. 4, n. 11, p. e00938, 2018. Cited on page 29.
- ALAM, Kazi Md Rokibul; SIDDIQUE, Nazmul; ADELI, Hojjat. A dynamic ensemble learning algorithm for neural networks. **Neural Computing and Applications**, Springer, v. 32, p. 8675–8690, 2020. Cited 2 times on pages 9 and 32.
- ALAM, Kazi Md Rokibul; SIDDIQUE, Nazmul; ADELI, Hojjat. A dynamic ensemble learning algorithm for neural networks. **Neural Computing and Applications**, Springer, v. 32, p. 8675–8690, 2020. Cited on page 20.
- ALBA, Enrique; LUQUE, Gabriel; NESMACHNOW, Sergio. Parallel metaheuristics: recent advances and new trends. **International Transactions in Operational Research**, v. 20, n. 1, p. 1–48, 2013. Disponível em: <<https://onlinelibrary.wiley.com/doi/abs/10.1111/j.1475-3995.2012.00862.x>>. Cited on page 40.
- ALETI, Aldeida; MOSER, Irene. A systematic literature review of adaptive parameter control methods for evolutionary algorithms. **ACM Comput. Surv.**, Association for Computing Machinery, New York, NY, USA, v. 49, n. 3, oct 2016. ISSN 0360-0300. Disponível em: <<https://doi.org/10.1145/2996355>>. Cited on page 39.
- AUDET, Charles et al. Performance indicators in multiobjective optimization. **European journal of operational research**, Elsevier, v. 292, n. 2, p. 397–422, 2021. Cited 3 times on pages 40, 41, and 42.
- BENALI, Fodil et al. A new reference-based algorithm based on non-euclidean geometry for multi-stakeholder media planning. In: **SAC '22: The 37th ACM/SIGAPP Symposium on Applied Computing**. Virtual Event, United States: ACM, 2022. p. 1056–1065. Disponível em: <<https://hal.science/hal-03692704>>. Cited on page 38.
- BINITHA, S.; SATHYA, S.S. A survey of bio inspired optimization algorithms. **International Journal of Soft Computing and Engineering**, v. 2, p. 137–151, 01 2012. Cited on page 35.
- BUDYNAS, Richard G; NISBETH, J Keith. **Elementos de Máquinas de Shigley-10ª Edição**. [S.l.]: McGraw Hill Brasil, 2016. Cited on page 26.
- CALLISTER, William D.; RETHWISCH, David G. **Materials science and engineering : an introduction / William D. Callister, Jr., David G. Rethwisch**. 8th ed.. ed. Hoboken, NJ: John Wiley & Sons, 2010. ISBN 9780470448649. Cited on page 26.
- CHAHAR, Vijay; KATOCH, Sourabh; CHAUHAN, Sumit. A review on genetic algorithm: Past, present, and future. **Multimedia Tools and Applications**, v. 80, 02 2021. Cited on page 35.
- CHENG, Ran et al. A reference vector guided evolutionary algorithm for many-objective optimization. **IEEE Transactions on Evolutionary Computation**, v. 20, n. 5, p. 773–791, 2016. Cited 2 times on pages 38 and 55.
- CORRIVEAU, Guillaume et al. Review and study of genotypic diversity measures for real-coded representations. **IEEE transactions on evolutionary computation**, IEEE, v. 16, n. 5, p. 695–710, 2012. Cited 2 times on pages 42 and 43.

DAS, Arun; RAD, Paul. Opportunities and challenges in explainable artificial intelligence (xai): A survey. **arXiv preprint arXiv:2006.11371**, 2020. Cited on page 65.

DEB, Kalyanmoy. **Multi-objective optimization using evolutionary algorithms**. [S.l.]: John Wiley & Sons, 2001. v. 16. Cited 2 times on pages 19 and 56.

DEB, Kalyanmoy; AGRAWAL, Ram Bhushan et al. Simulated binary crossover for continuous search space. **Complex systems**, Citeseer, v. 9, n. 2, p. 115–148, 1995. Cited on page 56.

DEB, Kalyanmoy; JAIN, Himanshu. An evolutionary many-objective optimization algorithm using reference-point-based nondominated sorting approach, part i: solving problems with box constraints. **IEEE transactions on evolutionary computation**, IEEE, v. 18, n. 4, p. 577–601, 2013. Cited 2 times on pages 37 and 55.

DEB, Kalyanmoy; JAIN, Himanshu. An evolutionary many-objective optimization algorithm using reference-point-based nondominated sorting approach, part i: Solving problems with box constraints. **IEEE Transactions on Evolutionary Computation**, v. 18, n. 4, p. 577–601, 2014. Cited on page 38.

DEB, Kalyanmoy; KALYANMOY, Deb. **Multi-Objective Optimization Using Evolutionary Algorithms**. USA: John Wiley & Sons, Inc., 2001. ISBN 047187339X. Cited 3 times on pages 32, 33, and 35.

DEB, Kalyanmoy et al. A fast and elitist multiobjective genetic algorithm: Nsga-ii. **IEEE transactions on evolutionary computation**, IEEE, v. 6, n. 2, p. 182–197, 2002. Cited 2 times on pages 19 and 37.

DESAI, Chitra. Comparative analysis of optimizers in deep neural networks. **International Journal of Innovative Science and Research Technology**, v. 5, n. 10, p. 959–962, 2020. Cited on page 30.

DING, Rui et al. A novel two-archive strategy for evolutionary many-objective optimization algorithm based on reference points. **Applied Soft Computing**, Elsevier, v. 78, p. 447–464, 2019. Cited on page 57.

DOMHAN, Tobias; SPRINGENBERG, Jost Tobias; HUTTER, Frank. Speeding up automatic hyperparameter optimization of deep neural networks by extrapolation of learning curves. In: **Twenty-fourth international joint conference on artificial intelligence**. [S.l.: s.n.], 2015. Cited on page 31.

DUTTA, Tanusree et al. Designing dual-phase steels with improved performance using ann and ga in tandem. **Computational Materials Science**, v. 157, p. 6–16, 2019. ISSN 0927-0256. Disponível em: <<https://www.sciencedirect.com/science/article/pii/S092702561830692X>>. Cited on page 49.

EIBEN, A.E.; SMIT, S.K. Parameter tuning for configuring and analyzing evolutionary algorithms. **Swarm and Evolutionary Computation**, v. 1, n. 1, p. 19–31, 2011. ISSN 2210-6502. Disponível em: <<https://www.sciencedirect.com/science/article/pii/S2210650211000022>>. Cited on page 39.

EIBEN, Agoston E; SMITH, James E. **Introduction to evolutionary computing**. [S.l.]: Springer, 2015. Cited on page 35.

ELSKEN, Thomas; METZEN, Jan Hendrik; HUTTER, Frank. Neural architecture search: A survey. **The Journal of Machine Learning Research**, JMLR. org, v. 20, n. 1, p. 1997–2017, 2019. Cited 2 times on pages 9 and 31.

FISCHER, F. D. et al. New view on transformation induced plasticity (TRIP). **International journal of plasticity**, v. 16, n. 7, p. 723–748, 2000. ISSN 07496419. Cited on page 25.

FONSECA, Carlos M; PAQUETE, Luís; LÓPEZ-IBÁÑEZ, Manuel. An improved dimension-sweep algorithm for the hypervolume indicator. In: IEEE. **2006 IEEE international conference on evolutionary computation**. [S.l.], 2006. p. 1157–1163. Cited 2 times on pages 9 and 41.

FONSTEIN, Nina. **Advanced high strength sheet steels**. [S.l.]: Springer, 2015. Cited 2 times on pages 23 and 25.

FURTADO, Maria Inês Vasconcellos. Redes neurais artificiais: uma abordagem para sala de aula. **Ponta Grossa, PR. Atena Editora**, p. 19, 2019. Cited on page 28.

GURAV, Depa; PATIL, S. R.; SOLANKI, Joginder. Optimizing tensile strength and yield point of steel bar with artificial neural network with enhanced parallel cat swarm optimizer. In: **2018 IEEE Global Conference on Wireless Computing and Networking (GCWCN)**. [S.l.: s.n.], 2018. p. 30–33. Cited on page 48.

HALL, J.N.; FEKETE, J.R. 2 - steels for auto bodies: A general overview. In: RANA, Radhakanta; SINGH, Shiv Brat (Ed.). **Automotive Steels**. Woodhead Publishing, 2017. p. 19–45. ISBN 978-0-08-100638-2. Disponível em: <<https://www.sciencedirect.com/science/article/pii/B978008100638200002X>>. Cited 2 times on pages 9 and 23.

HANSEN, Lars Kai; SALAMON, Peter. Neural network ensembles. **IEEE transactions on pattern analysis and machine intelligence**, IEEE, v. 12, n. 10, p. 993–1001, 1990. Cited on page 32.

HASTIE, Trevor et al. Overview of supervised learning. **The elements of statistical learning: Data mining, inference, and prediction**, Springer, p. 9–41, 2009. Cited 2 times on pages 27 and 28.

HOLLAND, John H. Genetic algorithms and the optimal allocation of trials. **SIAM Journal on Computing**, v. 2, n. 2, p. 88–105, 1973. Disponível em: <<https://doi.org/10.1137/0202009>>. Cited on page 35.

HOMMA, Toshimitsu; SALTELLI, Andrea. Importance measures in global sensitivity analysis of nonlinear models. **Reliability Engineering & System Safety**, Elsevier, v. 52, n. 1, p. 1–17, 1996. Cited on page 65.

HOSFORD, William F; CADDELL, Robert M. **Metal forming: mechanics and metallurgy**. [S.l.]: Cambridge university press, 2011. Cited on page 26.

HUANG, Chengpeng et al. Recent developments and perspectives of advanced high-strength medium mn steel: from material design to failure mechanisms. **Materials Futures**, IOP Publishing, v. 1, n. 3, p. 032001, sep 2022. Disponível em: <<https://dx.doi.org/10.1088/2752-5724/ac7fae>>. Cited on page 19.

ISHIBUCHI, Hisao; MASUDA, Hiroyuki; NOJIMA, Yusuke. Sensitivity of performance evaluation results by inverted generational distance to reference points. In: **IEEE. 2016 IEEE Congress on evolutionary computation (CEC)**. [S.l.], 2016. p. 1107–1114. Cited 2 times on pages 9 and 42.

JAIN, Himanshu; DEB, Kalyanmoy. An evolutionary many-objective optimization algorithm using reference-point based nondominated sorting approach, part ii: Handling constraints and extending to an adaptive approach. **IEEE Transactions on evolutionary computation**, IEEE, v. 18, n. 4, p. 602–622, 2013. Cited on page 55.

JANIESCH, Christian; ZSCHECH, Patrick; HEINRICH, Kai. Machine learning and deep learning. **Electronic Markets**, Springer, v. 31, n. 3, p. 685–695, 2021. Cited on page 27.

JIN, Haifeng; SONG, Qingquan; HU, Xia. Auto-keras: An efficient neural architecture search system. In: **Proceedings of the 25th ACM SIGKDD international conference on knowledge discovery & data mining**. [S.l.: s.n.], 2019. p. 1946–1956. Cited 3 times on pages 31, 53, and 54.

KITCHENHAM, Barbara; CHARTERS, Stuart. **Guidelines for performing systematic literature reviews in software engineering**. Citeseer, 2007. Cited on page 44.

KLOCK, Ana Carolina Tomé. Mapeamentos e revisões sistemáticos da literatura: um guia teórico e prático. **Cadernos de Informática**, v. 10, n. 1, p. 01–09, 2018. Cited on page 44.

KONFRST, Z. Parallel genetic algorithms: advances, computing trends, applications and perspectives. In: **18th International Parallel and Distributed Processing Symposium, 2004. Proceedings**. [S.l.: s.n.], 2004. p. 162–. Cited on page 40.

KONSTRUKCIJSKA, VISOKOTRDNA MALOLEGIRANA HSLA. High-strength low-alloy (hsla) steels. **Materiali in tehnologije**, v. 45, n. 4, p. 295–301, 2011. Cited on page 25.

Kouider Amar, Mohamed et al. A comparative study of multi-objective methods and algorithms for optimizing emulgels consistency and drug diffusion. **Journal of Drug Delivery Science and Technology**, v. 89, p. 104996, 2023. ISSN 1773-2247. Disponível em: <<https://www.sciencedirect.com/science/article/pii/S1773224723008481>>. Cited on page 55.

KRAMER, Oliver. Genetic algorithms. In: _____. **Genetic Algorithm Essentials**. Cham: Springer International Publishing, 2017. p. 11–19. ISBN 978-3-319-52156-5. Disponível em: <https://doi.org/10.1007/978-3-319-52156-5_2>. Cited 2 times on pages 35 and 36.

KRAUSS, G. Physical metallurgy of steels: An overview. In: RANA, Radhakanta; SINGH, Shiv Brat (Ed.). **Automotive Steels**. Woodhead Publishing, 2017. p. 95–111. ISBN 978-0-08-100638-2. Disponível em: <<https://www.sciencedirect.com/science/article/pii/B9780081006382000043>>. Cited 3 times on pages 19, 25, and 67.

KROGH, Anders. What are artificial neural networks? **Nature biotechnology**, Nature Publishing Group US New York, v. 26, n. 2, p. 195–197, 2008. Cited 2 times on pages 9 and 29.

KROGH, Anders; VEDELSBY, Jesper. Neural network ensembles, cross validation, and active learning. **Advances in neural information processing systems**, v. 7, 1994. Cited 2 times on pages 32 and 65.

KUMAR, Aman; CHAKRABARTI, Debalay; CHAKRABORTI, Nirupam. Data-driven pareto optimization for microalloyed steels using genetic algorithms. **steel research international**, Wiley Online Library, v. 83, n. 2, p. 169–174, 2012. Cited 3 times on pages 47, 48, and 49.

KUMAR, Sumit et al. A two-archive multi-objective multi-verse optimizer for truss design. **Knowledge-Based Systems**, Elsevier, v. 270, p. 110529, 2023. Cited on page 57.

LAMBORA, Annu; GUPTA, Kunal; CHOPRA, Kriti. Genetic algorithm- a literature review. In: **2019 International Conference on Machine Learning, Big Data, Cloud and Parallel Computing (COMITCon)**. [S.l.: s.n.], 2019. p. 380–384. Cited 2 times on pages 35 and 36.

LECUN, Yann; BENGIO, Yoshua; HINTON, Geoffrey. Deep learning. **nature**, Nature Publishing Group UK London, v. 521, n. 7553, p. 436–444, 2015. Cited on page 27.

LEE, Jin-Woong et al. A machine-learning-based alloy design platform that enables both forward and inverse predictions for thermo-mechanically controlled processed (tmcp) steel alloys. **Scientific Reports**, v. 11, n. 1, MAY 26 2021. ISSN 2045-2322. Cited 2 times on pages 48 and 49.

LI, Bingdong et al. An improved two archive algorithm for many-objective optimization. In: **IEEE. 2014 IEEE Congress on Evolutionary Computation (CEC)**. [S.l.], 2014. p. 2869–2876. Cited on page 56.

LI, Miqing; YAO, Xin. Quality evaluation of solution sets in multiobjective optimisation: A survey. **ACM Computing Surveys (CSUR)**, ACM New York, NY, USA, v. 52, n. 2, p. 1–38, 2019. Cited on page 41.

LIU, Bing; LIU, Bing. Supervised learning. **Web Data Mining: Exploring Hyperlinks, Contents, and Usage Data**, Springer, p. 63–132, 2011. Cited on page 28.

LIU, Chengcheng et al. Optimal design of the austenitic stainless-steel composition based on machine learning and genetic algorithm. **Materials**, MDPI, v. 16, n. 16, p. 5633, 2023. Cited on page 48.

LUNDBERG, Scott M; LEE, Su-In. A unified approach to interpreting model predictions. **Advances in neural information processing systems**, v. 30, 2017. Cited on page 67.

MITCHELL, Melanie. **An introduction to genetic algorithms**. [S.l.]: MIT press, 1998. Cited on page 35.

MOHANTY, Itishree; BHATTACHARJEE, Debashish; DATTA, Shubhabrata. Designing cold rolled if steel sheets with optimized tensile properties using ann and ga. **Computacional Materials Science**, v. 50, n. 8, p. 2331–2337, JUN 2011. ISSN 0927-0256. Cited 2 times on pages 47 and 49.

MOMENI, A et al. Bake hardening of a low carbon steel for automotive applications. **Metalurgija**, v. 13, n. 2, p. 131–138, 2007. Cited on page 24.

PANICHELLA, Annibale. An adaptive evolutionary algorithm based on non-euclidean geometry for many-objective optimization. In: **Proceedings of the Genetic and Evolutionary Computation Conference**. [S.l.: s.n.], 2019. p. 595–603. Cited 3 times on pages 38, 39, and 55.

PARPINELLI, Rafael Stubs et al. A review of techniques for online control of parameters in swarm intelligence and evolutionary computation algorithms. **International Journal of Bio-Inspired Computation**, Inderscience Publishers (IEL), v. 13, n. 1, p. 1–20, 2019. Cited on page 39.

PEREIRA, João Luiz Junho et al. A review of multi-objective optimization: methods and algorithms in mechanical engineering problems. **Archives of Computational Methods in Engineering**, Springer, v. 29, n. 4, p. 2285–2308, 2022. Cited on page 33.

PERELOMA, E; TIMOKHINA, Ilana. Bake hardening of automotive steels. In: **Automotive steels**. [S.l.]: Elsevier, 2017. p. 259–288. Cited on page 24.

PIRES, EJ Solteiro; MACHADO, JA Tenreiro; OLIVEIRA, Paulo B de Moura. Diversity study of multi-objective genetic algorithm based on shannon entropy. In: IEEE. **2014 Sixth World Congress on Nature and Biologically Inspired Computing (NaBIC 2014)**. [S.l.], 2014. p. 17–22. Cited on page 42.

QIU, Wenbo et al. An adaptive reference vector adjustment strategy and improved angle-penalized value method for rvea. **Complexity**, Hindawi Limited, v. 2021, p. 1–15, 2021. Cited on page 38.

RAHIMI, Iman et al. A comparative study on evolutionary multi-objective algorithms for next release problem. **Applied Soft Computing**, Elsevier, p. 110472, 2023. Cited on page 55.

RAY, RK; JONAS, John J; HOOK, RE. Cold rolling and annealing textures in low carbon and extra low carbon steels. **International materials reviews**, Taylor & Francis, v. 39, n. 4, p. 129–172, 1994. Cited on page 24.

REN, Pengzhen et al. A comprehensive survey of neural architecture search: Challenges and solutions. **ACM Computing Surveys (CSUR)**, ACM New York, NY, USA, v. 54, n. 4, p. 1–34, 2021. Cited on page 31.

REN, Ye; ZHANG, Le; SUGANTHAN, Ponnuthurai N. Ensemble classification and regression-recent developments, applications and future directions. **IEEE Computational intelligence magazine**, IEEE, v. 11, n. 1, p. 41–53, 2016. Cited on page 32.

RESENDIZ-FLORES, Edgar O. et al. Optimal design of hot-dip galvanized dp steels via artificial neural networks and multi-objective genetic optimization. **Metals**, v. 11, n. 4, APR 2021. Cited 3 times on pages 19, 47, and 48.

SARKAR, B et al. Processing and application of interstitial free (if) grade steel: Prospects in sail. In: **International conference on interstitial free steels: manufacturing and applications IF STEEL. India: Jamshedpur**. [S.l.: s.n.], 2010. Cited on page 24.

SARKAR, B et al. Processing and application of interstitial free (if) grade steel: Prospects in sail. In: **International conference on interstitial free steels: manufacturing and applications IF STEEL. India: Jamshedpur**. [S.l.: s.n.], 2010. Cited on page 66.

SCHWEITZER, Philip A et al. **Metallic materials: physical, mechanical, and corrosion properties**. [S.l.]: CRC press, 2003. v. 19. Cited 2 times on pages 19 and 66.

SEGURA, Carlos; CASTILLO, Joel Chacón; SCHÜTZE, Oliver. The importance of diversity in the variable space in the design of multi-objective evolutionary algorithms. **Applied Soft Computing**, Elsevier, v. 136, p. 110069, 2023. Cited on page 20.

- SELÇUKLU, Saltuk Buğra. Multi-objective genetic algorithms. In: **Handbook of Formal Optimization**. [S.l.]: Springer, 2023. p. 1–37. Cited on page 79.
- SGROTT, Douglas. **A multi-objective data-driven evolutionary algorithm applied to steel modeling**. Dissertação (Mestrado) — Santa Catarina State University, 2022. Cited 12 times on pages 9, 20, 21, 34, 47, 48, 49, 54, 55, 56, 63, and 79.
- SGROTT, Douglas Macedo et al. Modelling if steels using artificial neural networks and automated machine learning. In: SPRINGER. **Hybrid Intelligent Systems: 20th International Conference on Hybrid Intelligent Systems (HIS 2020), December 14-16, 2020**. [S.l.], 2021. p. 659–668. Cited 2 times on pages 20 and 67.
- SHAH, Karimulla et al. Optimization of annealing cycle parameters of dual phase and interstitial free steels by multiobjective genetic algorithms. **Materials and Manufacturing Processes**, Taylor & Francis, v. 32, n. 10, p. 1201–1208, 2017. Cited 2 times on pages 48 and 49.
- SHARMA, Sagar; SHARMA, Simone; ATHAIYA, Anidhya. Activation functions in neural networks. **Towards Data Sci**, v. 6, n. 12, p. 310–316, 2017. Cited on page 30.
- SHINDE, Pramila P; SHAH, Seema. A review of machine learning and deep learning applications. In: IEEE. **2018 Fourth international conference on computing communication control and automation (ICCUBEA)**. [S.l.], 2018. p. 1–6. Cited on page 27.
- SILVA, Krigor RR da et al. Ensemble of artificial neural networks and automl for predicting steel properties. In: SIMAS, E.; FERREIRA, D. D.; OLIVEIRA, L. R. (Ed.). **Anais do XVI Congresso Brasileiro de Inteligência Computacional (CBIC'2023)**. Salvador, BA: SBIC, 2023. p. 1–7. Cited 2 times on pages 9 and 53.
- SONG, Kai et al. A steel property optimization model based on the xgboost algorithm and improved pso. **Computational Materials Science**, Elsevier, v. 174, p. 109472, 2020. Cited 3 times on pages 47, 48, and 49.
- SRIVASTAVA, Nitish et al. Dropout: a simple way to prevent neural networks from overfitting. **The journal of machine learning research**, JMLR. org, v. 15, n. 1, p. 1929–1958, 2014. Cited on page 30.
- TANABE, Ryoji; ISHIBUCHI, Hisao; OYAMA, Akira. Benchmarking multi-and many-objective evolutionary algorithms under two optimization scenarios. **IEEE Access**, IEEE, v. 5, p. 19597–19619, 2017. Cited on page 55.
- TIWARI, Anurag et al. Hybrid lawyer recommendation system based on age-moea. In: **2022 IEEE International Conference on Distributed Computing and Electrical Circuits and Electronics (ICDCECE)**. [S.l.: s.n.], 2022. p. 1–6. Cited on page 55.
- TODOROVSKI, M.; RAJICIC, D. An initialization procedure in solving optimal power flow by genetic algorithm. **IEEE Transactions on Power Systems**, v. 21, n. 2, p. 480–487, 2006. Cited on page 36.
- UMBARKAR, Anant J; SHETH, Pranali D. Crossover operators in genetic algorithms: a review. **ICTACT journal on soft computing**, v. 6, n. 1, 2015. Cited on page 36.
- UZAIR, Muhammad; JAMIL, Noreen. Effects of hidden layers on the efficiency of neural networks. In: IEEE. **2020 IEEE 23rd international multitopic conference (INMIC)**. [S.l.], 2020. p. 1–6. Cited on page 29.

- VIKHAR, Pradnya A. Evolutionary algorithms: A critical review and its future prospects. In: **2016 International Conference on Global Trends in Signal Processing, Information Computing and Communication (ICGTSPICC)**. [S.l.: s.n.], 2016. p. 261–265. Cited on page 35.
- WANG, Bin et al. A hybrid ga-pso method for evolving architecture and short connections of deep convolutional neural networks. In: SPRINGER. **PRICAI 2019: Trends in Artificial Intelligence: 16th Pacific Rim International Conference on Artificial Intelligence, Cuvu, Yanuca Island, Fiji, August 26-30, 2019, Proceedings, Part III 16**. [S.l.], 2019. p. 650–663. Cited on page 31.
- WANG, Chenchong et al. Design of comprehensive mechanical properties by machine learning and high-throughput optimization algorithm in rafm steels. **Nuclear Engineering and Technology**, Elsevier, v. 52, n. 5, p. 1008–1012, 2020. Cited on page 49.
- WISTUBA, Martin; RAWAT, Ambrish; PEDAPATI, Tejaswini. A survey on neural architecture search. **arXiv preprint arXiv:1905.01392**, 2019. Cited on page 31.
- WU, Siwei et al. High dimensional data-driven optimal design for hot strip rolling of c-mn steels. **ISIJ International**, v. 57, n. 7, p. 1213–1220, 2017. ISSN 0915-1559. Cited 3 times on pages 47, 48, and 49.
- XIAO, Hanyue et al. Recent developments in the mechanical properties of hybrid fiber metal laminates in the automotive industry: A review. **REVIEWS ON ADVANCED MATERIALS SCIENCE**, v. 62, n. 1, p. 20220328, 2023. Disponível em: <<https://doi.org/10.1515/rams-2022-0328>>. Cited on page 19.
- ZHANG, Chiyuan et al. Understanding deep learning (still) requires rethinking generalization. **Communications of the ACM**, ACM New York, NY, USA, v. 64, n. 3, p. 107–115, 2021. Cited on page 29.
- ZHOU, Aimin et al. Multiobjective evolutionary algorithms: A survey of the state of the art. **Swarm and Evolutionary Computation**, Elsevier B.V., v. 1, n. 1, p. 32–49, 2011. ISSN 22106502. Disponível em: <<http://dx.doi.org/10.1016/j.swevo.2011.03.001>>. Cited on page 37.
- ZHU, Zhenlong; LIANG, Yilong; ZOU, Jianghe. Modeling and composition design of low-alloy steel's mechanical properties based on neural networks and genetic algorithms. **Materials**, MDPI, v. 13, n. 23, p. 5316, 2020. Cited on page 21.
- ZITZLER, Eckart. **Evolutionary algorithms for multiobjective optimization: Methods and applications**. [S.l.]: Shaker Ithaca, 1999. v. 63. Cited on page 58.
- ZITZLER, Eckart; THIELE, Lothar. An evolutionary algorithm for multiobjective optimization: The strength pareto approach. **TIK report**, ETH Zurich, v. 43, 1998. Cited on page 58.
- ZOPH, Barret; LE, Quoc V. **Neural Architecture Search with Reinforcement Learning**. 2017. Cited on page 31.